Scholars' Mine

Doctoral Dissertations   Student Theses and Dissertations

Spring 2021

High throughput analysis to study emerging pollutants and nanoparticle fate in biological systems

Xiaolong He

HIGH THROUGHPUT ANALYSIS TO STUDY EMERGING POLLUTANTS AND

NANOPARTICLE FATE IN BIOLOGICAL SYSTEMS

by

XIAOLONG HE

A DISSERTATION

Presented to the Graduate Faculty of the

MISSOURI UNIVERSITY OF SCIENCE AND TECHNOLOGY

In Partial Fulfillment of the Requirements for the Degree

DOCTOR OF PHILOSOPHY

in

CHEMISTRY

2021

Approved by:

Honglan Shi, Advisor
Joel G. Burken, Co-advisor
Paul Nam
Yinfa Ma
Philip D. Whitefield

PUBLICATION DISSERTATION OPTION

This dissertation consists of the following three articles, formatted in the style used by the Missouri University of Science and Technology:

Paper I (Pages 10-37) has been published in *Journal of Agricultural and Food Chemistry*. 2019, 67, 46, 12927–12935.

Paper II (Pages 38-59) was submitted to *Journal of Agricultural and Food Chemistry*, in review.

Paper III (Pages 60-93) has been published in *Mass Spectrometry*. 2020, 31, 2180−2190.

ABSTRACT

The increasing applications of emerging and fugitive contaminants (EFCs) and engineered nanoparticles (ENPs) attract significant research interest for their potential risks to human health and the environment. In order to assess the health risks of these emerging contaminants, rapid and reliable analytical methods to measure the concentrations and fates of these contaminants are imperative. This dissertation focuses on the developments of advanced analytical methods and their applications to study those emerging contaminants in crop plant and simulated gastric fluid (SGF). Three types of mass spectrometry based methodologies have been developed, one is freeze-thaw/centrifugation extraction followed by high performance liquid chromatography - tandem mass spectrometry (HPLC-MS/MS) method for non-volatile EFCs analysis in three species of crop plant and one is freeze-thaw-equilibration head space-solid phase microextraction (SPME) followed by gas chromatography-mass spectrometry (GC-MS) method for volatile EFCs analysis in three species of crop plant; and one is single particle-inductively coupled plasma-mass spectrometry (SP-ICP-MS) method for ENPs analysis in SGF. By using these SP-ICP-MS methods, various factors such as species, size, concentration of ingested ENPs, and body temperature on the fates of nanoparticles in the digestion system were investigated.

The studies in this dissertation offer green analyses with high throughput analytical methods for EFCs and ENPs. It represents significant advancement and contribution in rapid screening the concentrations of EFCs and ENPs, as well as understanding fates of EFCs and ENPs in biological systems, therefor will make significant contributions to environment research, food security, and human health.

ACKNOWLEDGMENTS

Foremost, I would like to express my deepest gratitude to my advisor, Professor Honglan Shi, for her great and continuous support of my PhD program. Except the fundamental knowledge, experiment skills, she also gave me so much priceless wealth, logical thinking, ability of solving problem and the leadership abilities. At the same time, undoubtedly, her passion and attitude towards research inspired me to overcome difficulties and go through the trough during my PhD program. I believe these characteristics will help me 3000 times in my whole life.

I would like to thank my co-advisor Dr. Joel Burken, my committee members, Dr. Paul Nam, Dr. Yinfa Ma, and Dr. Philip D. Whitefield. I still remember clearly how you gave me confidence on research and language at the beginning of PhD program and how you asked me hard questions one by one on the countless group meetings to help me improve my research ability. I greatly appreciate your patient, encouragement, and professional advisings. These most precious gifts make this work become possible.

I would like to thank Dr. Sahle-Demessie, Endalkachew, who gave me huge support and a lot of useful advices for my research. In addition, I want to thank my friends and other group members for their great help for my research experiment, instrument troubleshooting, document editing, and all the happy time together. At last, I want to express my sincere gratitude to my parents, my 3.5 years old son, especially my wife, Haiting Zhang. Their love and encouragement inspired me to finish this Ph.D. program.

TABLE OF CONTENTS

LIST OF ILLUSTRATIONS

LIST OF TABLES

1. INTRODUCTION

In recent years, increasing number of novel compounds and engineered nanoparticles (ENPs) have been produced and applied in various fields with the advancement of society. The increasing applications of these compounds and ENPs has led to significant increases of emerging and fugitive contaminants (EFCs) pollutions in the environment. The potential risks related to human health and environment caused by these EFCs and ENPs have raised serious concerns.

1.1. EMERGING AND FUGITIVE CONTAMINANTS

As the shortage of water and the humans' demand for alternative irrigation resources continues to grow, the humans' potential exposure to EFC through plants, especially crop plants, is inevitably increasing. Plants can be contaminated by various EFCs[1-3], and the direct irrigation of crop plants with contaminated water raises the EFCs contamination[4, 5] considering the tightly water cycle[6]. EFCs are highly associated with serious diseases, such as heart disease, diabetes, liver disease in human, and they also lead to problems in ecosystem[7-11]. The potential risks of EFCs to human and environment has attracted serious concerns. EFCs have been listed in the related regulations in U.S.A. [12]. The U.S Environmental Protection Agency (EPA) published Draft Contaminant Candidate List (CCL)-4, including contaminants occurring or that are anticipated to occur in water systems. Potential regulations will be applied for these contaminants[12]. EPA Federal Facilities Restoration and Reuse Office (FFRRO) classified part of EFCs as possible human carcinogens and listed them as emerging contaminants[13, 14]. Once EFCs are released

into the water system, they will remain in water systems for a long period of time, due to their relative resistance to biodegradation[13, 14].

There are sufficient evidences that demonstrate the ability of plants to uptake contaminants from water systems[15-18]. Edible crops' uptake of EFCs is one major way of EFCs for direct exposure and entry into the food chain. The preemptive, efficient risk assessment and risk management for edible crops can help people to avert potential human health risks of EFCs. It is imperative to investigate the crop plants uptake EFCs with different biochemical and physicochemical properties to evaluate the potential risk of EFCs enter into the food chain. The octanol/water partitioning coefficient (K_{ow}) was applied by Briggs *et al* to predicate the efficiency of plants' uptake of contaminants in 1982[19]. Aitchison *et al* and Limmer *et al* investigated the transpiration stream concentration factor (TSCF), defined as the ratio of pollutant concentration in the transpiration stream (aqueous chemical concentration in the plant shoot xylem) to the aqueous concentration in solutions, to quantify the uptake efficiency[17, 20]. However, TSCF cannot be applied to all contaminants for uptake efficiency evaluation. The log K_{ow} value of 1,4-Dioxane is -0.27, then the TSCF value of 1,4-Dioxane was 0.14 and 0.3 based on Briggs' and Burken's correlation.[19, 20]. It should has extreme low potential uptake by plants in theory. However, it is observed that Carolina hybrid polar tree uptake 1,4-Dioxane rapidly from a hydroponic solution and the contaminated soil in Aitchison's study[17]. It is necessary to get more comprehensive and realistic data related the concentrations of contaminants in the stem of plants and solutions to evaluate the plants uptake efficiency. Thus, a sensitive and rapid method is important to measure EFCs contamination in brownfield and plants, especially edible crops.

1.2. ENGINEERED NANOPARTICLES

International Standards Organization (ISO) defined the nanoscale substance being less than 100 nm in size at least one dimension. According to their chemical composition, ENPs are classified as metal-based, carbon-based, organics and composites. Nanoparticle toxicity was introduced first by the World Economic Forum in its 2006 Global Risks Reports[21]. Large amount of studies in recent years implied that some ENPs are responsible to serious physiological maladies and genetic damage [22-25]. ENPs were utilized in various fields such as food, feed, biocides, and veterinary drugs due to their unique magnetic, thermal, electronic, optical, and photoactive properties with the rapid development of nanoscience and nanotechnology[26-30]. Wang *et al*[31] summarized common ENPs in the environment, as shown in Table 1.1, and Keller *et al*[32] summarized the global flow of ENPs (Figure 1.1). The ENPs were released into air, water, and soil system after the products containing ENPs entered environment. The ENPs released into the environment have high possibility to accumulate and concentrate in food chains through soil and water systems[31]. ENPs are widely used in food, packaging, and specific drugs, as additives and catalysts. These applications directly increase the risk for humans to ingest ENPs.

Table 1.1. Common ENPs in the environment[31]

ENPs	Applications/Sources
CNT (SWCNT & MWCNT)	Vaccine, scaffolds, biosensors, flexible electrodes in displays, electronic paper, antistatic coatings, bullet-proof vests, protective clothing, and high-performance composites for aircraft and automotive industries
Graphene-based (graphene, GO, & rGO)	Scaffolds, grafts, biosensors, and drug delivery vehicles
Fullerene	Lubricant additive, solar cells, and semiconductors
TiO_2	Pigment in paints, glazes, enamels, plastics, paper, fibers, foods, pharmaceuticals, cosmetics, sunscreens, toothpastes, photocatalytic degradation, and solar cells
ZnO	Sunscreens, cosmetics, wide bandgap semiconductor, UV-light-emitting diodes (LEDs), lasers, solar cells, field-emission displays, and gas sensors
Ag	Catalyst, biosensors, food containers, paints, printer inks, textiles, and antibacterial detergents
Au	Printer inks, catalyst, and biosensors
Fe-based (NZVI, Fe_2O_3, & Fe_3O_4)	Environmental remediation, water purification, and catalyst
Cu-based (CuO, Cu_2O, & CuS)	Catalyst, sensors, and photothermal agent

1. Cosmetics   48,000   5. Electronics & Optics   48,700
2. Coatings, Paints, & Pigments   80,500   6. Automotive   23,500
3. Medical   13,400   7. Catalysts   37,500
4. Energy & Environment   43,700   8. Other   22,900
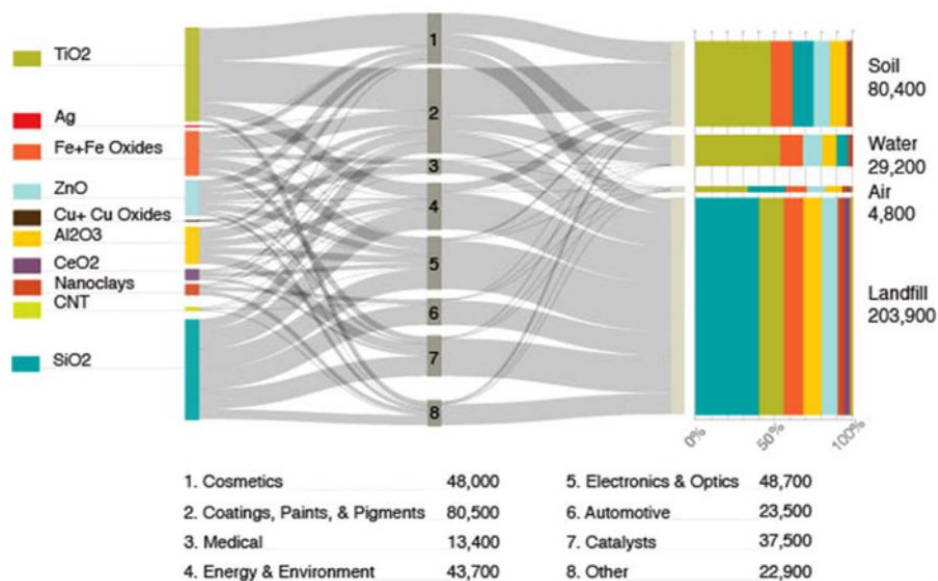
Figure 1.1 Global flow of ENPs (metric tons/year). Life cycle stages from left (production of ENPs) to right (final disposal or release)[32]

The toxicity of ENPs is determined by various factors, such as size, concentration, shape, stability, and agglomeration. The ENPs stay in the stomach for a long time after ingestion and the characteristics of ENPs may change there. Therefore, it is necessary to study the character and fate of nanoparticles in digestive environment.

1.3. CURRENT ANALYTICAL METHODS OF EFCs

In general, assessments of brownfield contamination are done through soil and water analysis. There are several EPA standard methods to measure EFCs listed in the drafted contaminant Candidate List-4, as shown in the Table 1.2[12].

Table 1.2. EPA standard methods

method	analytes	Web site
EPA Method 530	semivolatile organic chemicals	http://www2.epa.gov/water-research/epa-drinking-water-research-methods
EPA Method 543	selected organic chemicals	http://www2.epa.gov/water-research/epa-drinking-water-research-methods
EPA Method 544	microcystins and nodularin	http://www2.epa.gov/water-research/epa-drinking-water-research-methods
EPA Method 545	cylindrospermopsin and anatoxin a	water.epa.gov/scitech/drinkingwater/labcert/upload/epa815r15009.pdf

Based on these EPA method, determination of non-polar, thermostable, volatile, semivolatile, and part of small polar organic EFCs were analyzed by Solid Phase Extraction (SPE) and Gas Chromatography-Mass Spectrometry (GC-MS). SPE-GC-MS is a popular technique for analysis of volatile, semivolatile, and small organic compounds due to its advantages of rapid, simplicity, high sensitivity, and solvent elimination[33-35]. Other EFCs can be analyzed by advanced technique of high performance liquid chromatography-tandem mass spectrometry (HPLC-MS/MS). The EFCs analysis becomes more rapid, sensitive, and accurate due to the great advantages of HPLC-MS/MS and the quantitative detection limit can reach down to part per trillion level in water. However, these EPA methods were all developed to measure EFCs in water samples. The analyses of EFCs in plant tissues are much more complicated. Few methods are available to measure EFCs in plant materials. The major challenges of determination of EFCs in plant tissues are: (1). Time consuming and high cost extraction procedure; (2) Complex matrix of plant tissues, which contains pigments, waxes, fats, cellulose, lignin, etc., leading quantification detection more difficult.

The most popular EFCs-tissue extraction method is solid liquid extraction (SLE). Polar or ionic nature EFCs were extracted with polar organic solvents[36]. Fu *et al*[37] used methyl tert-butyl ether and acetonitrile to extract Triclosan and Triclocarban from radish and carrot in their study. Mechanical shaking, Soxhlet extraction, pressurized liquid extraction (PLE), microwave assisted extraction (MAE), and ultrasound-assisted extraction (USE) were also applied in some studies[38-40]. The cleanup was necessary to reduce the matrix effect after extraction. SPE is a commonly used cleanup method, which offers excellent results[41]. However, above extraction and cleanup methods are not only time-

consuming and high cost, each method is generally only suitable for a specific type of contaminants or plant. More importantly, the volatile and semi-volatile EFCs may evaporate during the extraction and purification procedure, to cause unreliable results. Novel methods are imperative to improve the efficiency and accuracy of EFCs analysis in plant tissues.

1.4. CURRENT ANALYTICAL TECHNIQUES FOR NANOPARTICLE ANALYSIS

There are two main challenges for analysis of ENPs: (1) Development of innovative method to detect, characterize and quantify ENPs in complex samples; (2) Analysis of ENPs at realistic low concentrations and in the presence of nature particles. In past decades, various techniques and methodological approaches were applied to ENPs analysis. The most common techniques are electron microscopy, light scattering, atomic spectrometry, and electroanalytical. Laborda *et al*[21] summarized these analytical techniques and their analytical information, as shown in Table 1.3. Electron microscopy is considered a standard tool for the ENPs size measurement because it has the capability to visualize nanoparticles[42]. Thus, it is typically used as a support technique to guide the interpretation of results from other techniques. It is widely applied in a lot of studies with transmission electron microscopy (TEM), scanning electron microscopy (SEM), and scanning transmission electron microscopy (STEM) [43-47]. However, it is difficult to detect ENPs with low concentrations in environmental or biological samples due to sensitivity of Electron microscopy. Dynamic light scattering (DLS) is the most commonly used light scattering technique. It is used to analyze ENPs size and aggregation behaviors in aqueous suspensions by combining to size separation techniques, like field flow fraction and

Hydrodynamic chromatography. However, there are two main limitations for a light scattering technique: (1) The presence of interfering nanoparticles in an environment or biological samples makes the data obtained from light scattering difficult to interpret; (2) The viscosity and refractive index information from complex samples, which is required by light scattering techniques, is often not available or difficult to obtain[21]. Inductively Coupled Plasma Mass Spectrometry (ICP-MS) is recognized as the state-of-art atomic spectrometry technique for determination of metal and metal containing biomolecules, semimetals, and some nonmetal elements at concentrations of parts per billion (ppb) or parts per trillion (ppt) [48]. Single particle (SP) ICP-MS is able to provide the information of ENPs concentration, size, size distribution, and dissolved concentration of analyte, as well as the element content per nanoparticle. To date, SP-ICP-MS has been significantly developed and utilized in various complex samples, such as plant tissues, water, animal tissues, etc, and shown a great deal of promise[44, 49-51]. However, SP-ICP-MS has not been widely applied to analyze ENPs in gastric fluid. The fate and characterization of commonly used ENPs, such as Au-NPs and CeO_2-NPs, has not been investigated in gastric fluid. Several studies investigate the Ag-NPs and ZnO_2-NPs in gastric conditions[52-57]. Most of these studies were focused on a single unrealistic high concentration of ENPs, one specific contact time, and one single temperature when they investigated the fate of ENPs in gastric conditions. The information about particle concentration, particle size distribution, and dissolved analyte concentration were not collected simultaneously in these previous studies due to the limits of experimental methodologies. Therefore, the fate of ENPs under more realistic conditions need to be investigated and more comprehensive information of ENPs

Table 1.3. Analytical techniques to be suitable for analysis of ENPs[21]

Technique	Acronym	Size LOD	Concentration LOD	Analytical information
Electron microscopy				
Transmission electron microscopy	TEM	<1 nm		- Size (average and distribution) - Shape - Elemental composition (+EDS) - Chemical structure (+EELS) - Crystal structure (+SAED/CBED)
Field-emission scanning electron microscopy	FESEM	1 nm		- Size (average and distribution) - Shape - Elemental composition (+EDS)
Environmental scanning electron microscopy	ESEM	30 nm	10^{12} L^{-1}	- Size (average and distribution) - Shape
Light scattering				
Nanoparticle tracking analysis	NTA	20 nm	10^9 L^{-1}	- Size (average and distribution) - Number concentration
Atomic spectrometry				
Inductively coupled plasma mass spectrometry	ICP-MS	–	ng L^{-1}	- Bulk element composition - Total mass concentration
Single particle ICP-MS	SP-ICP-MS	10–20 nm	10^6 L^{-1} ng L^{-1}	- Detection of dissolved element/NP - Element mass per NP (average and distribution) - Size (average and distribution) - Number concentration - Mass concentration
X-ray absorption spectroscopy	XAS	–	mg kg^{-1}	- Chemical composition - Identification/quantitative distribution of chemical species
Electroanalytical techniques				
Voltammetry of immobilized particles	VIP	10 nm	µg L^{-1}	- Element composition - Oxidation state - Size (average) - Mass concentration
Particle collision coulometry	PCC	5 nm	10^{10} L^{-1}	- Detection of NPs - Size (average and distribution) - Number concentration - Mass concentration

under gastric condition need to be confirmed. The investigation of fate of ENPs in gastric fluid can help us to predicate their organ biodistribution after they enter into circulatory system and evaluate their toxicity to human.

1.5. RESEARCH OBJECTIVE

The research aims to develop the rapid, simple, and sensitive analytical methods to analyze different types of EFCs in plant for rapid evaluation of brownfield contamination and food safety, and to develop method to analyze broadly used metal-based ENPs by SP-ICP-MS and to study their fate in simulate gastric fluid (SGF):

(1) Develop method of Freeze-Thaw-Centrifuge sample preparation followed by HPLC-MS/MS to analyze a large panel of representative EFCs with different biochemical and physicochemical properties in three species of representative plants, corn, tomato, and wheat.

(2) Develop method of Freeze-Thaw-Equilibration sample preparation followed by SPME-GC-MS to analyze representative volatile EFCs in stem of three species of representative plants, corn, tomato, and wheat.

(3) Establish SP-ICP-MS method to analyze Ag-NPs, Au-NPs, CeO_2-NPs, and ZnO-NPs in SGF and study fates of these ENPs in SGF under different conditions.

PAPER

I. GREEN ANALYSIS: HIGH THROUGHPUT ANALYSIS OF EMERGING POLLUTANTS IN PLANT SAP BY FREEZE-THAW-CENTRIFUGAL MEMBRANE FILTRATION SAMPLE PREPARATION-HPLCMS/MS ANALYSIS

Xiaolong He[1], Haiting Zhang[1], Runmiao Xue[1], Wenyan Liu[1,2], Majid Bagheri[2], Matt. A. Limmer[4], Joel G. Burken[2, 3] Honglan Shi[1,2*]

[1]Department of Chemistry, Missouri University of Science and Technology, Rolla, MO, 65409, USA

[2]Center of Research for Energy and Environment, Missouri University of Science and Technology, Rolla, MO, 65409, USA

[3]Department of Civil, Architectural, and Environment Engineering, Missouri University of Science and Technology, Rolla, MO, 65409, USA

[4]Department of Plant and Soil Sciences, University of Delaware, Newark, DE 19716, USA

Corresponding author
Address: Department of Chemistry
Missouri University of Science and Technology
400 W 11th Street
Rolla, MO 65409
E-mail: honglan@mst.edu
Tel: 573-341-4433

ABSTRACT

Emerging and fugitive contaminants (EFCs) released to our biosphere have caused a legacy and continuing threat to human and ecological health, contaminating air, water, and soil. Polluted media are closely linked to food security through plants, especially agricultural crops. However, measuring EFCs in plant tissues remains difficult, and high-throughput screening is a greater challenge. A novel rapid freeze-thaw/centrifugation extraction followed by high performance liquid chromatography-tandem mass

spectrometry (HPLC-MS/MS) analysis was developed for high-throughput quantification of 11 EFCs with diverse chemical properties, including estriol, codeine, oxazepam, 2,4-dinitrotoluene, 1,3,5-trinitroperhydro-1,3,5-triazine, bisphenol A, triclosan, caffeine, carbamazepine, lincomycin, and DEET, in three representative crops, corn, tomato, and wheat. The internal aqueous solution, i.e., sap, is liberated via a freeze/thaw cycle, and separated from macromolecules utilizing molecular weight cutoff membrane centrifugal filtration. Detection limits ranged from 0.01 µg L^{-1} to 2.0 µg L^{-1}. Recoveries of spiked analytes in three species ranged from 83.7% to 109%. Developed methods can rapidly screen EFCs in agriculture crops and can assess pollutant distribution at contaminated sites and gain insight on EFCs transport in plants to assess transmembrane migration in vascular organisms. The findings contribute significantly to environmental research, food security, and human health, as it assesses the first step of potential entry into the food chain, that being transmembrane migration and plant uptake, the primary barrier between polluted waters or soils and our food.

Keywords: Rapid plant sample preparation, freeze-thaw-centrifugation, emerging and fugitive contaminants, HPLC-MS/MS method, agriculture crops, food safety.

1. INTRODUCTION

As our society continues to advance, the generation and production of many chemical compounds continues to expand. As we generate and use new compounds for societal benefit, we have unintended consequences through broad applications, unintended spills, and inappropriate disposal of these novel compounds, resulting in emerging and fugitive contaminants (EFCs) and pollutants. These EFCs are linked with industrialization

and the increase of anthropogenic activities, continuously increasing contamination of water, soils, and air.[1−3] These EFCs pose a serious threat to human health as they can be persistent in food and water, and lead to human exposure.[1] Elevated exposures to certain EFCs are significantly associated with heart disease, diabetes, liver disease, and many other health problems in humans, as well as in ecosystems.[4−8] The potential human exposure to EFCs through plants, especially agriculture crops, is inevitably increasing with the growing demand for alternative irrigation resources as water scarcity expands and other potential exposure pathways increase. The water cycle is becoming tighter, and consequently, food security and safety are increasing concerns. Plants can be contaminated by a range of EFCs[9−11] and the contamination by EFCs is expected to rise as direct irrigation of crops with treated wastewater,[12, 13] particularly on brownfields and in urban agriculture.[14] Uptake of EFCs into plants,[15-20] especially edible crops, may be a significant pathway of these chemicals for direct exposure and entry into the food chain via direct food consumption and livestock feeding. Evaluation of the potential plant uptake of EFCs with different biochemical and physicochemical properties is becoming more important for food safety and human health. Therefore, development of sensitive and rapid methods to assess EFCs contamination in brownfields and plants, especially food crops, is becoming crucially important.

Assessments of brownfield and plant contaminations are generally through soil and groundwater analysis. Contamination of plants is generally through analyses of plant tissues including edible portions of crops. Current methods for soil, groundwater, and plant tissue analyses generally include time-consuming procedures for sample preparation.[21−27] Sensitivity and specificity are also not sufficient for some low levels of EFCs analysis.

Advancement of high performance liquid chromatography-tandem mass spectrometry (HPLC-MS/MS) has made EFC analyses much more rapid, sensitive, and accurate with the quantitative detection limit down to parts per trillion levels in water.[28, 29] Advanced HPLC-MS methods were also applied for plant sample analyses, such as pressurized liquid extraction and LC/ESI/MS detection of pharmaceuticals in carrot and cabbage,[30] ultraperformance liquid chromatography−MS/MS to detect triclosan and triclocarban in radish and carrot after extraction with methyl tert-butyl ether and acetonitrile,[25] and solid phase extraction and HPLC-MS/ MS to detect carbamazepine in zucchini.[26] An extraction methodology that is quick, easy, cheap, effective, rugged, and safe, QuEChERS extraction, was also developed to detect pesticide in plant materials.[31−33] Explosive contaminants were analyzed by multicomponent solvent extraction followed by HPLC-MS/MS analysis in tree tissue,[34] and results suggested that the solvent extraction efficiency of explosives in plants was influenced by the plant species and solvent used. These developed methods were generally applicable at analyzing a specific type of contaminant or one type of plant, in addition to the requirement of time-consuming sample extraction or specific setup. Although a rapid and simple freeze−thaw−centrifugation method has been developed for field contamination screening of perchlorate using tree sap in our previous study,35 the method is not suitable to simultaneously analyze a large variety of contaminants in crop samples.

The objective of this study was to develop a rapid, simple, and sensitive analytical method to analyze different types of EFCs simultaneously in plants saps for rapid brownfield contamination and food safety assessments. We have chosen 11 representative compounds with different biochemical and physicochemical properties as analytes, and

three kinds of representative plants, corn (*Zea mays*), tomato (*Solanum lycopersicum*) and wheat (*Tritcum* spp). Pharmaceuticals (estriol, codeine, oxazepam, caffeine, carbamazepine, lincomycin), explosives (2,4-DNT, RDX), an antimicrobial (triclosan), a pesticide (DEET), and a plasticizer (bisphenol-A) in the three crop plants were analyzed by using the developed freeze-thaw molecular weight cut-off membrane centrifugal filtration technique for sample preparation followed by HPLC-MS/MS detection.

2. MATERIALS AND METHODS

2.1. CHEMICALS AND OTHER MATERIALS

Standards of 16α-hydroxyestradiol (estriol) (≥97%), (5α,6α)-7,8-didehydro-4,5-epoxy-3-methoxy-17-methylmorphinan-6-ol (codeine) (1 mg mL^{-1} in methanol), 7-chloro-3-hydroxy-5-phenyl-1,3-dihydro-1,4-benzodiazepin-2-one (oxazepam) (≥98%), 2,4-DNT (100 μg mL^{-1} in acetonitrile), RDX (100 μg mL^{-1} in acetonitrile), and 4,4′-(propane-2,2-diyl)diphenol (bisphenol A) (≥99%) were purchased from Sigma-Aldrich (St. Louis, MO, USA). 5-Chloro-2-(2,4-dichlorophenoxy)phenol (triclosan) (99%), 1,3,7-trimethylpurine-2,6-dione (caffeine) (99%), 5Hdibenzo[b,f]azepine-5-carboxamide (carbamazepine) (98%), (2S,4R)-N-[(1R,2R)-2-hydroxy-1-[(2R,3R,4S,5R,6R)-3,4,5-trihydroxy-6-(methylsulfanyl) oxan-2-yl] propyl] -1-methyl-4propylpyrrolidine-2-carboxamide (lincomycin) (99.9%), and N,N-diethyl-3-methylbenzamide (DEET) (97%) were purchased from Alfa Aesar (Ward Hill, MA, USA). Formic acid (>98%) and ammonium acetate (>99.99%) was purchased from Sigma-Aldrich (St. Louis, MO, USA). LC-MS grade methanol and acetonitrile were purchased from Fisher Scientific (Fair Lawn, NJ, USA). Ultrahigh purity (MQ) water (18.2 MΩ.cm) was prepared by an Elix-3 water

purification system (Millipore, Billerica, MA, USA) and was degassed and filtered by vacuum filtration using a 0.22-μm nylon membrane filter prior to use for standard or mobile phase preparation. Tomato seeds and corn seeds were purchased from Johnny's selected seeds (Winslow, ME, USA); wheat seeds were purchased from Power Grow Systems (Lindon, UT, USA). Hoagland solution was purchased from Laboratories (Lenexa, KS, USA). Molecular weight cutoff (MWCO) membrane centrifugal filter tubes (Modified PES) with cutoff molecular weight of 3000 Da was purchased from VWR, NY, USA.

2.2. PLANT GROWTH AND FREEZE-THAW-CENTRIFUGATION SAMPLE PREPARATION

Plants were grown by following the same procedure we used for nanoparticle plant uptake study.[36] Briefly, tomato, corn, and wheat seeds were germinated for 3−5 days, and then were transferred to 50 mL size polypropylene tubes which contain quarter strength Hoagland solution (one seedling per tube). The seedlings were grown under T5 fluorescent light operated with 16 h light/8 h dark cycle. Plant shoots were harvested when they grew to approximately 20 cm high. The plant shoots separated from roots were wrapped by aluminum foil and stored in ziptop bags individually in the freezer (−20 °C) for several hours or longer to freeze the samples. The time required for freezing depends on the size of the plant shoots. It took longer for larger shoots than the smaller ones to freeze completely. We generally left the samples in the freezer overnight. The plant shoot samples were then thawed at room temperature (20 °C) for 30 to 60 min (time needed also depend on the size of the plant shoots) to ensure that they were thawed completely. The thawed samples were then cut to small pieces and placed into 3000 Da MWCO membrane

centrifugal filter tubes and centrifuged at 13,000 g at 20 °C for 30 min. The liquid filtrate was then transferred into amber glass autosampler vials for HPLC-MS/MS analysis.

2.3. DETERMINATION OF PLANT SAP VOLUME AND EFCs

The sap of plant tissues were measured for calculation of the analytes in the tissue sap. All three different types of plants without dosing the EFCs were grown and harvested as described above. Ten replicates of each type of shoots were weighed individually, and dried in an oven at 60 °C until constant weight. The weight lost from each plant shoot was recorded as sap volume of the tissue (assuming the same density with water). The amount of the EFCs in the whole plant shoot was calculated from the sap volume and EFCs concentration detected by HPLC-MS/MS.

2.4. PREPARATION OF MATRIX-MATCHED CALIBRATION STANDARDS

Individual stock standard solution of estriol, codeine, oxazepam, bisphenol A, triclosan, caffeine, carbamazepine, lincomycin, acetaminophen, and DEET was prepared in methanol at concentration of 1000 mg L^{-1}, and in acetonitrile for 2,4-DNT and RDX at 100 mg L^{-1}. A secondary standard solution mixture containing all the analytes was prepared by diluting the stock solutions in MQ water at a concentration of 10 mg L^{-1} each compound. The instrument calibration standard solutions were prepared by further dilution from this secondary standard solution. The calibration standard solutions were prepared in control (analyte free) plant liquid prepared with the same freeze-thaw procedure of the plant samples in order to match matrix of samples. Standard concentrations were from

quantification detection limits to 50 μg L^{-1}. All the calibration standards and samples were stored at 4 °C until analyzed. The analyses were finished in 3 days.

2.5. HPLC-MS/MS METHOD

The general information and properties of analytes are shown in Table 1. Based on this information, both positive electrospray ionization (ESI) and negative ESI were used for HPLC-MS/MS analyses of the plant samples. A Shimadzu highperformance liquid chromatography (HPLC) system (Columbia, MD, USA) including two pumps (LC-20 AD XR), an autosampler (SIL-20AC XR), an online degasser (DGU-30A3), and a column oven (CTO-20A) with a C18 column (75 × 2.1 mm, Kinetex. 2.6 μm particle size, Phenomenex, Torrance, CA, USA) was used for separation. Analyst 1.5 software was used for data acquisition and quantification. For compounds determined by positive ionization mode, samples were eluted with a flow rate set to 0.25 mL min^{-1} under a gradient elution program with eluent A (ultrapure water with 0.1% (v/v) formic acid) and eluent B (Acetonitrile (ACN) with 0.1% (v/v) formic acid). The gradient program was set as the following: 10% B linearly increased from beginning to 50% B over 8 min and then quickly increased to 95% over 0.5 min, and maintained at 95% B for 3.5 min; then decreased to 10% B over 0.5 min and equilibrated for 5 min before the next sample injection. The total run time was 17.5 min. The sample injection volume was 20 μL. The temperature of the oven was set to 35 °C. For compounds determined by negative ionization mode, samples were eluted with a flow rate set to 0.25 mL min^{-1} under a gradient elution program with eluent A (1 mM ammonium acetate in ultrapure water) and eluent B (1 mM ammonium acetate in methanol (MeOH)). The gradient program was set as the following: 15% B linear increased to 90%

B in 3 min and further increased to 95% over 3 more minutes; then decreased to 15% B over 0.5 min and maintained for 5 min before next injection. The total runtime was 11.5 min. The sample injection volume was 20 μL. The temperature of oven was set to 35 °C.

Table 1. General information and properties of EFCs

Contaminant	Log K_{ow}[a]	Formula	CAS #	Molecular weight
Codeine	1.2	$C_{18}H_{21}NO_3$	76-57-3	299.364
Lincomycin	0.91	$C_{18}H_{34}N_2O_6S$	154-21-2	406.538
Caffeine	-0.13	$C_8H_{10}N_4O_2$	58-08-2	194.19
Carbamazepine	2.7	$C_{15}H_{12}N_2O$	298-46-4	236.269
Oxazepam	2.3	$C_{15}H_{11}ClN_2O_2$	604-75-1	286.71
DEET	2.0	$C_{12}H_{17}NO$	134-62-3	191.27
RDX	-2.2	$C_3H_6N_6O_6$	121-82-4	222.12
Estriol	2.9	$C_{18}H_{24}O_3$	50-27-1	288.39
2,4 DNT	2.1	$C_7H_6N_2O_4$	121-14-2	182.134
Bisphenol-A	3.4	$C_{15}H_{16}O_2$	80-05-7	228.29
Triclosan	5.2	$C_{12}H_7Cl_2O_2$	3380-34-5	289.54

[a] $\log_{10}$ of the octanol-water partition coefficient.

A 4000Q Trap tandem mass spectrometer (AB Sciex, Foster City, CA, USA) was operated using multiple reaction monitoring (MRM) for quantitation. Nitrogen gas was used for curtain and collision gases. Specifically, declustering potentials (DP), collision energies (CE), and collision cell exit potentials (CXP) were optimized for the two most sensitive ion transitions for each analyte. For compounds determined by positive ionization

mode, MS was operated under positive ESI mode, and flow injection analysis (FIA) was performed to optimize ion source conditions: ion source temperature of 550 °C, ion spray voltage of 5500 V, curtain gas pressure at 50 psi, ion source gas 1 pressure at 50 psi, and ion source gas 2 pressure at 50 psi. The entrance potential was 10 V for all compounds. For compounds determined by negative ionization mode, MS was operated under negative ESI mode, and FIA was performed to optimize ion source conditions: ion source temperature of 450 °C, ion spray voltage of −3500 V, curtain gas pressure at 30 psi, ion source gas 1 pressure at 50 psi, and ion source gas 2 pressure at 10 psi. The entrance potential was 10 V for all compounds.

2.6. TESTING IF FREEZE-THAW PROCEDURE AFFECTS EFCs IN PLANT SAP

In order to evaluate if the freeze−thaw process effects the EFCs, such as any biological reaction during thaw at room temperature, EFCs standard mixture (20 μg L^{-1} of each EFC) was spiked in extracted plant sap. The sap samples were then divided into two aliquots. One aliquot was directly filtered by the centrifugal filtration followed by HPLC-MS/MS analysis without freeze-thaw process, and the other aliquot was processed through a freeze-thaw-centrifugal filtration procedure, and then analyzed by HPLC-MS/MS methods. This experiment was also repeated to test the repeatability.

2.7. METHOD APPLICATION FOR EFCs DETECTION IN PLANT TISSUES

The developed methods were applied to detect the EFCs in plant tissues. Six plant shoots of each species, two shoots (duplicated) for each concentration of 0.2, 1, or 4 mg

L^{-1} EFCs standard solution with all the analytes, were used for this experiment. Each freshly harvested shoot (bottom end down) was placed in a small glass tube containing 50 μL of EFCs standard. The top of each tube was covered with parafilm to avoid evaporation of solvent. It took about 15 min for the plant shoot to take up all the EFC standard solution in the tube. A 50 μL aliquot of MQ water was then added into the glass tube, and the plant shoot was allowed to take up the MQ water (take about 15 min). This MQ water uptake procedure was repeated for 3 times to make sure all the EFCs were taken up into the plant tissue. The plant shoot samples were then processed through the freeze-thaw-centrifugal filtration followed by HPLC-MS/MS analysis as described above. To double confirm no residual EFCs left in the glass tube, 500 μL MQ water was used to wash the glass tube and the wash was analyzed by HPLC-MS/MS, and it was confirmed that no detectable EFCs left in the washing solution.

3. RESULTS AND DISCUSSIONS

3.1. METHOD PARAMETER OPTIMIZATION OF HPLC SEPERATION

The main aim of this research was to develop a method to detect and quantify 11 EFCs in plant saps. We tested different column types and sizes, flow rates, mobile phases, and gradient systems during the method development to get optimized method performance. A Phenomenex Kinetex C18 column with dimension of 2.6 μm particle size, 75 mm length, and 2.1 mm internal diameter was selected for the HPLC-MS/MS methods of both positive electrospray ionization (ESI) and negative ESI. For negative ESI compounds, mobile phase components of MQ water and methanol with different concentrations of ammonium acetate were tested at different flow rates and column oven

Table 2. Optimized HPLC-MS/MS conditions

	Compound	Quantification ion transition (m/z)	Confirmation ion transition (m/z)	DP[a] (V)	CE$_1$[b] (V)	CE$_2$[c] (V)	CXP$_1$[d] (V)	CXP$_2$[e] (V)
Positive ionization mode	Codeine	300.1>152	300.1>128.2	86	93	81	8	6
	Lincomycin	407.1>126.3	407.1>359.1	101	45	29	8	10
	Caffeine	194.9>138.2	194.9>110	66	27	33	8	6
	Carbamazepine	237.0>194.1	237.0>193.1	71	27	49	12	12
	Oxazepam	287.0>241.1	287.0>104	91	31	47	16	6
	DEET	192.0>119	192.0>91.1	76	27	45	6	4
Negative ionization mode	RDX	281.1>45.7	281.1>58.9	-25	-22	-38	-5	-9
	Estriol	287.1>170.9	287.1>143	-135	-50	-72	-9	-7
	2,4 DNT	181.0>46	181.0>134.9	-50	-50	-28	-5	-7
	Bisphenol-A	227.0>211.9	227.0>133	-80	-26	-32	-13	-1
	Triclosan	286.9>35	286.9>48.6	-40	-32	-114	-1	-1

[a] DP-Declustering potential. [b] CE$_1$-Collision energy for quantification ion pair. [c] CE$_2$ Collision energy for confirmation ion pair. [d] CXP$_1$- Collision cell energy for quantification ion pair. [e] CXP$_2$-Collision cell energy for confirmation ion pair.

temperatures. For the positive ESI compounds, the mobile phase of MQ water and ACN with different concentrations of formic acid were tested at different flow rates and column oven temperatures. The optimized positive ESI method is Mobile phase A in MQ water with 0.1% formic acid, and mobile phase B is ACN with 0.1% formic acid. The mobile phase flow rate was 0.25 mL min^{-1}. The elution gradient is 10% B linearly increased from the beginning to 50% B over 8 min and then quickly increased to 95% over 0.5 min, and maintained at 95% B for 3.5 min, and then decreased to 10% B over 0.5 min and

equilibrated for 5 min before the next sample injection. The sample injection volume was 20 µL. The temperature of the oven was set to 35 °C. For negative ESI compounds, the optimized method is Mobile phase A in MQ water with 1 mM ammonium acetate, and mobile phase B is MeOH with 1 mM ammonium acetate. The mobile phase flow rate was 0.25 mL min^{-1}. The gradient elusion program was 15% B linearly increased to 90% B in 3 min and further increase to 95% over 3 more minutes, and then decreased to 15% B over 0.5 min and maintained for 5 min before the next injection. The sample injection volume was 20 µL. The temperature of the oven was set to 35 °C.

3.2. METHOD PARAMETER OPTIMIZATION OF TANDEM MASS SPECTROMETRY

Caffeine, carbamazepine, lincomycin, codeine, oxazepam, and DEET were detected by positive ESI. Each individual compound was infused to mass spectrometer at a concentration of 500 µg L^{-1} in 50% of mobile phase A and 50% of mobile phase B at a flow rate of 0.6 mL h^{-1} using a syringe pump. The MS/MS parameters and the MRM transitions for each selected compound were optimized to achieve the best sensitivity. Two MRM transitions of the one precursor ion and two abundant product ions were monitored for each compound. The most abundant ion pair was used for quantitation and the second one was used for confirmation. The MS/MS parameters that were optimized for each transition included DP, CE, and CXP. All these optimized parameters have been summarized in Table 2. Ion source parameters were subsequently optimized at the following values: ion source temperature 500 °C, ion spray voltage 4000 V, curtain gas pressure 20 psi, GS1 50 psi, GS230 psi, and entrance potential 10 V for all transitions.

Estriol, bisphenol A, RDX, 2,4 DNT, and triclosan were analyzed with a negative ESI method. Each individual compound was infused at a concentration of 500 µg L^{-1} in 50% of mobile phase A (1 mM ammonium acetate in ultrapure water) and 50% of mobile phase B (1 mM ammonium acetate in MeOH at a flow rate of 0.6 mL h^{-1}. The MS/MS parameters and the MRM transitions for each compound were optimized to achieve best sensitivity. Similarly, two MRM transitions between the precursor ion and two abundant product ions were monitored for each compound. The most abundant ion pair was used for quantification, whereas the second was used for confirmation. The MS/MS parameters that were optimized for each transition included DP, CE, and CXP. All these optimized parameters have been summarized in Table 2. Ion source parameters were optimized as the following values: ion source temperature 550 °C, ion spray voltage −4500 V, curtain gas pressure 20 psi, GS1 30 psi, GS2 10 psi, and the entrance potential 10 V for all transitions.

3.3. PERFORMANCE OF METHODS

For positive ESI method, codeine, lincomycin, caffeine, carbamazepine, oxazepam, and DEET were all separated and detected in 10 min. A representative chromatogram of the standard mixture is provided in Figure 1. The repeatability of retention time (RT) for each plant species was tested by injections of standard mixture spiked in the extracted plant sap (n = 6 for each species of plant) (Table 3). Excellent repeatability of the retention time for each plant species was observed as shown in percent relative standard deviation (%RSD) of the six replicates, ranging within 0.01−0.07%. The concentration repeatability of each analyte for each plant species was tested by injections of a standard mixture (10 µg L^{-1} of each analyte) spiked in the extracted plant sap (n = 6 for each type of plant) (Table

3). Repeatability of each analyte for each plant species was high as shown in %RSD of six replicates of each contaminant-species combination tested, ranging within 1.29−11.2%. For the negative ESI method, all analytes were eluted and detected in less than 6 min. A representative chromatogram of a standard mixture is provided in Figure 2. The repeatability of the retention time for each plant species was tested by injections of standard mixture spiked in the extracted plant sap (n = 6 for each plant species) (Table 3). The retention time repeatability was also excellent with %RSD ranging from 0.01% to 0.04%. The concentration repeatability of each analyte was tested by injections of standard mixture (10 µg L$^{−1}$ of each analyte) spiked in the extracted plant sap (n= 6 for each plant species) (Table 3). Good concentration repeatability of analyte for each plant species was observed as shown in %RSD with the six replicates, ranging within 1.63−13.5%.

The performance of this HPLC-MS/MS method was validated in different types of plant matrices including corn, wheat, and tomato (Table 4) by spiking the different concentrations of standards in filtered plant sap matrixes. The instrument detection limits (IDLs), defined as the lowest observable concentration giving a signal-to-noise ratio (S/N) between 3 to 5,[37] ranged from 0.01 to 2 µg L^{-1}. Because calibration standards were prepared in samples extracted from each plant tissues directly and respectively, the method detection limits (MDLs) is ranged from 0.01 to 2 µg L^{-1}. Linear regression analyses were performed using an external calibration curve that begin from limits of quantification (S/N=10)[37] up to the concentration of 50 µg L^{-1} with linearity coefficients (R^2) higher than 0.99. Spiked recovery analyses were performed to evaluate method accuracy by spiking 5 µg L^{-1} analytes in the corresponding plant sap matrix. In corn, recoveries ranged from 83.6% to 109% with reproducibility of <10% RSD; in wheat, recoveries ranged from 85.1% to 103%

with reproducibility of <11% RSD; in tomato, recoveries ranged from 87.1% to 105% with reproducibility of <6% RSD. This demonstrated that the newly developed method was suitable for determination of the selected compounds in all the selected plants.

The spiked recoveries of plant saps with and without freeze-thaw process are all good (Table 5) for all the EFCs with the recoveries in the range of 86.8% to 117%. The repeatability is also good with the %RPD ranged from 0.21% to 6.9%. This indicated that the EFCs did not change during the freeze-thaw process.

Table 3. Repeatability of retention time (RT, in minute) and concentration (10 µg L^{-1}, n=6 for each plant species) of HPLC-MS/MS methods[a]

	Compound	Elution Order	RT (%RSD[b])			Concentration (%RSD[b])		
			Corn	Wheat	Tomato	Corn	Wheat	Tomato
Positive ionization	Codeine	1	3.27 (0.03)	3.24 (0.03)	3.26 (0.01)	9.67 (7.60)	9.34 (11.2)	9.62 (6.86)
	Lincomycin	2	4.11 (0.04)	4.12 (0.02)	4.12 (0.01)	9.25 (2.12)	9.68 (11.0)	9.77 (2.33)
	Caffeine	3	5.20 (0.04)	5.20 (0.02)	5.21 (0.01)	9.76 (4.03)	9.84 (10.7)	9.38 (3.78)
	Carbamazepine	4	8.00 (0.05)	8.33 (0.01)	8.23 (0.03)	10.32 (1.29)	9.93 (1.40)	10.15 (1.08)
	Oxazepam	5	8.25 (0.06)	8.64 (0.01)	8.52(0.03)	9.69 (4.60)	10.25 (10.2)	10.36 (4.72)
	DEET	6	9.14 (0.07)	9.56 (0.02)	9.43 (0.03)	10.64 (3.11)	9.88 (10.6)	9.68 (3.34)
Negative ionization	RDX	1	2.98 (0.02)	2.98 (0.02)	2.96 (0.03)	9.47 (3.30)	9.61 (10.2)	9.47 (3.25)
	Estriol	2	3.79 (0.01)	3.79 (0.02)	3.80 (0.01)	9.89 (5.84)	9.37 (8.66)	9.88 (6.75)
	2,4 DNT	3	3.98 (0.01)	3.99 (0.04)	4.00 (0.02)	9.94 (1.63)	10.64 (12.2)	9.17 (13.5)
	Bisphenol-A	4	4.16 (0.01)	4.17 (0.03)	4.18 (0.03)	9.38 (4.82)	10.36 (12.1)	9.36 (5.85)
	Triclosan	5	4.69 (0.01)	4.70 (0.02)	4.71 (0.04)	10.11 (11.1)	10.11 (9.42)	9.43 (10.4)

[a] Concentration of each analyte spiked was 10 µg L^{-1} in plant sap [b]The percent relative standard deviation.
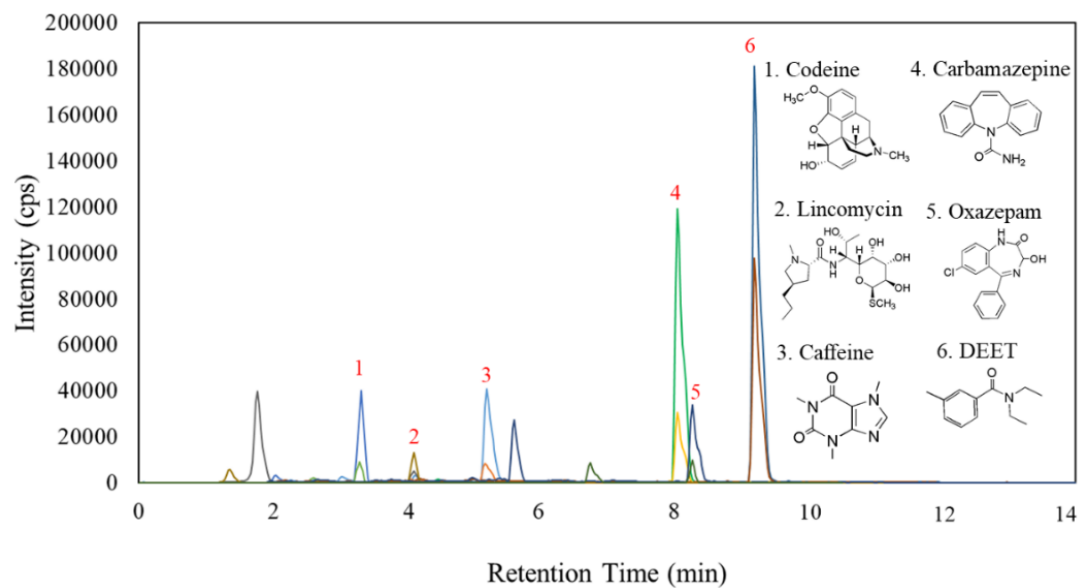
Figure 1. Representative chromatogram of HPLC-MS/MS method for positive ESI standard mixture
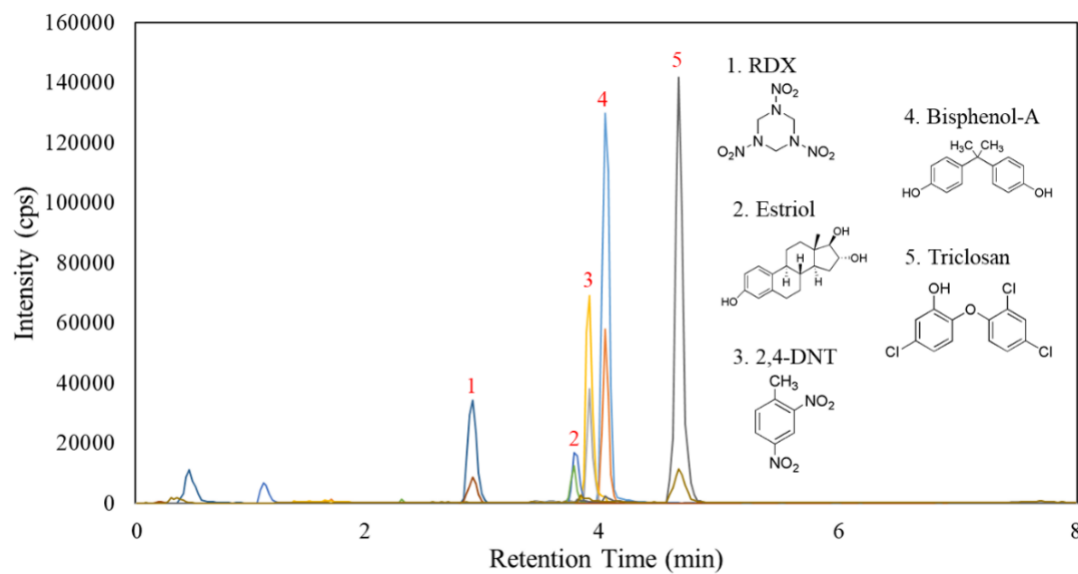
Figure 2. Representative chromatogram of HPLC-MS/MS method for negative ESI standard mixture

Table 4. Detection limits and spike recovery (mean recovery in percentage) and %RSD
(n=3 for each plant species) of the HPLC-MS/MS methods[a]

| | corn | | | wheat | | | tomato | | |
compound	MDL[b] (μg L^{-1})	LOQ[c] (μg L^{-1})	Recovery (% RSD)	MDL[b] (μg L^{-1})	LOQ[c] (μg L^{-1})	Recovery (% RSD)	MDL[b] (μg L^{-1})	LOQ[c] (μg L^{-1})	Recovery (% RSD)
Codeine	0.2	1	87.6 (4.31)	0.5	2	98.2 (5.65)	0.2	1	101 (3.37)
Lincomycin	0.05	0.1	109 (1.35)	0.02	0.05	85.1 (2.04)	0.02	0.05	94.7 (2.24)
Caffeine	0.1	0.2	96.3 (1.83)	0.05	0.1	94.0 (0.22)	0.05	0.1	96.7 (3.67)
Carbamazepine	0.01	0.05	95.5 (0.61)	0.01	0.02	95.4 (0.91)	0.01	0.02	97.8 (0.41)
Oxazepam	0.2	0.5	90.0 (1.07)	0.1	0.2	99.8 (2.05)	0.1	0.5	100 (2.02)
DEET	0.01	0.02	107 (2.35)	0.01	0.02	98.0 (2.47)	0.01	0.02	102 (0.70)
RDX	0.01	0.05	97.2 (0.87)	0.02	0.05	96.2 (4.93)	0.01	0.05	95.6 (2.13)
Estriol	2	5	94.9 (4.84)	1	5	103 (10.74)	1	5	105 (5.04)
2,4 DNT	0.2	0.5	91.6 (0.87)	0.1	0.5	95.7 (5.65)	0.1	0.5	103 (3.36)
Bisphenol-A	1	2	104 (9.18)	0.2	0.5	96.9 (2.06)	0.5	1	88.8 (4.17)
Triclosan	0.05	0.2	83.7 (3.02)	0.05	0.2	89.0 (8.44)	0.1	0.2	87.1 (3.96)

[a]Spiked standard concentration was 5 μg L^{-1} of each analyte. [b]Method detection limits (MDLs) were determined where the S/N = 3−5. [c]Limits of quantification (LOQ) were determined where S/N = 9−10.

Table 5. Concentrations (µg L^{-1}) of spiked EFCs and percent relative percent difference (%RPD) of duplicated samples with and without freeze-thaw (FT) procedure[a]

Compound	EFC concentration in corn sap		EFC concentration in wheat sap		EFC concentration in tomato sap	
	FT (%RPD)	No FT (%RPD)	FT (%RPD)	No FT (%RPD)	FT (%RPD)	No FT (%RPD)
Codeine	18.91 (0.21)	19.34 (2.34)	19.63 (3.51)	19.67 (3.58)	19.34 (4.22)	19.62 (3.86)
Lincomycin	19.91 (1.35)	19.64 (1.89)	20.68 (2.98)	19.24 (2.12)	19.64 (1.65)	19.67 (2.67)
Caffeine	22.72 (2.47)	19.37 (5.79)	21.35 (1.65)	19.65 (3.94)	19.48 (2.36)	18.36 (3.76)
Carbamazepine	23.44 (1.69)	19.64 (3.57)	18.24 (4.68)	20.34 (0.95)	18.46 (3.38)	20.69 (1.59)
Oxazepam	17.90 (3.68)	20.67 (6.92)	18.55 (3.14)	19.64 (3.98)	17.36 (6.21)	18.56 (4.33)
DEET	19.74 (2.49)	21.34 (4.94)	19.47 (2.99)	20.69 (1.79)	20.69 (2.95)	22.65 (5.34)
RDX	18.94 (3.01)	22.98 (1.67)	22.46 (6.31)	19.64 (1.65)	21.69 (4.31)	21.89 (4.21)
Estriol	20.94 (1.69)	18.62 (4.62)	21.88 (2.54)	19.63 (2.96)	22.34 (2.59)	21.33 (3.75)
2,4 DNT	21.03 (4.31)	20.69 (0.99)	19.69 (3.62)	20.34 (3.37)	19.56 (3.67)	19.17 (3.64)
Bisphenol-A	19.88 (2.87)	20.31 (1.64)	21.69 (1.54)	20.39 (4.95)	20.69 (1.67)	19.64 (4.85)
Triclosan	18.66 (1.95)	19.77 (2.95)	22.61 (3.65)	19.68 (6.25)	20.98 (2.59)	20.43 (3.41)

[a]Spiked standard concentration was 20 µg L^{-1} of each analyte.

3.4. RESULT OF PLANT TISSUE ANALYSES

Based on the weight of dry and fresh plants, the moisture percentages of corn, wheat, and tomato plants are ranged from 88%-92%, average value is 90%. Using a moisture content of 90%, the following equation was used to calculate the amount of chemicals in plant sap:

$$M_c = C \times M_p \times 90\%$$

Mc is the mass of chemical in the plant sap, C is the EFC concentration in the sap determined by HPLC-MS/MS, and Mp is the wet mass of plant. Then the fraction of parent compound in plant sap, rather than adsorbed to the plant tissue (R, %) can be calculated by following equation:

$$R = M_c \times 100/M_t$$

Mt is the total mass of chemicals dosed into the plant. The recovery of chemicals in washing tube solution after uptake experiment are ranged from 0 %-1.50 %, indicating only a negligible portion of the chemicals were not taken up by the plant. The percent of chemicals in the sap (R) are shown in Figure 3 for tomato (a), wheat (b), and corn (c). Among all the selected compounds, codeine had the highest fraction in the sap, which ranged from 59.6%-72.4% in tomato plants, 57.4%-73.8% in wheat plants, 78.3%-92.4% in corn plants. The fraction of lincomycin ranged from 47.4%-51.3% in tomato plants, 14.0%-71.2% in wheat plants, 47.0%-63.1% in corn plants. For DEET, the fraction ranged from 33.0%-38.2% in tomato plants, 18.0-23.2% in wheat plants, 46.1%-58.2% in corn plants. The fraction of RDX ranged from 21.7%-40.6% in tomato plants, 40.5%-42.0% in wheat plants, 46.3%-51.5% in corn plants. Shanks found several types of plants have the ability to degrade RDX in their research.[38] Caffeine had low fraction in sap of tomato and wheat, which were ranged from 13.4%-16.5%, and 16.2%-21.1%, but 60.0%-61.4% in corn plants sap, indicating plant species specification. For carbamazepine, the fraction ranged from 19.7%-24.2% in tomato plants sap, 10.0%-21.8% in wheat sap, 32.3%-42.3% in corn sap. Our results largely agree with the published studies, for example, carbamazepine was reported lost during the cucumber plant uptake experiment because of leaching, evaporation, degradation and adsorption;[18] Winker *et al* also found that about 34% of the carbamazepine applied was recovered in plant material after three months in their ryegrass uptake experiment.[39] The methods have also been shown to maintain the integrity of analytes RDX and HMX in this high-throughput method from tissues collection to membrane sterilization.[28-29,34-35]
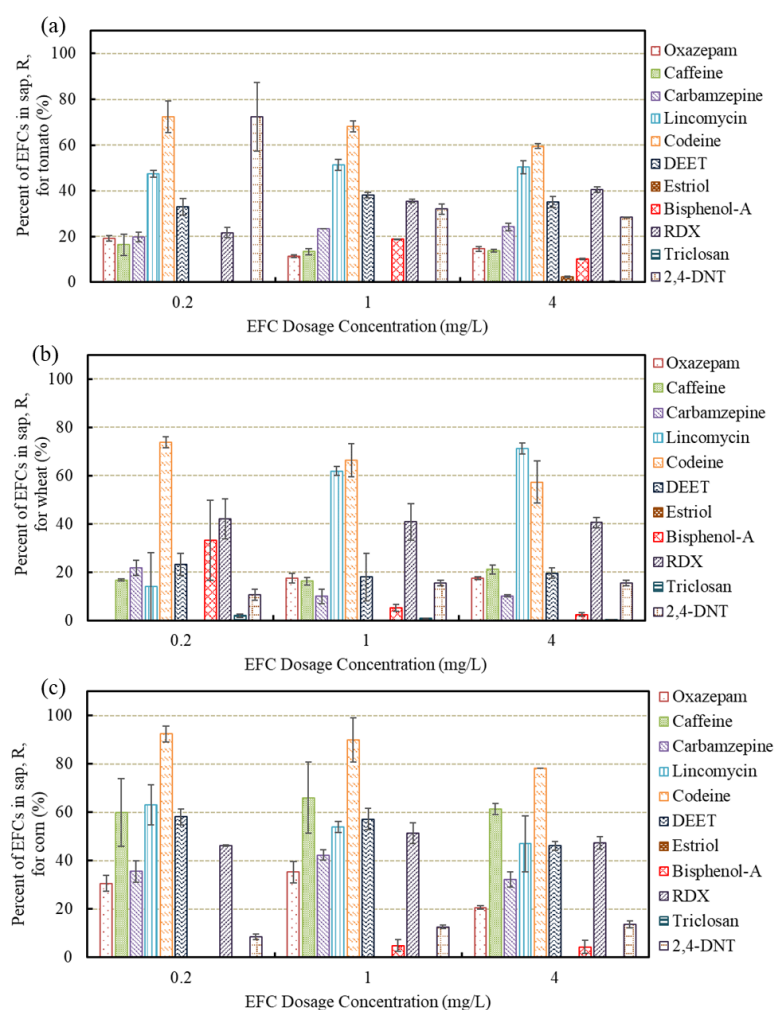
Figure 3. The fraction (%) of EFCs in plant sap: (a) tomato, (b) wheat, (c) corn. R is the ratio of parent compound in plant sap to the total amount adsorbed by the plant. The bars are the averages of duplicated samples and the error bars are the relative present differences of duplicated samples

The fraction of oxazepam were ranged from 11.4%-19.2% in tomato plant sap, 0%-17.5% in wheat plants, and 20.6%-35.3% in corn plants. Carter *et al* also found only 20% of initial oxazepam remained in radish and silverbeet plants due to biotic and abiotic degradations,[40] which is agreed with our results. For 2,4-DNT, the fraction were in the range from 28.4%-72.4% in tomato plant sap, 10.7%-15.6% in wheat sap, and 8.6%-13.7% in corn plant sap. Very low or non-detectable bisphenol-A were found in tomato and corn

plants sap. In wheat plant sap, the fraction of bisphenol-A were 2.48%-33.2%. Fukui has found that convolvulus, a vegetable, can absorb and metabolize bisphenol-A,[41] and Schmidt also found that about 9% of bisphenol-A retained in plant after metabolism of plant.[42] The fraction of triclosan and estriol were very low ($< 3\%$) in in all tomato, wheat and corn sap, presumably degraded biologically by plants, as Reemtsma reported in carrot cells,[43] or plant-microbe symbiotic pairings.

For all the detectable chemicals, their fractions in corn sap were higher than in tomato and wheat sap, except bisphenol-A. From the published research, RDX, carbamazepine, oxazepam, bisphenol-A, and triclosan could be degraded in the plants[18, 38, 40-43] leading to the low percentages of EFCs in the sap. For most of the compounds, the fractions were stable with different dosage amounts in same type of plant. However, the fractions of lincomycin in wheat sap and 2,4-DNT in tomato sap increased with the increase of dosage concentrations, suggesting saturable degradation kinetics. Overall, the developed method could be applied in the real plant sample analysis. More degradation and partition experiments of the EFCs in plants are needed to fully understand all the results.
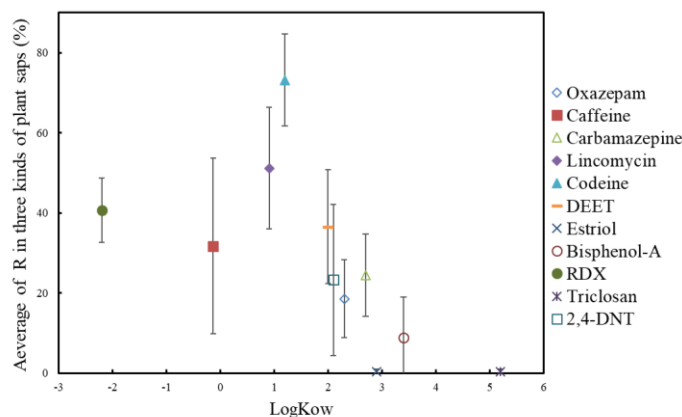
Figure 4. The relationship between the average percent of EFCs in three kinds of plant sap *vis* log K_{ow} of EFCs. The values are the mean of six replicates (two replicates for each kind of plant) with error bars indicating relative standard deviations

The fraction of each EFC in the plant sap was related to its log K_{ow}. From the results in Figure 4, the fraction of EFCs remaining in these three types of plant sap have a negative correlation with Log K_{ow} when log K_{ow} exceeds 1. Higher log K_{ow} values increase partitioning to the hydrophobic plant solids. For RDX and caffeine, their Log K_{ow} values are lowest, however, the fractions remaining in plant saps were lower than lincomycin and codeine. One possible reason is the degradation of these two nitrogenous contaminants by the plant, which also have been discovered in some research that caffeine and RDX were catabolized in some plants and microorganisms.[38, 44] Alternatively, these contaminants maybe sorbed to plant solids through polar interactions. More research experiments are undergoing to further confirm these hypotheses.

4. CONCLUSIONS

In summary, we have developed a rapid and simple freeze- thaw-centrifugal filtration followed by HPLC-MS/MS analysis method for detection of 11 EFCs with different properties in three types of representative agricultural plant sap. The method can quantify EFCs in sap without the use of solvents and complicated multistep sample preparation procedures. The solvent-less sample extraction and purification offer new insight to green analysis, particularly for plant tissues in food security screening. As shown in this study, estriol, codeine, oxazepam, 2,4-DNT, RDX, bisphenol A, triclosan, caffeine, carbamazepine, lincomycin, and DEET, 11 representative compounds with different biochemical and physicochemical properties, were measured in corn, tomato, and wheat sap simultaneously with low detection limits. Matrix effects were avoided by performing a plant sap matrix-matched external calibration. The novel methods provide a quick

screening tool to assess the EFC contaminations of brownfields and food crops through plant sampling, using green analytical chemistry methods. This sample preparation method could also be potentially used as an initial screening for phytodegradation of contaminants in plants and would be ideal for identifying metabolites and plant metabolic pathways as well as presence of pollutants in plants for phytoforensic applications.

ACKNOWLEDGEMENT

REFERENCES

1. Kolpin, D. W.; Furlong, E. T.; Meyer, M. T.; Thurman, E. M.; Zaugg, S. D.; Barber, L. B.; Buxton, H. T., Pharmaceuticals, hormones, and other organic wastewater contaminants in US streams, 1999-2000: A national reconnaissance. *Environmental Science & Technology* **2002,** *36* (6), 1202-1211.

2. Lacey, C.; McMahon, G.; Bones, J.; Barron, L.; Morrissey, A.; Tobin, J. M., An LC-MS method for the determination of pharmaceutical compounds in wastewater treatment plant influent and effluent samples. *Talanta* **2008,** *75* (4), 1089-1097.

3. Hirsch, R.; Ternes, T. A.; Haberer, K.; Mehlich, A.; Ballwanz, F.; Kratz, K. L., Determination of antibiotics in different water compartments via liquid chromatography electrospray tandem mass spectrometry. *Journal of Chromatography A* **1998,** *815* (2), 213-223.

4. Rochester, J. R., Bisphenol A and human health: a review of the literature. *Reprod Toxicol* **2013,** *42*, 132-55.

5. Hussain, G.; Rasul, A.; Anwar, H.; Aziz, N.; Razzaq, A.; Wei, W.; Ali, M.; Li, J.; Li, X., Role of Plant Derived Alkaloids and Their Mechanism in Neurodegenerative Disorders. *Int J Biol Sci* **2018,** *14* (3), 341-357.

6. Niemuth, N. J.; Klaper, R. D., Emerging wastewater contaminant metformin causes intersex and reduced fecundity in fish. *Chemosphere* **2015,** *135*, 38-45.

7. Pal, S.; Blais, J. M.; Robidoux, M. A.; Haman, F.; Krummel, E.; Seabert, T. A.; Imbeault, P., The association of type 2 diabetes and insulin resistance/secretion with persistent organic pollutants in two First Nations communities in northern Ontario. *Diabetes Metab* **2013,** *39* (6), 497-504.

8. McKinney, M. A.; De Guise, S.; Martineau, D.; Beland, P.; Lebeuf, M.; Letcher, R. J., Organohalogen contaminants and metabolites in beluga whale (Delphinapterus leucas) liver from two Canadian populations. *Environ Toxicol Chem* **2006,** *25* (5), 1246-57.

9. Huelster, A.; Mueller, J. F.; Marschner, H., Soil-Plant Transfer of Polychlorinated Dibenzo-p-dioxins and Dibenzofurans to Vegetables of the Cucumber Family (Cucurbitaceae). *Environ Sci Technol* **1994,** *28* (6), 1110-5.

10. Groom, C. A.; Halasz, A.; Paquet, L.; Olivier, L.; Dubois, C.; Hawari, J., Accumulation of HMX (octahydro-1,3,5,7-tetranitri-1,3,5,7-tetrazocine) in indigenous and agricultural plants grown in HMX-contaminated anti-tank firing-range soil. *Environmental Science & Technology* **2002,** *36* (1), 112-118.

11. Wu, W. Z.; Schramm, K. W.; Xu, Y.; Kettrup, A., Contamination and distribution of polychlorinated dibenzo-p-dioxins and dibenzofurans (PCDD/F) in agriculture fields in Ya-Er Lake area, China. *Ecotoxicology and Environmental Safety* **2002,** *53* (1), 141-147.

12. Pereira, L. S.; Oweis, T.; Zairi, A., Irrigation management under water scarcity. *Agricultural Water Management* **2002,** *57* (3), 175-206.

13. Manas, P.; Castro, E.; de las Heras, J., Irrigation with treated wastewater: Effects on soil, lettuce (Lactuca sativa L.) crop and dynamics of microorganisms. *Journal of Environmental Science and Health Part a-Toxic/Hazardous Substances & Environmental Engineering* **2009,** *44* (12), 1261-1273.

14. Brown, K. H.; Jameton, A. L., Public health implications of urban agriculture. *Journal of Public Health Policy* **2000,** *21* (1), 20-39.

15. Collins, C.; Fryer, M.; Grosso, A., Plant uptake of non-ionic organic chemicals. *Environmental Science & Technology* **2006,** *40* (1), 45-52.

16. Boxall, A. B. A.; Johnson, P.; Smith, E. J.; Sinclair, C. J.; Stutt, E.; Levy, L. S., Uptake of veterinary medicines from soils into plants. *Journal of Agricultural and Food Chemistry* **2006,** *54* (6), 2288-2297.

17. Wu, C. X.; Spongberg, A. L.; Witter, J. D.; Fang, M.; Czajkowski, K. P., Uptake of Pharmaceutical and Personal Care Products by Soybean Plants from Soils Applied with Biosolids and Irrigated with Contaminated Water. *Environmental Science & Technology* **2010,** *44* (16), 6157-6161.

18. Shenker, M.; Harush, D.; Ben-Ari, J.; Chefetz, B., Uptake of carbamazepine by cucumber plants - A case study related to irrigation with reclaimed wastewater. *Chemosphere* **2011,** *82* (6), 905-910.

19. Holling, C. S.; Bailey, J. L.; Heuvel, B. V.; Kinney, C. A., Uptake of human pharmaceuticals and personal care products by cabbage (Brassica campestris) from fortified and biosolids-amended soils. *Journal of Environmental Monitoring* **2012,** *14* (11), 3029-3036.

20. Wu, C. X.; Spongberg, A. L.; Witter, J. D.; Sridhar, B. B. M., Transfer of wastewater associated pharmaceuticals and personal care products to crop plants from biosolids treated soil. *Ecotoxicology and Environmental Safety* **2012,** *85*, 104-109.

21. Obana, H.; Kikuchi, K.; Okihashi, M.; Hori, S., Determination of organophosphorus pesticides in foods using an accelerated solvent extraction system. *Analyst* **1997,** *122* (3), 217-20.

22. Wennrich, L.; Popp, P.; Koller, G.; Breuste, J., Determination of organochlorine pesticides and chlorobenzenes in strawberries by using accelerated solvent extraction combined with sorptive enrichment and gas chromatography/mass spectrometry. *J AOAC Int* **2001,** *84* (4), 1194-201.

23. Bogialli, S.; Curini, R.; Di Corcia, A.; Nazzari, M.; Tamburro, D., A simple and rapid assay for analyzing residues of carbamate insecticides in vegetables and fruits: hot water extraction followed by liquid chromatography-mass spectrometry. *J Agric Food Chem* **2004,** *52* (4), 665-71.

24. Herklotz, P. A.; Gurung, P.; Vanden Heuvel, B.; Kinney, C. A., Uptake of human pharmaceuticals by plants grown under hydroponic conditions. *Chemosphere* **2010,** *78* (11), 1416-21.

25. Fu, Q.; Wu, X.; Ye, Q.; Ernst, F.; Gan, J., Biosolids inhibit bioavailability and plant uptake of triclosan and triclocarban. *Water Res* **2016,** *102*, 117-124.

26. Carter, L. J.; Williams, M.; Bottcher, C.; Kookana, R. S., Uptake of Pharmaceuticals Influences Plant Development and Affects Nutrient and Hormone Homeostases. *Environ Sci Technol* **2015,** *49* (20), 12509-18.

27. Snow, D. D.; Cassada, D. A.; Biswas, S.; Shafieifini, M.; Li, X.; D'Alessio, M.; Carter, L.; Sallach, J. B., Detection, Occurrence and Fate of Emerging Contaminants in Agricultural Environments. *Water Environ Res* **2018,** *90* (10), 1348-1370.

28. Wang, C.; Shi, H.; Adams, C. D.; Gamagedara, S.; Stayton, I.; Timmons, T.; Ma, Y., Investigation of pharmaceuticals in Missouri natural and drinking water using high performance liquid chromatography-tandem mass spectrometry. *Water research* **2011,** *45* (4), 1818-28.

29. Mu, R. P.; Shi, H. L.; Yuan, Y.; Karnjanapiboonwong, A.; Burken, J. G.; Ma, Y. F., Fast Separation and Quantification Method for Nitroguanidine and 2,4-Dinitroanisole by Ultrafast Liquid Chromatography-Tandem Mass Spectrometry. *Analytical Chemistry* **2012,** *84* (7), 3427-3432.

30. Herklotz, P. A.; Gurung, P.; Heuvel, B. V.; Kinney, C. A., Uptake of human pharmaceuticals by plants grown under hydroponic conditions. *Chemosphere* **2010,** *78* (11), 1416-1421.

31. Han, Y.; Zou, N.; Song, L.; Li, Y.; Qin, Y.; Liu, S.; Li, X.; Pan, C., Simultaneous determination of 70 pesticide residues in leek, leaf lettuce and garland chrysanthemum using modified QuEChERS method with multi-walled carbon nanotubes as reversed-dispersive solid-phase extraction materials. *J Chromatogr B Analyt Technol Biomed Life Sci* **2015,** *1005*, 56-64.

32. Lehotay, S. J.; Son, K. A.; Kwon, H.; Koesukwiwat, U.; Fu, W.; Mastovska, K.; Hoh, E.; Leepipatpiboon, N., Comparison of QuEChERS sample preparation methods for the analysis of pesticide residues in fruits and vegetables. *J Chromatogr A* **2010,** *1217* (16), 2548-60.

33. Costa, F. P.; Caldas, S. S.; Primel, E. G., Comparison of QuEChERS sample preparation methods for the analysis of pesticide residues in canned and fresh peach. *Food Chem* **2014,** *165*, 587-93.

34. Karnjanapiboonwong, A.; Mu, R.; Yuan, Y.; Shi, H.; Ma, Y.; Burken, J. G., Plant tissue analysis for explosive compounds in phytoremediation and phytoforensics. *J Environ Sci Health A Tox Hazard Subst Environ Eng* **2012,** *47* (14), 2219-29.

35. Limmer, M. A.; West, D. M.; Mu, R.; Shi, H.; Whitlock, K.; Burken, J. G., Phytoscreening for perchlorate: rapid analysis of tree sap. *Environmental Science: Water Research & Technology* **2015,** *1* (2), 138-145.

36. Dan, Y. B.; Zhang, W. L.; Xue, R. M.; Ma, X. M.; Stephan, C.; Shi, H. L., Characterization of Gold Nanoparticle Uptake by Tomato Plants Using Enzymatic Extraction Followed by Single-Particle Inductively Coupled Plasma-Mass Spectrometry Analysis. *Environmental Science & Technology* **2015,** *49* (5), 3007-3014.

37. Vial, J.; Jardy, A., Experimental comparison of the different approaches to estimate LOD and LOQ of an HPLC method. *Analytical Chemistry* **1999,** *71* (14), 2672-2677.

38. Bhadra, R.; Wayment, D. G.; Williams, R. K.; Barman, S. N.; Stone, M. B.; Hughes, J. B.; Shanks, J. V., Studies on plant-mediated fate of the explosives RDX and HMX. *Chemosphere* **2001,** *44* (5), 1259-64.

39. Winker, M.; Clemens, J.; Reich, M.; Gulyas, H.; Otterpohl, R., Ryegrass uptake of carbamazepine and ibuprofen applied by urine fertilization. *Sci Total Environ* **2010,** *408* (8), 1902-8.

40. Carter, L. J.; Williams, M.; Martin, S.; Kamaludeen, S. P. B.; Kookana, R. S., Sorption, plant uptake and metabolism of benzodiazepines. *Sci Total Environ* **2018,** *628-629*, 18-25.

41. Noureddin, I. M.; Furumoto, T.; Ishida, Y.; Fukui, H., Absorption and metabolism of bisphenol A, a possible endocrine disruptor, in the aquatic edible plant, water convolvulus (Ipomoea aquatica). *Biosci Biotechnol Biochem* **2004,** *68* (6), 1398-402.

42. Schmidt, B.; Schuphan, I., Metabolism of the environmental estrogen bisphenol A by plant cell suspension cultures. *Chemosphere* **2002,** *49* (1), 51-9.

43. Macherius, A.; Eggen, T.; Lorenz, W.; Moeder, M.; Ondruschka, J.; Reemtsma, T., Metabolization of the bacteriostatic agent triclosan in edible plants and its consequences for plant uptake assessment. *Environ Sci Technol* **2012,** *46* (19), 10797-804.

44. Mazzafera, P., Catabolism of caffeine in plants and microorganisms. *Front Biosci* **2004,** *9*, 1348-59.

II. GREEN ANALYSIS: RAPID THROUGHPUT ANALYSIS OF VOLATILE CONTAMINANTS IN PLANTS BY FREEZE-THAW-EQUILIBRATION SAMPLE PREPARATION AND SPME-GC-MS

Xiaolong He[1], Bagheri Majid[2], Haiting Zhang[1], Wenyan Liu[2,3], Matt. A. Limmer[4], Joel G. Burken[2, 3], Honglan Shi[1,2*]

[1]Department of Chemistry, Missouri University of Science and Technology, Rolla, MO, 65409, USA

[2]Center of Research for Energy and Environment, Missouri University of Science and Technology, Rolla, MO, USA

[3]Department of Civil, Architectural, and Environment Engineering, Missouri University of Science and Technology, Rolla, MO, 65409, USA

[4]Department of Plant and Soil Sciences, University of Delaware, Newark, DE 19716, USA

Corresponding author
Address: Department of Chemistry
Missouri University of Science and Technology
400 W 11th Street
Rolla, MO 65409
E-mail: honglan@mst.edu
Tel: 573-341-4433

ABSTRACT

Emerging and fugitive contaminants (EFCs) can be introduced into the food chain through plants, particularly crop plants, and have threatened food safety and human health. The method for determination of volatile EFCs in plant tissues remains challenging. A new rapid, simple, precise, and accurate freeze-thaw-equilibration followed by head space (HS)-solid phase microextraction (SPME) and gas chromatography-mass spectrometry (GC-MS) analytical method was developed in this study for high-throughput analysis of 1,4-dioxane and 1,2,3-trichloropropane (TCP) in tissues of three representative crop plants,

corn, wheat, and tomato. The samples were treated by a freeze-thaw procedure, then equilibrated in a saturated sodium sulfate solution and analyzed by HS-SPME-GC-MS method. Method detection limits ranged from 0.625-16 ng/g. The calibration showed good linearity (R^2>0.9). Recoveries of spiked analytes in the three plant species ranged from 82.69-106.3%. The ability of plants uptake of the compounds from soil has been investigated. As demonstrated in this study, this method is used to measure the concentrations of volatile contaminants in the stems of crop plants. This method should also be applicable for other plant tissues, therefore will contribute significantly to the sight of EFCs transport in plants, and to assess the potential risks EFCs pose to food safety and human health.

Key words: Volatile emerging and fugitive contaminants, freeze-thaw-equilibration, solid phase microextraction-GC-MS method, crop uptake of emerging contaminant, food safety

1. INTRODUCTION

Over the past decades, emerging and fugitive contaminants (EFCs) have attracted considerable attention from the scientific and regulatory communities owing to their input to the environment and the potential risks they posed to human health.[1-3] Among them, 1,4-dioxane and 1,2,3-trichloropropane (TCP) have been classified as possible human carcinogens and listed as emerging contaminants by the U.S. Environmental Protection Agency Federal Facilities Restoration and Reuse Office.[4-5] 1，4-Dioxane is a cyclic ether that is widely utilized as a stabilizer in chlorinated organic solvents.[6] 1,2,3-TCP is a synthetic chlorinated hydrocarbon with high chemical stability, and is commonly used as

an industrial solvent, paint remover, cleaning agent, fumigant, and as a chemical intermediate in the production of other chemicals such as polymers.[7]

As emerging contaminants, 1，4-dioxane and 1,2,3-TCP have been detected in surface water and groundwater resources over the previous decades and can pose risks to human health.[8-10] Once released into the subsurface, they remain for long periods of time as a result of their relative resistance to biodegradation[4-5] and are subsequently transferred to the food chain through the uptake by plants, especially edible crops,[2, 11-14] leading to potential human exposure. Therefore, it is important to evaluate the plant uptake efficiency of 1,4-dioxane and 1,2,3-TCP to investigate their potential risks to food safety and human health.

The efficiency of plant uptake contaminants was predicted by Briggs *et al*. using the octanol/water partitioning coefficient (K_{ow}).[15] The transpiration stream concentration factor (TSCF) was introduced to quantify the uptake efficiency, which is defined as the ratio of pollutant concentration in the transpiration stream (aqueous chemical concentration in the plant shoot xylem) to the aqueous concentration in solution.[13, 16] A chemical with TSCF value of 1.0 can move freely with water into a plant, whereas there is no potential uptake for chemicals with TSCF value of 0. The TSCF value of 1,4-dioxane was only 0.14 based on Briggs' correlation, due to its log K_{ow} of -0.27.[15, 17] However, it was observed that the 1,4-dioxane removal increased rapidly in hydroponic solution and contaminated soil by Carolina hybrid polar tree.[13] Therefore, more comprehensive data related the concentrations of 1,4-dioxane and 1,2,3-TCP in the plant and solution are necessary to evaluate their potential risks for crops uptake.

The methods to determine concentrations of 1,4-dioxane and 1,2,3-TCP in solution have been well developed.[7, 18-21] However, it is difficult to quantify their concentrations in plant tissue by these methods. Currently, solid-phase microextraction gas chromatography-mass spectrometry (SPME-GC-MS) has become a popular technique for volatile compounds analysis in plant tissues[22-25] due to its rapidity, simplicity, high sensitivity, and solvent elimination. Though some methods have been developed to monitor 1,4-dioxane and 1,2,3-TCP in plant tissues, most of them focused on the identification of the volatile chemicals in the plant tissues, rather than their quantification.[14, 24-29] There is no precise and accurate quantification method to measure 1,4-dioxane and 1,2,3-TCP in plant tissues currently. Therefore, a reliable quantification method to determine the concentration of 1,4-dioxane and 1,2,3-TCP in plant tissues is urgently needed. Moreover, typical methods require sample pretreatment, such as homogenization, grinding, centrifugation, and/or sonication, prior to the use of HS-SPME procedure,[27, 30-31] which is time consuming and inevitably results in the loss of volatile analytes. Therefore, it is desirable to develop a suitable method to effectively quantify 1,4-dioxane and 1,2,3-TCP in crop plants with minimal sample preparation.

The aim of the present work was to develop a new advanced analytical method, which is a simple, rapid, sensitive and reliable, for the simultaneous determination of 1,4-dioxane and 1,2,3-TCP in three different representative crop plants, corn (*Zea mays*), tomato (*Solanum lycopersicum*) and wheat (*Tritcum* spp). The freeze-thaw method provides significant advantages when it is used to extract EFCs from plant tissues due to the limited sample processing.[2] Thus, in this research, 1,4-dioxane and 1,2,3-TCP in the stem of the three crop plants were analyzed by using the developed freeze-thaw-

equilibration with saturated Na$_2$SO$_4$ solution for sample preparation followed by HS-SPME extraction and GC-MS detection.

2. EXPERIMENTAL SECTIONS

2.1. CHEMICALS AND OTHER MATERIALS

1,2,3-TCP standard (≥99%) was purchased from TCI (Portland, OR, USA). 1,4-Dioxane standard (≥99%) was purchased from Sigma Aldrich (St. Louis, MO, USA). Sodium sulfate (≥99%) was purchased from Fisher Scientific (Pittsburgh, PA, USA). Optima grade methanol was purchased from Fisher Scientific (Fair Lawn, NJ, USA). Tomato seeds and corn seeds were purchased from Johnny's selected seeds (Winslow, ME, USA), and wheat seeds were purchased from Power Grow Systems (Lindon, UT, USA). An Elix-3 water purification system (Millipore, Billerica, MA, USA) was utilized to prepare ultra-high purity water (18.2 MΩ.cm). Hoagland solution was purchased from PhytoTechnology Laboratories (Lenexa, KS, USA).

2.2. PLANTS GROWTH AND FREEZE-THAW-EQUILIBRATION SAMPLE PREPARATION

The same plant growth protocol used routinely in our laboratory[32, 33] was used to grow all three types of plants. Briefly, the seeds were surface-sterilized by 4% (w/v) sodium hypochlorite solution, followed by rinsing with ultra-high purity (MQ) water before being placed on a wet filter paper in a Petri dishes for seed germination. A sufficient number of seeds (2-3 times more than the main replicates) were used for germination to provide enough seedlings for each species. It took 7 days for tomato and up to 5 days for corn and wheat to germinate and seedling growth to take place, before they were

transplanted to the chemical dosing reactor. The seedlings were transplanted into individual 250-ml size amber glass jar (reactors) filled with glass beads (filled to 2.5 cm from the top of the jar) to support the root of the plants. The same amount of glass beads were filled to all reactors in order to maintain the same condition for all plants. The plants were grown in a growth chamber at temperature of 25 °C and 70% humidity under simulated natural light (LED light, light intensity of 350 μmol/m^{2}s) with 16 h light/8 h dark cycles. The reactors on the shelves under the light were positioned randomly, and the reactors were also covered with aluminum foil to avoid evapotranspiration. The plants were fed daily with 25% Hoagland nutrient solution and harvested when they grew to approximately 20 cm by cutting the plants approximately 1 cm above their roots. Two 1 cm stem segments (~0.3 cm diameter for tomato and wheat plant, ~0.5 cm diameter for corn plant) were collected and weighted from each plant and stored in a 20-mL headspace GC vial, and sealed immediately with a Teflon lined septum cap. The vials with samples were put in a freezer (-20 °C) to freeze (generally overnight, or until the sample complete frozen). After taking the frozen samples out of the freezer, 5 mL saturated Na_2SO_4 were added quickly into each vial, and the vials were sealed again immediately. The samples were thawed and equilibrated in the sealed vial at room temperature for 2 hours then analyzed by HS-SPME-GC-MS method. 1, 2, 3 and 4 hours equilibration time were tested to improve the performance of method.

2.3. PREPARATION OF CALIBRATION STANDARDS

Individual standard stock solutions of 1,2,3-TCP and 1,4-dioxane were prepared in methanol at a concentration of 10,000 mg/L. A secondary standard stock solution

containing both analytes was prepared by diluting the stock solutions in MQ water at a concentration of 1000 mg/L for each compound. The calibration standard solutions were prepared by further dilution from this secondary standard solution mixture with MQ water at a series of concentrations (0.05, 0.1, 0.2, 0.5, 1, 5, 10, 20, 50, 100, 500 mg/L). A 10 µL syringe was utilized for the preparation of the calibration standard samples by injecting 10 µL of each standard solution into each control (analyte free) plant stem segment. Each calibration standard sample contained two 1 cm stem segments, and all calibration standard samples went through the same freeze-thaw and equilibration procedure for procedural standard calibration. For each type of plant, the corresponding control plant was used for the calibration standard preparation.

2.4. HS-SPME-GC-MS METHOD

Different fibers, extraction times and temperatures, desorption times and temperatures were examined to optimize the method performance. The finalized method used a 75 µm coating thickness carboxen/ polydimethylsiloxane (PDMS) fiber purchased from Sigma-Aldrich (Bellefonte, PA, USA) for extraction of the volatile analytes. The fiber was preconditioned by following the manufacture's instructions. Extraction time was 20 min from the headspace of the sample in the capped headspace GC vial. The extraction temperature was 60 °C. An Agilent 6890 gas chromatography coupled with a 5973 mass spectrometer was used for this study. The sample injection port equipped with a Merlin Microseal High Pressure Septum (Merlin Instrument Company, Half Moon Bay, California) manual SPME device. The extracted analytes were injected to the GC inlet at 250 °C in splitless mode with a desorption time of 4 min. The separation was achieved using a HP-5

column (30 m ×0.25 mm i.d., 0.25 µm film thickness) with a helium carrier gas flow of 0.8

mL/min. The oven temperature program was set as follows: 40 °C for 2.0 min, 20 °C/min

up to 280 °C, 280 °C for 3.0 min, with a total runtime of 17.0 min. The temperature of the

transfer line and the MS source was set at 280 °C and 230 °C, respectively. The mass

spectrometer electron ionization voltage was 70 eV. The MSD acquisition was carried out

in the selected ion monitoring (SIM) with a dwell time of 100 µs. The quantification ion

was 58 m/z and the confirmation ion was 88 m/z for 1,4-dioxane. The quantification ion

was 75 m/z and the confirmation ion was 110 m/z for 1,2,3-TCP. The basic information of

1,4-dioxane and 1,2,3-TCP and the monitored ions are listed in Table 1 and Figure 1.

Table 1. General information and properties of 1,4-Dioxane and 1,2,3-TCP

Contaminant	Log K_{ow}[a]	Formula	Boiling point (°C)	CAS #	Molecular weight
1,4-Dioxane	-0.27	$C_4H_8O_2$	101	123-91-1	88.106
1,2,3-TCP	1.98~2.27	$C_3H_5Cl_3$	156	96-18-4	147.43

[a] Log K_{ow} is $\log_{10}$ of the octanol-water partition coefficient.

2.5. METHOD APPLICATION FOR VOLATILE EFCs DETECTION IN PLANT STEM

The developed method was applied to analyze 1,4-dioxane and 1,2,3-TCP in plant

stems. Three species of plants, corn, wheat, and tomato, grew by feeding with 25%

Hoagland nutrient solution daily to a height of approximately 20 cm, then dosed daily with

1,4-dioxane and 1,2,3-TCP at concentrations of 1, 4, and 8 mg/L in 25% Hoagland solution.

The blank plant samples were dosed with 25% Hoagland solution only. The experiments

for each plant species and each dosing concentrations were all performed in three

replicates. The plant samples were collected after dosing of 1,4-dioxane and 1,2,3-TCP for 20 days. Two of 1 cm stem segments (~0.3 cm diameter for tomato and wheat plants, ~0.5 cm diameter for corn plants) were collected from each plant. The samples were then processed through the freeze-thaw and equilibration procedure and analyzed by HS-SPME-GC-MS method as described above.
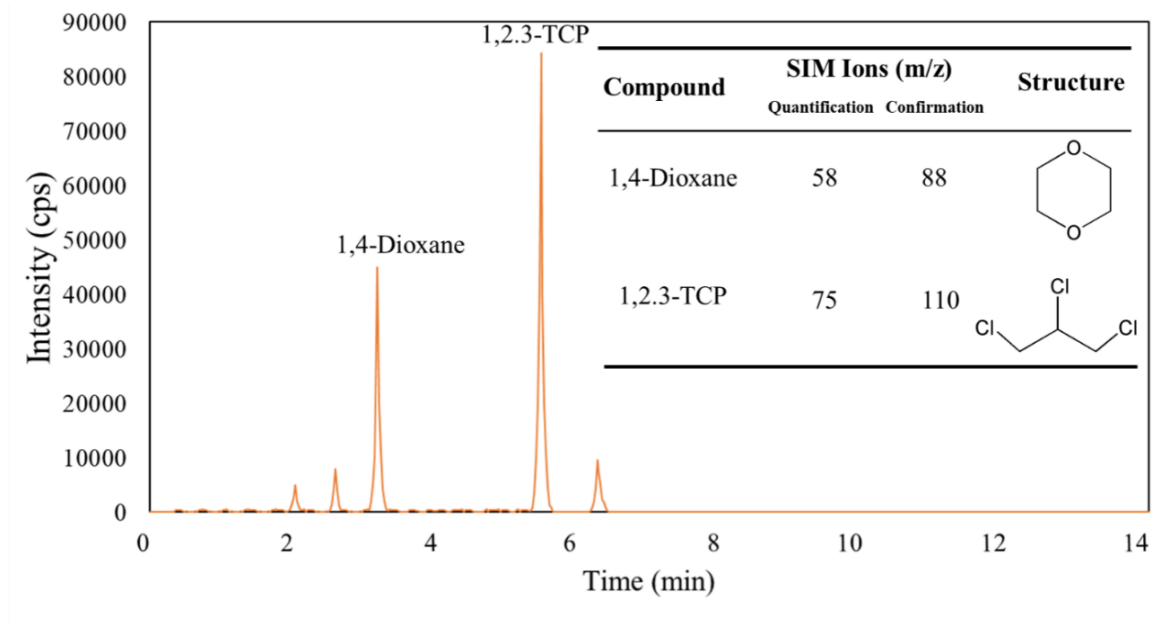
Figure 1. Representative chromatogram of GC-MS method for a 1,4-dioxane and 1,2,3-TCP standard mixture

3. RESULTS AND DISCUSSION

3.1. FREEZE-THAW-EQUILIBRATION AND HS-SPME EXTRACTION PERFORMANCE

To obtain optimized precision and accuracy of the method, sampling conditions such as equilibration time, extraction temperature and time, SPME fiber type, desorption time and temperature, were all optimized. The results indicate that the sensitivities of 1,4-

dioxane and 1,2,3-TCP did not change significantly with 2 hours or longer equilibration time at room temperature, indicating that 2 hours equilibration time is enough.

Because the selected volatile compounds have very different octanol-water partition coefficients (log K_{ow}) (Table 1), three types of SPME fibers, including Carboxen/PDMS, PDMS, and PDMS/DVB, were tested. It can be seen from Figure 2A that the 75 µm Carboxen/PDMS fiber resulted in the best sensitivity and reproducibility for both 1,4-dioxane and 1,2,3-TCP. The impact of extraction temperature on the compound extraction efficiency was investigated at 40, 50, 60, and 70 °C. Figure 2B shows that the maximum signals of the 1,4-dioxane and 1,2,3-TCP were obtained at 60 °C, which is in consistent with the results reported by Adalberto Menezes Filho for water sample analysis.[34] The influence of different extraction times (10, 15, 20, 25, and 30 min) was also examined at 60 °C extraction temperature. Figure 2C shows that the sensitivities of the 1,4-dioxane and 1,2,3-TCP increased sharply when the extraction time was increased from 10 min to 20 min but no significant further increase was observed with longer extraction time. The complete desorption of the analytes from the SPME fiber is also necessary to improve the detector response and to eliminate memory effects. The desorption temperature was therefore tested from 200 to 270 °C. As shown in Figure 2D, the response of the detector increased with increasing temperature from 200 to 250 °C, and did not change significantly when the temperature was further increased from 250 to 270 °C. In addition, the test of different desorption times (3, 4, 5, and 6 min) showed that the 1,4-dioxane and 1,2,3-TCP were desorbed completely from the fiber in 4 min.
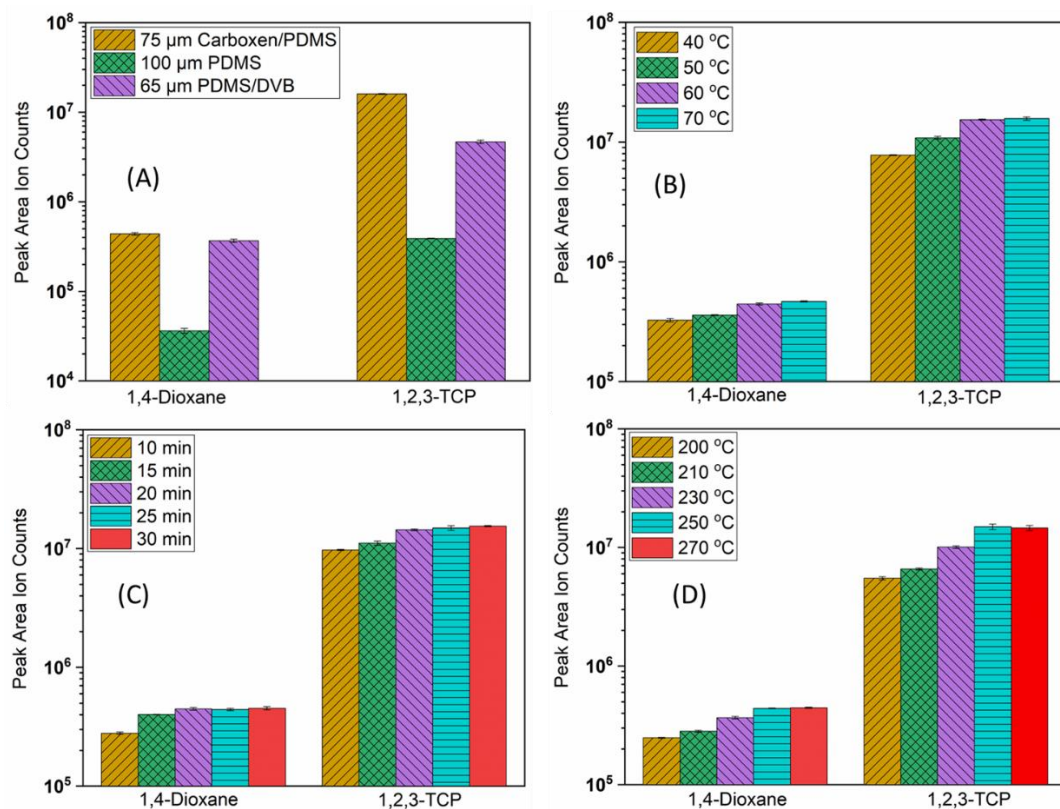
Figure 2. Effects of (A) fiber type, (B) extraction temperature, (C) extraction time, and (D) desorption temperature on the sensitivies of 1,4-dioxane and 1,2,3-TCP. Error bar is mean relative standard deviations

Therefore, considering the above results, overnight freezing, 2 hours equilibration time at room temperature, the extraction time of 20 min at 60 °C and the desorption time of 4 min at 250 °C with Carboxen/PDMS fiber were chosen as optimal freeze-thaw-equilibration procedure and HS-SPME conditions for this method.

3.2. PERFORMANCE OF THE METHOD

The method was validated through the examination of the limits of detection (LOD), limits of quantification (LOQ), the linearity of calibration, the spike recovery, the repeatability of retention time (RT) and the sensitivity of the target compounds. As can be

seen in a representative chromatogram shown in Figure 1, 1,4-dioxane and 1,2,3-TCP in the standard mixture were separated and detected in 6 min. The repeatabilities of RT and concentration were determined by injecting 20 µL of the standard mixture (10 mg/L) into each stem sample of 6 replicates for each species of the plant. The weights of the stem samples were similar to those of the stem samples used for calibration curves (Table 2). The performance of this HS-SPME-GC-MS method is shown in Table 3. The percent relative standard deviations (%RSD) of RTs for 1,4-dioxane and 1,2,3-TCP in these 6 replicate samples ranged from 0.26-0.94% for corn stem, 0.07-0.74% for wheat stem and 0.15-1.37% for tomato stem, therefore, exhibiting an excellent repeatability of RT. Good repeatability of concentration were observed with RSD% of six replicate samples ranged from 3.89-13.34% for corn stems, 7.45-16.74% for wheat stems, and 6.15-15.37% for tomato stems. Eleven concentration levels of the standard mixture were injected into the stems of the plants with the same volume to generate linear regression calibration curve for each compound and to estimate their LOD and LOQ (see Table 2 for details). The LOD was defined as the lowest concentration that shows a signal to noise ratio between 3-5.[31] The LOD ranged in 6.25-16 ng/g for 1,4-dioxane and 0.625-8 ng/g for 1,2,3-TCP in plant stems. The developed method for these three plant species showed good linearity (correlation coefficients (R^2) > 0.98) over the concentration range of 20-10,000 ng/g, 40-8,000 ng/g and 12.5-6,250 ng/g for 1,4-dioxane, and 2-2,000 ng/g, 16-8,000 ng/g and 1.25-6,250 ng/g for 1,2,3-TCP in the stems of corn, wheat, and tomato, respectively.

Table 2. Information of calibration curve standard samples

Concentration of mixture standard (mg/L)	Injection volume (µL)	Mass of fresh stems (g)			Concentration of standard in stem (ng/g)		
		Corn	Wheat	Tomato	Corn	Wheat	Tomato
0.05	20	0.9125	0.2684	1.5946	1	4	0.625
0.1	20	0.9423	0.2625	1.6941	2	8	1.25
0.2	20	0.9389	0.2728	1.5896	4	16	2.5
0.5	20	1.0445	0.2635	1.6121	10	40	6.25
1	20	1.0571	0.2575	1.6478	20	80	12.5
5	20	0.9966	0.2702	1.6588	100	400	62.5
10	20	0.9217	0.2667	1.5789	200	800	125
20	20	0.9845	0.2488	1.5868	400	1600	250
50	20	1.0652	0.2507	1.6112	1000	4000	625
100	20	0.9763	0.2527	1.6561	2000	8000	1250
500	20	0.9992	0.2642	1.6369	10000	40000	6250

Several methods had been developed to measure the concentration of pesticide residues and volatile compounds in mangoes, grapes and vegetables by SPME-GC-MS and SPME-GC-ECD.[30-31, 35] However, the spike recovery of some compounds in these methods were relatively low due to the loss of analyte during the sample preparation. In this study, 200 ng/g and 2000 ng/g of 1,4-dioxane and 1,2,3-TCP were injected into plant stem samples to test the spike recovery. The spike recovery of 1,4-dioxane and 1,2,3-TCP in these three species of plant stems are shown in Table 3. The recoveries ranged from 82.69% to 106.34% in the method developed. There are two possible reasons for the various performance of method for these three species of plants. First, the significantly different in weight of the three species stem samples led to different LOD and concentration ranges for 1,4-dioxane and 1,2,3-TCP. Second, the different properties of various species of stem,

which is caused by the varying composition of each stem, may cause different performance when they are mixed with 1,4-dioxane and 1,2,3-TCP.

Table 3. Performance of the method developed

Plant type	Contaminant	RT (min) ± RSD[a] (%)	RSD (%) of peak area	Linear range (ng/g)	LOD[c] (ng/g)	LOQ[d] (ng/g)	Linearty (R²)[b]	Mean Rocovery (%) ± RPD[e] (%)	
								200 ng/g	2000 ng/g
Corn	1,4-Dioxane	3.19±0.94	13.34	20~10000	10	20	0.9899	89.76±4.79	91.66±8.84
	1,2,3-TCP	5.51±0.26	3.89	2~2000	1	2	0.9906	92.69±11.35	106.34±11.24
Wheat	1,4-Dioxane	3.17±0.74	16.74	40~8000	16	40	0.9843	84.34±4.67	82.69±4.17
	1,2,3-TCP	5.51±0.07	7.45	16~8000	8	16	0.9985	88.92±9.31	90.68±3.26
Tomato	1,4-Dioxane	3.17±1.37	15.37	12.5~6250	6.25	12.5	0.9932	95.48±13.33	101.39±7.24
	1,2,3-TCP	5.50±0.15	6.15	1.25~6250	0.625	1.25	0.9956	101.38±6.48	83.36±14.67

[a] %RSD is the percent relative standard deviation (n=6). [b] R^2 is the linearity coefficients of calibration curve. [c] Limits of detection (LOD) were determined where the S/N=3-5. [d] Limits of quantification (LOQ) were determined where the S/N=9-10. [e] %RPD is the Relative Percent Difference (n=2).

3.3. ANALYSIS OF VOLATILE COMPOUNDS IN THREE KINDS OF PLANT STEM

Triplicate plant samples for each plant species and each dosing concentration of 1,2,3-TCP and 1,4-dioxance were harvested after 20 days dosing. Two stem segments of the same weight with the calibration standard samples were harvested from each plant. The plant stem samples were processed through the above freeze-thaw and equilibration processing procedure and then analyzed by HS-SPME-GC-MS method. The concentrations of the 1,2,3-TCP and 1,4-dioxane in the plant stem samples were obtained from the calibration curves. Figure 3 shows the concentrations of the two volatile compounds, 1, 2, 3-TCP and 1, 4-dioxane in the stems of the corn, wheat, and tomato plants which were daily dosed with 1, 2, 3-TCP and 1, 4-dioxane in 25% Hoagland solution at concentrations of 1, 4, and 8 mg/L. The concentrations of 1, 2, 3-TCP and 1, 4-dioxane in

field blank plants were below the LODs. After 20 days' daily dosing 1 mg/mL of 1, 2, 3-TCP and 1, 4-dioxane, the concentrations of 1, 2, 3-TCP ranged from 134 to 198 ng/g in corn stem samples, from 491 to 649 ng/g in wheat stem samples, and from 172 to 248 ng/g in tomato stems, while the concentrations of 1, 4-dioxane ranged from 304 to 477 ng/g in corn stem samples, from 432 to 524 ng/g in wheat stem samples, and from 329 to 504 ng/g in tomato stems. After 20 days' daily dosing with 4 mg/mL of 1, 2, 3-TCP and 1, 4-dioxane, the concentrations of 1, 2, 3-TCP ranged from 254 to 379 ng/g in corn stem samples, 1410 to 2738 ng/g in wheat stem samples, and 483~807 ng/g in tomato stems, while the concentrations of 1, 4-dioxane ranged from 951 to1162 ng/g in corn stem samples, from 949 to 1483 ng/g in wheat stem samples, and from 1392 to 2414 ng/g in tomato stems. After daily dosing 8 mg/mL of 1, 2, 3-TCP and 1, 4-dioxane for 20 days, the concentrations of 1, 2, 3-TCP were ranged from 212 to 574 ng/g in corn stem samples, from 4423 to 6091 ng/g in wheat stem samples, and from 2143 to 4500 ng/g in tomato stems, while the concentrations of 1, 4-dioxane were ranged from 1410 to 2003 ng/g in corn stem samples, from 2021 to 3807 ng/g in wheat stem samples, and from 5011to 6192 ng/g in tomato stems. In Aitchsion's study, the concentration of 1,4-dioxane in stem of hybrid poplar tree were approximately 5000~10,000 ng/g (fresh weight) when the initial concentration of 1,4-dioxane in soil was 21 ± 32.3 mg/kg.[13] The wide concentration distributions of 1, 2, 3-TCP and 1, 4-dioxane in same species of plant stem with same dosing concentration may be caused by the diversity of plant uptake ability due to their various growth status and activities.
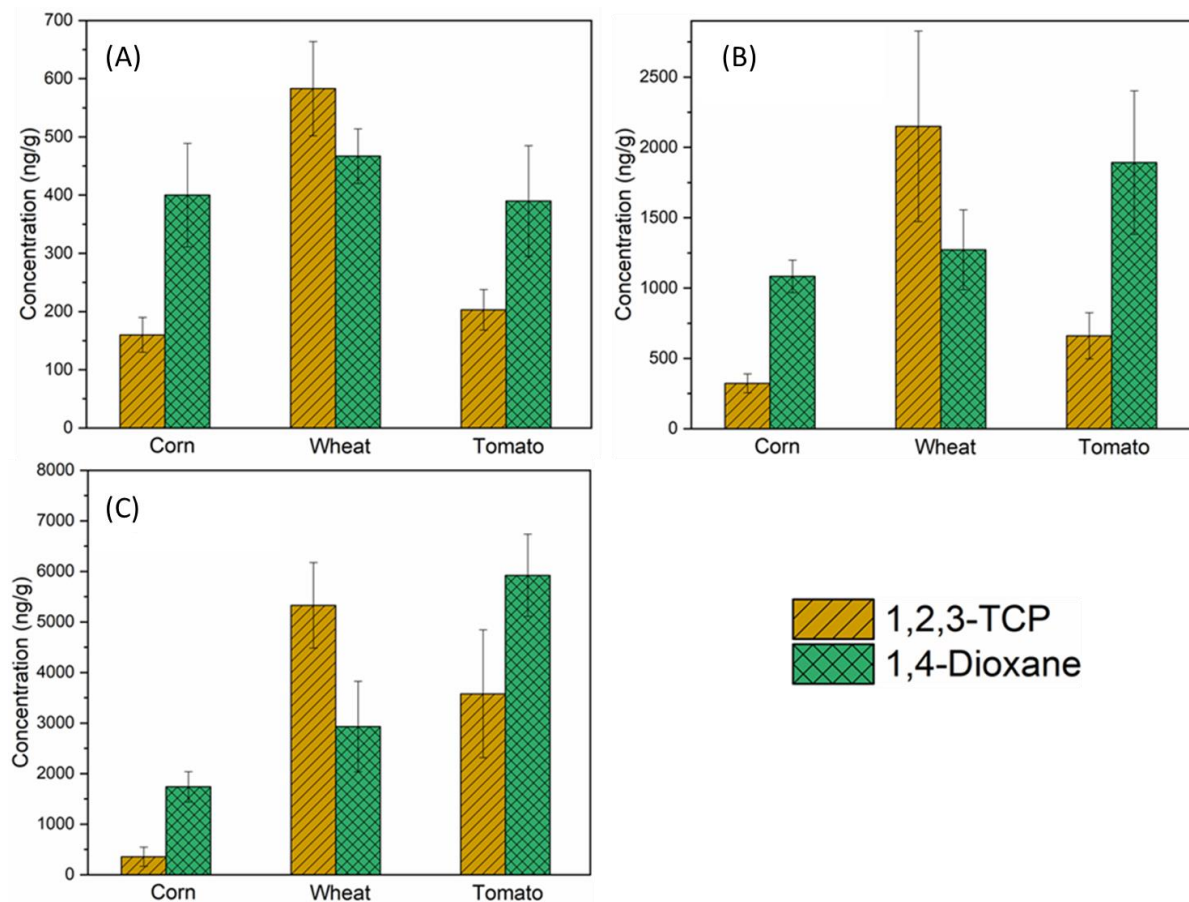
Figure 3. The average concentrations of 1,4-dioxane and 1,2,3-TCP in three species of plant stems with dosing concentrations of (A) 1 mg/mL, (B) 4 mg/mL, and (C) 8 mg/mL. Error bars indicating relative standard deviations

The contaminants with log K_{ow} value close to 2 has the highest TSCF value based on the correlations of a previous study.[13] Contaminants with high TSCF value are easily uptake by plant. The log K_{ow} value of 1, 2, 3-TCP and 1,4-dioxane are 1.98~2.27 and -0.27, respectively. However, the average concentrations of 1,4-dioxane in the stems of corn and tomato are significantly higher than 1, 2, 3-TCP at all dosing concentrations, as shown in the Figure 3. The opposite result was observed in wheat stem samples. On the other hand, the concentrations of 1, 2, 3-TCP and 1,4-dioxane increased significantly in wheat and tomato stems with the increasing of dosing concentration. However, the concentrations

of 1, 2, 3-TCP did not increase when the dosing concentration increased from 4 mg/L to 8 mg/L. Different factors may cause these discrepancies. First, contaminants need to bind with and pass through semi-permeable cell membranes. However, water and compounds can enter into plants because exist of nondiscriminating pathways. It is possible that the 1,4-dioxane and other relatively low molecular weight compounds are available to form hydrogen bonding with water and then achieve an efficient uptake.[13] Second, the differences of composition and root structure of various plants may cause the different uptake performance for the same compound. More comprehensive study is needed to evaluate the potential health risk of 1,4-dioxine and other EFCs through plant uptake.

In summary, we have developed a simple, sensitive, and reliable quantification method of 1,4-dioxane and 1,2,3-TCP in three representative crop tissues based on freeze-thaw-equilibration, followed by HS-SPME-GC-MS analysis. The method shows good performance for the quantification of 1,4-dioxane and 1,2,3-TCP in the plant stems without the need of complicated sample preparation procedure and loss of analyte. This novel method provides a quick, precise, and accurate screening tool to evaluate the plant uptake efficiency for volatile compounds. The method will be very useful to assess the brownfields contamination and food safety. This sample preparation method has high potential to extend its application to analyses of other volatile EFCs in plant tissues.

Abbreviations used:

EFCs   emerging and fugitive contaminants

HS   head space

SPME   solid phase microextraction

GC-MS	gas chromatography-mass spectrometry
TSCF	transpiration stream concentration factor
MQ water	Ultra-high purity water
LOD	limits of detection
LOQ	limit of quantification
RT	retention time
Log K_{ow}	octanol/water partition coefficient

ACKNOWLEDGMENTS

REFERENCES

1. Bagheri, M.; Al-Jabery, K.; Wunsch, D.; Burken, J. G., Examining plant uptake and translocation of emerging contaminants using machine learning: Implications to food security. *Sci Total Environ* 2020, *698*, 133999.

2. He, X.; Zhang, H.; Xue, R.; Liu, W.; Bagheri, M.; Limmer, M. A.; Burken, J. G.; Shi, H., Green Analysis: High Throughput Analysis of Emerging Pollutants in Plant Sap by Freeze-Thaw-Centrifugal Membrane Filtration Sample Preparation-HPLC-MS/MS Analysis. *J Agric Food Chem* 2019, *67* (46), 12927-12935.

3. Madrigano, J.; Osorio, J. C.; Bautista, E.; Chavez, R.; Chaisson, C. F.; Meza, E.; Shih, R. A.; Chari, R., Fugitive Chemicals and Environmental Justice: A Model for Environmental Monitoring Following Climate-Related Disasters. *Environ Justice* 2018, *11* (3), 95-100.

4. EPA, U. S., Technical Fact Sheet –1,4-Dioxane. 2017. URL (https://www.epa.gov/fedfac/technical-fact-sheet-14-dioxane)

5. EPA, U. S., Technical Fact Sheet –1,2,3-Trichloropropane (TCP). 2017. URL (https://www.epa.gov/fedfac/technical-fact-sheet-123-trichloropropane-tcp)

6. Li, M.; Conlon, P.; Fiorenza, S.; Vitale, R. J.; Alvarez, P. J., Rapid analysis of 1, 4-dioxane in groundwater by frozen micro-extraction with gas chromatography/mass spectrometry. *Groundwater Monitoring & Remediation* 2011, *31* (4), 70-76.

7. Babcock, R. W., Jr.; Harada, B. K.; Lamichhane, K. M.; Tsubota, K. T., Adsorption of 1,2,3-Trichloropropane (TCP) to meet a MCL of 5 ppt. *Environ Pollut* 2018, *233*, 910-915.

8. Zenker, M. J.; Borden, R. C.; Barlaz, M. A., Occurrence and treatment of 1, 4-dioxane in aqueous environments. *Environmental Engineering Science* 2003, *20* (5), 423-432.

9. Oki, D. S.; Giambelluca, T. W., Groundwater contamination by nematicides: influence of recharge timing under pineapple crop 1. *JAWRA Journal of the American Water Resources Association* 1989, *25* (2), 285-294.

10. Williams, M.; Ingerman, L.; McIlroy, L., Toxicological profile for 1, 2, 3-Trichloropropane: draft for public comment. 2019.

11. Wu, C.; Spongberg, A. L.; Witter, J. D.; Sridhar, B. B., Transfer of wastewater associated pharmaceuticals and personal care products to crop plants from biosolids treated soil. *Ecotoxicol Environ Saf* 2012, *85*, 104-109.

12. Holling, C. S.; Bailey, J. L.; Vanden Heuvel, B.; Kinney, C. A., Uptake of human pharmaceuticals and personal care products by cabbage (Brassica campestris) from fortified and biosolids-amended soils. *J Environ Monit* 2012, *14* (11), 3029-3036.

13. Aitchison, E. W.; Kelley, S. L.; Alvarez, P. J.; Schnoor, J. L., Phytoremediation of 1, 4-dioxane by hybrid poplar trees. *Water Environment Research* 2000, *72* (3), 313-321.

14. De Paoli, M.; Taccheo Barbina, M.; Damiano, V.; Fabbro, D.; Bruno, R., Simplified determination of combined residues of prochloraz and its metabolites in vegetable, fruit and wheat samples by gas chromatography. *J Chromatogr A* 1997, *765* (1), 127-131.

15. Briggs, G. G.; Bromilow, R. H.; Evans, A. A., Relationships between lipophilicity and root uptake and translocation of non-ionised chemicals by barley. *Pesticide science* 1982, *13* (5), 495-504.

16. Limmer, M. A.; Burken, J. G., Plant translocation of organic compounds: molecular and physicochemical predictors. *Environmental Science & Technology Letters* 2014, *1* (2), 156-161.

17. Burken, J. G.; Schnoor, J. L., Predictive relationships for uptake of organic contaminants by hybrid poplar trees. *Environmental Science & Technology* 1998, *32* (21), 3379-3385.

18. Yasuhara, A.; Shiraishi, H.; Nishikawa, M.; Yamamoto, T.; Uehiro, T.; Nakasugi, O.; Okumura, T.; Kenmotsu, K.; Fukui, H.; Nagase, M., Determination of organic components in leachates from hazardous waste disposal sites in Japan by gas chromatography–mass spectrometry. *Journal of Chromatography A* 1997, *774* (1-2), 321-332.

19. Kawata, K.; Ibaraki, T.; Tanabe, A.; Yagoh, H.; Shinoda, A.; Suzuki, H.; Yasuhara, A., Gas chromatographic–mass spectrometric determination of hydrophilic compounds in environmental water by solid-phase extraction with activated carbon fiber felt. *Journal of Chromatography A* 2001, *911* (1), 75-83.

20. Yano, M.; Kawamoto, T.; Makihata, N.; Tanimoto, T.; Kono, Y., Highly sensitive detertnination of 1, 4-dioxane in tap water and raw water in hyogo prefecture by GC/MS coupled with an improved solid-phase extraction-GC/MS. *Bunseki Kagaku* 2005, *54* (9), 917-921.

21. Wejnerowska, G.; Gaca, J., Application of Headspace Solid-Phase Microextraction for Determination of Chloro-Organic Compounds in Sewage Samples. *Toxicol Mech Methods* 2008, *18* (6), 543-550.

22. Zhao, D.; Tang, J.; Ding, X., Analysis of volatile components during potherb mustard (Brassica juncea, Coss.) pickle fermentation using SPME–GC-MS. *LWT-Food Science and Technology* 2007, *40* (3), 439-447.

23. KRZYŻANOWSKI, R.; LESZCZYŃSKI, B.; GADALIŃSKAKRZYŻANOWSKA, A., Application of DI-SPME/GC-MS method for the analysis of MCPA residues in winter wheat tissues. Herba Polonica 2008, 54 (3).

24. Vandendriessche, T.; Nicolai, B.; Hertog, M., Optimization of HS SPME fast GC-MS for high-throughput analysis of strawberry aroma. *Food analytical methods* 2013, *6* (2), 512-520.

25. Souza Silva, E. A.; Saboia, G.; Jorge, N. C.; Hoffmann, C.; Dos Santos Isaias, R. M.; Soares, G. L. G.; Zini, C. A., Development of a HS-SPME-GC/MS protocol assisted by chemometric tools to study herbivore-induced volatiles in Myrcia splendens. *Talanta* 2017, *175*, 9-20.

26. Reid, L. M.; O'Donnell, C. P.; Downey, G., Potential of SPME-GC and chemometrics to detect adulteration of soft fruit purees. *Journal of agricultural and food chemistry* 2004, *52* (3), 421-427.

27. Steingass, C. B.; Grauwet, T.; Carle, R., Influence of harvest maturity and fruit logistics on pineapple (Ananas comosus [L.] Merr.) volatiles assessed by headspace solid phase microextraction and gas chromatography-mass spectrometry (HS-SPME-GC/MS). *Food Chem* 2014, *150*, 382-391.

28. Lim, D. K.; Mo, C.; Lee, D. K.; Long, N. P.; Lim, J.; Kwon, S. W., Non-destructive profiling of volatile organic compounds using HS-SPME/GC-MS and its application for the geographical discrimination of white rice. *J Food Drug Anal* 2018, *26* (1), 260-267.

29. Deng, C.; Zhang, X.; Zhu, W.; Qian, J., Investigation of tomato plant defence response to tobacco mosaic virus by determination of methyl salicylate with SPME-capillary GC-MS. *Chromatographia* 2004, *59* (3-4), 263-268.

30. Zeng, J.; Chen, J.; Lin, Z.; Chen, W.; Chen, X.; Wang, X., Development of polymethylphenylsiloxane-coated fiber for solid-phase microextraction and its analytical application of qualitative and semi-quantitative of organochlorine and pyrethroid pesticides in vegetables. *Anal Chim Acta* 2008, *619* (1), 59-66.

31. Menezes Filho, A.; dos Santos, F. N.; Pereira, P. A., Development, validation and application of a methodology based on solid-phase micro extraction followed by gas chromatography coupled to mass spectrometry (SPME/GC-MS) for the determination of pesticide residues in mangoes. *Talanta* 2010, *81* (1-2), 346-354.

32. Dan, Y. B.; Zhang, W. L.; Xue, R. M.; Ma, X. M.; Stephan, C.; Shi, H. L., Characterization of gold nanoparticle uptake by tomato plants using enzymatic extraction followed by single-particle inductively coupled plasma-aass spectrometry analysis. Environ Sci Technol. 2015, 49, 3007-3014.

33. Dan, Y. B.; Ma, X. M.; Zhang, W. L.; Liu, K.; Stephan, C.; Shi, H. L., Single particle ICP-MS method development for the determination of plant uptake and accumulation of CeO2 nanoparticles. *Anal Bioanal Chem*. 2016, 408, 5157-5167.

34. Shirey, R. E.; Linton, C. M., The extraction and analysis of 1,4-dioxane from water using solid-phase microextraction coupled with gas chromatography and gas chromatography-mass spectrometry. *J Chromatogr Sci* 2006, *44* (7), 444-450.

35. Sanchez-Palomo, E.; Diaz-Maroto, M. C.; Perez-Coello, M. S., Rapid determination of volatile compounds in grapes by HS-SPME coupled with GC-MS. Talanta 2005, 66 (5), 1152-1157.

III. FATES OF Au, Ag, ZnO, AND CeO₂ NANOPARTICLES IN SIMULATED GASTRIC FLUID STUDIED USING SINGLE PARTICLE-INDUCTIVELY COUPLED PLASMA-MASS SPECTROMETRY

Xiaolong He[1,2], Haiting, Zhang[1,2], Honglan Shi[1,2,3, *], Wenyan Liu[1,3], Endalkachew Sahle-Demessie[4,*]

[1]Department of Chemistry, Missouri University of Science and Technology, Rolla, MO 65409, USA

[2]Center for Single Nanoparticle, Single Cell, and Single Molecule Monitoring (CS³M), Missouri University of Science and Technology, Rolla, MO, 65409, USA

[3]Center for Research in Energy and Environment, Missouri University of Science and Technology, Rolla, MO, USA

[4]The U.S. Environmental Protection Agency, ORD, CESER, LRTD, 26 W. Martin Luther King Jr. Drive, Cincinnati, OH, 45268, USA

*Corresponding authors
Honglan Shi
honglan@mst.edu
573-341-4433
Endalkachew Sahle-Demessie
Sahle-Demessie.Endalkachew@epa.gov
Tel: +1-513-569-7739

ABSTRACT

The increasing use of engineered nanoparticles (ENPs) in many industries has generated significant research interest regarding their impact on the environment and human health. The major routes of ENPs to enter the human body are inhalation, skin contact, and ingestion. Following ingestion, ENPs have a long contact time in human stomach. Hence, it is essential to know the fate of the ENPs under gastric conditions. This study aims to investigate the fate of the widely used nanoparticles Ag-NP, Au-NP, CeO2-NP, and ZnO-NP in simulated gastric fluid (SGF) under different conditions through the

application of single-particle inductively coupled plasma-mass spectrometry (SP-ICP-MS). The resulting analytical methods have size detection limits for Ag-NP, Au-NP, ZnO-NP, and CeO$_2$-NP, from 15 nm to 35 nm, and the particle concentration detection limit is 135 particles/mL. Metal ions corresponding to the ENPs of interest were detected simultaneously with detection limits from 0.02 to 0.1 µg/L. The results showed that ZnO-NPs dissolved completely and rapidly in SGF, whereas Au-NPs and CeO$_2$-NPs showed apparent aggregation and did not dissolve significantly. Both aggregation and dissolution were observed in Ag-NP samples following exposure to SGF. The size distributions and concentrations of ENPs were affected by the original ENP concentration, ENP size, the contact time in SGF, and temperature. This work represents a significant advancement in the understanding of ENP characteristics under gastric conditions.

Keywords: Nanoparticles, single particle (SP)-ICP-MS, simulated gastric fluid (SGF), ingestion exposure

1. INTRODUCTION

In recent years, the increased use of nanotechnology and nanoenabled consumer products has penetrated every field of science and the economic sector. The increasing value of engineered nanoparticles (ENPs) for various applications has led to a significant increase in their presence in the environment. The emerging utility of ENPs has raised concerns about their potential risks related to human health and the environment.[1] Engineered nanomaterials and nanoagrochemicals could be taken up by plants and accumulate in plant tissues, which provides a potential pathway for entering the food chain, subsequently posing health risks.[2] ENPs are also widely used in the food industry as food

additives for enhancing the texture and color of food, as antimicrobials for improving food preservation in food packaging, and as nutritional supplements. In the pharmaceutical/medical field, ENPs are used as catalysts to make specific drugs, such as potential anticancer agents. These applications could directly increase human exposure to ENPs.[3-6] Many studies imply that exposure to ENPs is strongly correlated to some pathophysiological mechanisms.[7-9] The toxicity of nanoparticles is determined by various factors, such as size, concentration, shape, stability, and agglomeration.[10] While there are a few pathways by which ENPs can enter the body, ingestion is of interest due to the use of ENPs as food additives and in agriculture and pharmaceuticals. Ingested ENPs first pass the digestive system before distributing to the circulatory or lymphatic systems or being removed from the body as waste.[11, 12] The fate of the ENP depends on its characteristics. Therefore, it is necessary to study the aspects of ENPs under gastric conditions.

Nanoparticles of silver (Ag-NPs), gold (Au-NPs), zinc oxide (ZnO-NPs), and cerium oxide (CeO_2-NPs) are the most commonly used metallic ENPs.[7, 13-17] The fates of Au-NPs and CeO_2-NPs in simulated gastric fluid (SGF) have not been investigated, to the best of our knowledge. There are several studies for Ag-NPs and ZnO_2-NPs in gastric conditions,[4, 14, 18-26] and these studies provided very valuable information. However, these previous studies mostly tested limited experimental conditions, such as a single high concentration of ENPs, one specific contact time, as well as one single temperature. More importantly, particle concentration, particle size distribution, and dissolved concentration could not be simultaneously and quantitatively measured in most of these studies due to the limits of experimental methodologies. Thus, the fates of these ENPs under more realistic conditions were not well confirmed.

Single-particle inductively coupled plasma-mass spectrometry (SP-ICP-MS) is a high throughput and ultrasensitive emerging technology for the simultaneous analysis of nanoparticle and metal ion concentrations[27, 28] with size detection limits in the range 10-20 nm for some monoelemental nanoparticles.[29] The results of size distribution experiments with SP-ICP-MS have shown good agreement with scanning electron microscopy (SEM).[30-32] The development of SPICP-MS technology has advanced nanoparticle analysis and is expected to play an increasing role, thereby becoming a standard method for nanoparticle analysis.[28, 32] SP-ICP-MS has been applied to several metal-based ENP analyses in different sample matrices, such as plant tissues, water, animal tissues, etc.[2, 27, 31-41] However, to the best of our knowledge, SP-ICPMS has not been widely applied to the analysis of ENPs in gastric fluid. Therefore, this SP-ICP-MS application for rapid and sensitive tracking of the metal-based ENP fate in gastric fluid represents a useful advancement in the field of ENP analysis.

This study aims to establish SP-ICP-MS methods for characterization and quantification of several broadly used metal-based ENPs, including Ag-NPs, Au-NPs, CeO_2-NPs, and ZnO-NPs, in SGF and systematically investigates the fates of these ENPs in SGF with different contact times, particle sizes, particle concentrations, and exposure temperatures using the state-of-the-art SP-ICP-MS technology. The particle concentrations, size distributions, and concentrations of metal ions were also monitored simultaneously.

2. MATERIALS AND METHODS

2.1. MATERIALS AND REAGENTS

Different sizes (10, 20, 40, 70, and 100 nm) of citrate-stabilized Ag-NPs (0.02 mg/mL) and Au-NPs (10, 15, 20, 30, 40, 50, and 80 nm at a concentration of 0.05 mg/mL) were purchased from nanoComposix (San Diego, CA). These ENPs are spherical with narrow size distributions (coefficient of variation of <15%). ZnO-NPs (<100 nm) were obtained from Sigma-Aldrich (St. Louis, MO). ZnO-NP (80-200 nm) and CeO_2-NPs (30-50 nm, stock suspension of 40% CeO2-NPs in H2O) were purchased from US Research Nanomaterials Inc. (Houston, TX). SEM analysis was carried out to determine the shapes and size distributions of the CeO_2 and ZnO NPs. The SEM images of these ENPs are provided in the Supporting Information (Figures S1 and S2). Ultrahigh purity (MQ) water (18.2 M$\Omega \cdot$cm) was produced by an Elix-3 water purification system from Millipore (Billerica, MA). Hydrochloric acid (HCl) (trace metal grade) and glycine (>99%) were purchased from Fisher Scientific (Fair Lawn, NJ) and Sigma-Aldrich (St. Louis, MO), respectively. Dissolved Au, Ag, Zn, and Ce ions (1000 mg/L) were purchased from High-Purity Standards (Charleston, SC). For the pH value of SGF, the pH of the biological gastric fluid is biologically regulated in a narrow pH range. Other researchers have studied it for Ag-NPs.[26] The SGF in this study was prepared in MQ water with 0.42 mol/L of HCl and 0.40 mol/L of glycine[18, 19] It is a broadly used formula of SGF in the scientific research field. The pH value of the SGF was 1.2, measured with a pH meter.

2.2. SP-ICP-MS METHOD

An ICP-MS (NexION 300/350D, PerkinElmer, Shelton, CT, USA) equipped with Syngistix Single-Particle Application software was used for the single-particle analysis of ENPs in SGF. [197]Au, [107]Ag, [64]Zn, and [140]Ce with natural abundances of 100%, 51.84%, 48.6%, and 88.45%, respectively, were monitored by the SP−ICP−MS. Details of the optimized ICP-MS operating conditions and SP-ICP-MS parameters are shown in Table 1. The 40 nm Au-NP suspension served as a standard to determine the transportation efficiency of the SP-ICP-MS method that was optimized for each batch of samples. Citrate-stabilized Au-NP (10, 15, 20, 30, 40, 50, and 80 nm) and Ag-NP (10, 20, 40, 70, and 100 nm) standards diluted in MQ water were used to test the particle size detection limits under optimal SP-ICP-MS conditions. Dissolved Au and Ag calibration standards at concentrations of 0.1, 0.2, 0.5, 1, 2, 5, 10, and 20 μg/L were also incorporated into the methods to measure the concentrations of corresponding dissolved ions. For ZnONPs and CeO₂-NPs, there were no commercially available ENP standards with relatively narrow size distribution. Therefore, dissolved Zn and Ce calibration curves were used for the determination of dissolved ion concentrations, particle sizes, and particle number concentrations. The dissolved standard SP-ICP-MS signals were converted to the corresponding ENP sizes according to the mass fraction and density of the material.[40, 42] The particle size detection limits of ZnO-NPs and CeO₂-NPs were determined to be five times the standard deviation above the background intensity in MQ water.[28, 29] Equation 1 was employed to measure the particle concentration detection limit (LOD):

$$LOD_{NP} = 3 \times \frac{1}{\eta_{neb} Q_{sam} t_i} \tag{1}$$

where η_{neb} is the nebulization efficiency, Q_{sam} is the sample flow rate, and t_i is the total acquisition time.[43]

Table 1. Optimized ICP-MS operating conditions and SP-ICP-MS method parameters

Optimized ICP-MS operating condition				
nebulizer gas flow (L/min)[a]	1.02			
auxiliary gas flow (L/min)	1.2			
plasma gas flow (L/min)	18			
ICP radio-frequency (RF) power (W)	1600			
analog stage voltage (V)	-1675			
pulse stage voltage (V)	1250			
cell entrance voltage (V)	-6			
cell exit voltage (V)	-6			
cell rod offset	-15			
sampler cones	Platinum			
skimmer cones	Platinum			
sample introduction system	cyclonic spray chamber with a Meinhard nebulizer			
Transport Efficiency (%)[a]	7~9			
SP-ICP-MS method parameters				
Analyte	Au	Ag	Zn	Ce
Mass	197	107	64	140
Dwell time (ms)	0.05	0.05	0.05	0.05
Settling time (ms)	0	0	0	0
Density (g/cm3)	19.3	10.5	5.606	7.215

[a] Parameters optimized daily

The lowest spiked concentration that maintained regression linearity ($R^2 > 0.99$) was set to be the dissolved detection limit of the element. The calibration range of dissolved element ions was set to 0.1-20 μg/L in a single-particle mode of ICP-MS.

2.3. NANOPARTICLES EXPOSURE IN SGF

To test the fates of different ENPs in SGF, each nanoparticle sample was prepared in the SGF at 1, 10, and 100 μg/L in ICP-MS individual autosampler tube, followed by incubation in a water bath shaker (120 rpm)[44] at 23 or 37 °C for different time periods (from 0 to 360 min). The same experiments were conducted for all the ENPs. Control samples were conducted in parallel with the equal amounts of ENPs spiked into Milli-Q (MQ) water. At the selected contact times (at the beginning of spiking (about 2 min), 15, 30, 60, 120, and 360 min), samples were collected and diluted appropriately (to approximately 10^5 ENPs/mL or lower) with MQ water and subsequently analyzed by SP-ICP-MS. MQ water was used as a dilution solvent because all the NPs studied in this paper are stable in MQ water in the selected concentration ranges, except ZnO-NPs. The dilution factor and the matrix effect were also tested for different dilution factors (1, 5, 10, 50, 100, 500, and 1000 depending on the initial concentration) for SP-ICP-MS analysis. The results showed that the initial concentrations of dissolved ions and nanoparticles are basically the same in specific ranges of dilution factors except for ZnO-NPs, which dissolve quickly in SGF. We selected these ranges of the dilution factors for the NPs analyses .

3. RESULTS AND DISCUSSIONS

3.1. SP-ICP-MS METHOD PERFORMANCE

The size detection limits for Au-NPs and Ag-NPs were determined by analyzing ENP standard suspensions of Au-NPs at 10, 15, 20, 30, 40, 50, and 80 nm and Ag-NPs at 10, 20, 40, 70, and 100 nm. The ICP-MS response intensities of Au-NPs vis size were linear from 15 to 80 nm, whereas for Ag-NPs, the linear range was from 20 to 100 nm.

Therefore, the size detection limits for AuNPs and Ag-NPs were determined to be 15 and 20 nm. The particle concentration detection limits of the Au-NPs, Ag-NPs, and CeO2-NPs were estimated on the basis of the published method[43] to be ∼135 NPs/mL. However, due to the rapid dissolution of ZnO-NPs in MQ water and SGF, the data shows that the detection limit for the particle number concentration could not be measured accurately. The particle size detection limits of CeO_2-NP and ZnO-NP were determined to be 25 and 35 nm, respectively, by the same way of our previously published method.[31] The particle size detection limits, particle concentration detection limits, and dissolved ions concentration detection limits determined using SP-ICP-MS are shown in Table 2.

Table 2. Detection limits of different ENPs

particle ID	detection limits		
	size (nm)	particle concentration (particles/mL)	dissolved ion (µg/L)
Ag-NPs	20	135	0.05
Au-NPs	15	135	0.05
CeO_2-NPs	25	135	0.02
ZnO-NPs	35	N/A[a]	0.1

[a] N/A means not available.

3.2. FATE OF Ag-NPS IN SGF

The fates of Ag-NPs (40 and 70 nm) at concentrations (1, 10, and 100 µg/L) in SGF were monitored for over 6 h at 23 and 37 °C. The corresponding controls were conducted in filtered deionized MQ water. Figure 1a shows that Ag-NP particle concentrations did not change significantly for the 6 h of contact time in the water at 23 °C, which was also confirmed by the stable size distributions of Ag-NPs shown in Figures S3a-c and S4a-c.

Ag-NPs in MQ water at 37 °C also exhibited similar stability from the beginning to 6 h of contact time (data is not shown here). At a low concentration of 1 μg/L Ag-NPs, both 40 and 70 nm Ag-NP particle concentrations decreased rapidly to below size detection limit within 15 min in SGF. This decrease was due to the dissolution, as confirmed by the increased concentration of dissolved Ag+ ion shown in Table 3. Figure 1b illustrates the decrease of particle concentration with contact time for 40 nm Ag-NPs at a concentration of 10 μg/L. Figure 1c shows profiles of 40 nm Ag-NPs in SGF at a high concentration of 100 μg/L. The particle concentrations decreased slower when the concentration is higher. The particles were still present in the samples up to 6 h of contact time. Similarly, Figure 1d and 1e represent the profiles of 70 nm Ag-NPs in SGF. At 10 μg/L, the particle concentration decreased with time and all dissolved in 2 h at a decreasing rate lower than that of 40 nm Ag-NPs at the same mass concentration. For high concentrations (100 μg/L) of 70 nm Ag-NPs in SGF, the particle concentration decreased first and then slowed down. Comparing the Ag-NPs profiles based on their particle sizes, the smaller Ag-NPs dissolved faster than the larger ones under the same condition, as expected. A possible reason is that the higher specific surface area of the smaller AgNP contributes to a higher dissolution/reaction rate in SGF. Moreover, analysis of obtained data suggests that the particles dissolve/react faster at body temperature (37 °C) than at room temperature (23 ° C) from Figure 1, indicating that temperature also has a significant impact on the fate of Ag-NPs in SGF.

Figure 2 shows the change of the most frequent size and mean size of Ag-NPs at 100 μg/L in MQ water and SGF at time intervals of 2, 15, 30, 60, 120, and 360 min. It is
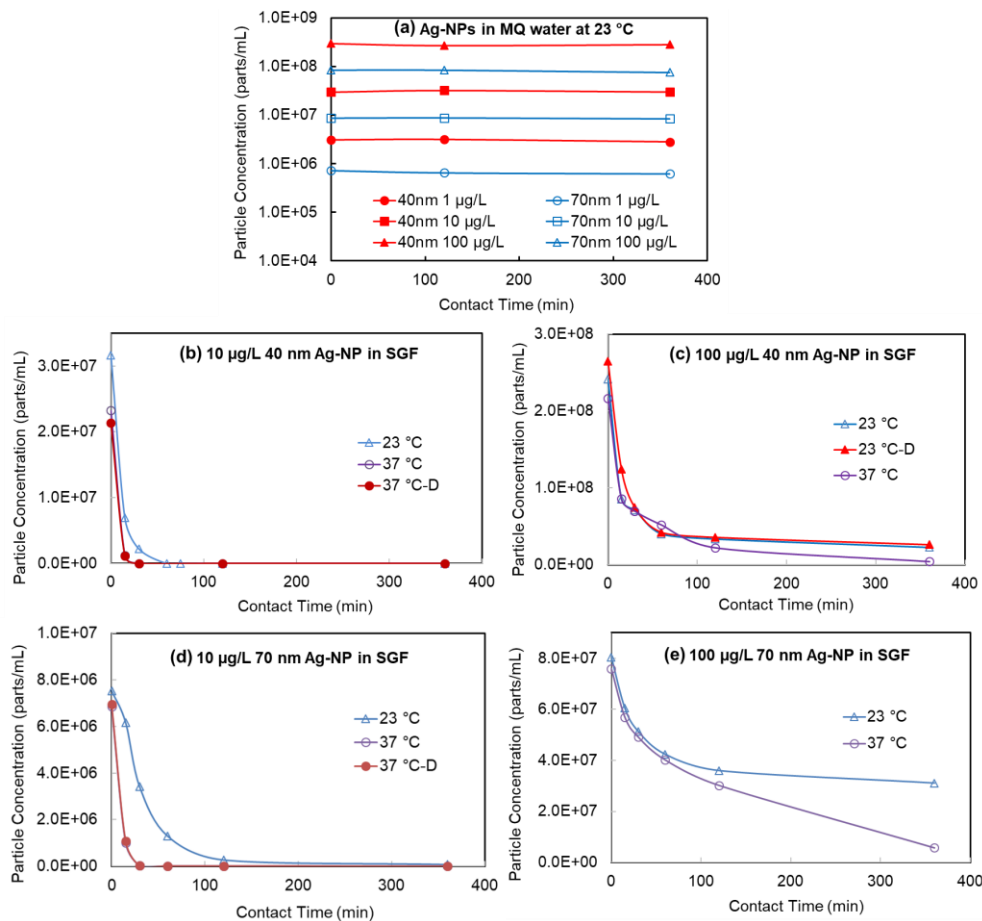
Figure 1. Particle concentration profiles of Ag-NPs with time in MQ and SGF at different temperatures. -D means duplicate sample. The samples were diluted appropriately at the time of SP-ICP-MS analysis, and the concentrations were before the dilutions

worth noting that, though the samples were analyzed immediately after mixing well, the mixing and analysis take roughly 2 min. Thus, the first data point was at time 2 min contact time, not at 0 min. The control tests where ENPs were spiked in MQ water indicated that the size distributions of Ag-NPs remained stable for both 40 and 70 nm Ag-NPs during the 6 h tested period (Figures S3a-c and S4a-c). However, the size distributions of Ag-NPs changed significantly in SGF during the test, implicating SGF as a causative factor in the decreasing signal. The Ag-NPs dissolved very rapidly at a low concentration of 1

μg/L for both 40 and 70 nm Ag-NPs in SGF at 23 and 37 °C. As a result, the histograms at this concentration could not be reliably measured. The size distribution histograms of spiked 40 nm Ag-NPs at a concentration of 10 μg/L in SGF at 23 and 37 °C are shown in Figure S3d, f, which indicate that the most common particle size decreased with exposure time. When high concentration (100 μg/L) 40 nm Ag-NPs were spiked in SGF at 23 °C, the most frequent size of the particles increased rapidly from 47 nm at the beginning of dosing (about 2 min) to 62 nm within 60 min and then stayed the same until 6 h tested (Figure 2a). This indicated that the aggregation of the Ag-NP likely occurred at a high concentration at room temperature, which could contribute to the rapid decreasing of the particle concentration during the early contact time. Additionally, Figure 2a shows that the most frequent size AgNPs increased from 21 to 50 nm first and then decreased to 35 nm in SGF at the temperature of 37 °C. The mean size of 40 nm Ag-NPs spiked at a concentration of 100 μg/L in SGF at 37 °C was smaller than those incubated at 23°C, as also shown in Figure 2b. The fate of Ag-NPs in a biological system is complicated by different factors. Liu *et al.*[45] also referred that the dissolution and aggregation of Ag-NPs is a complicated dynamic process that was influenced by particle size, concentration, surface coating material, and exposure environment. For 70 nm Ag-NP, the most frequent particle size decreased with time for the 10 μg/L 70 nm Ag-NP in SGF at 23 and 37 °C, as shown in Figure S4d, f. However, the most frequent and mean sizes increased when spiked 100 μg/L 70 nm Ag-NP in SGF at 23 and 37 °C. The most frequent and mean size of 70 nm Ag-NPs at 37 °C were slightly lower than at 23 °C, as shown in Figure 2c, d.

The rate of dissolution of the Ag-NPs spiked into SGF at body temperature (37 °C) was rapid at the beginning of the exposure and then slowed down. This phenomenon was likely attributed to the fact that the dissolved Ag^+ ions reacted with the chloride in SGF to form AgCl precipitation on the surface of the Ag-NPs or as separate AgCl particles, due to the low K_{sp} value of AgCl and high Cl^- concentration in solution.[46] A similar phenomenon was found and explained when Ag-NPs were exposed to highly acidic conditions (pH 2) in other publications.[19, 26] At a longer contact time, the particles might also redistribute, making more change in the Ag-NPs, together with AgCl. Mwilu *et al.*[18] observed that the size of Ag-NPs increased significantly after spiking a high concentration (2 mg/L) of 10 and 75 nm Ag-NPs into SGF for up to 30 min. However, Walczak *et al.*[20] reported that the size of Ag-NPs decreased from 60 nm to 20-30 nm after spiking 60 nm AgNPs (500 µg/L) into SGF for 2 h without reporting the shorter exposure time. In this study, Figure 2 shows the fate profiles of Ag-NPs with different exposure times in the SGF from the beginning to 6 h, which is the longest possible exposure time in the stomach.

The concentrations of Ag^+ tend to increase from the initial spiking to 6 h in all suspensions (Table 3), which indicates that both 40 and 70 nm Ag-NPs dissolved in SGF. At concentrations of 1 and 10 µg/L, all the Ag-NPs were dissolved within 15 and 120 min. Correspondingly, the detected Ag^+ ion concentration is about equivalent to Ag-NPs concentrations of 1 and 10 µg/L. At a high concentration (100 µg/L) of Ag-NPs, the situation is more complex. Ag^+ ion concentration increased initially and then slowed down and only slightly increased from 1 to 6 h of exposure. The temperature of SGF in all previous studies was set at 37 °C, based on a basic understanding of human physiology. However, Bekkby *et al.*[47] and Bateman[48] showed that the gastric fluid temperature is

affected by the temperature and volume of ingested meals. This study showed that temperature played a vital role in the fate of Ag-NPs in SGF. Both the most frequent and mean size of Ag-NPs are smaller at 37 °C than at 23 °C. At the same time, the dissolved Ag concentration reached 78.61 μg/L after 6 h for 40 nm Ag-NPs and 70.54 μg/L for 70 nm Ag-NP at 37 °C. Lower dissolved Ag was observed at 23 °C and 54.96 and 43.93 μg/L for 40 and 70 nm Ag-NPs, respectably, at 6 h of exposure time. The actual Ag^+ ion concentration might be lower than the detected concentrations because, if AgCl particles were formed at sizes smaller than the size detection limit of Ag-NP, they would also be identified as "dissolved" Ag. Due to the limitation of the SP-ICP-MS technology, it detects metal in particulate form but cannot distinguish the different chemical species and the exact types of particles, thus the actual form of the Ag is not clear. Therefore, the Ag-NPs determined by SP-ICP-MS in this study should be Ag-NPs and other silver-containing NPs. It has been reported that that Ag-NPs may convert to Ag_2S during water treatment and AgCl in SGF.[19, 49] Furthermore, the detected particle concentration in SGF might also be influenced by aggregation and redistribution of the particles. Therefore, the fate of AgNPs in SGF appeared to be affected by multiple factors, including particle size, initial mass concentration, temperature, reaction with a component of SGF, dissolution, aggregation, particle redistribution, and possibly more. The particle surface coating may be another factor that affects the fate of the particles. For example, Axson *et al.*[26] found that the citrate-coated Ag-NPs aggregate more than the PVP Ag-NPs after 17 min exposure to SGF at pH 2. Thus, the fate of Ag-NPs in the gastric system is a complex process that warrants further study.
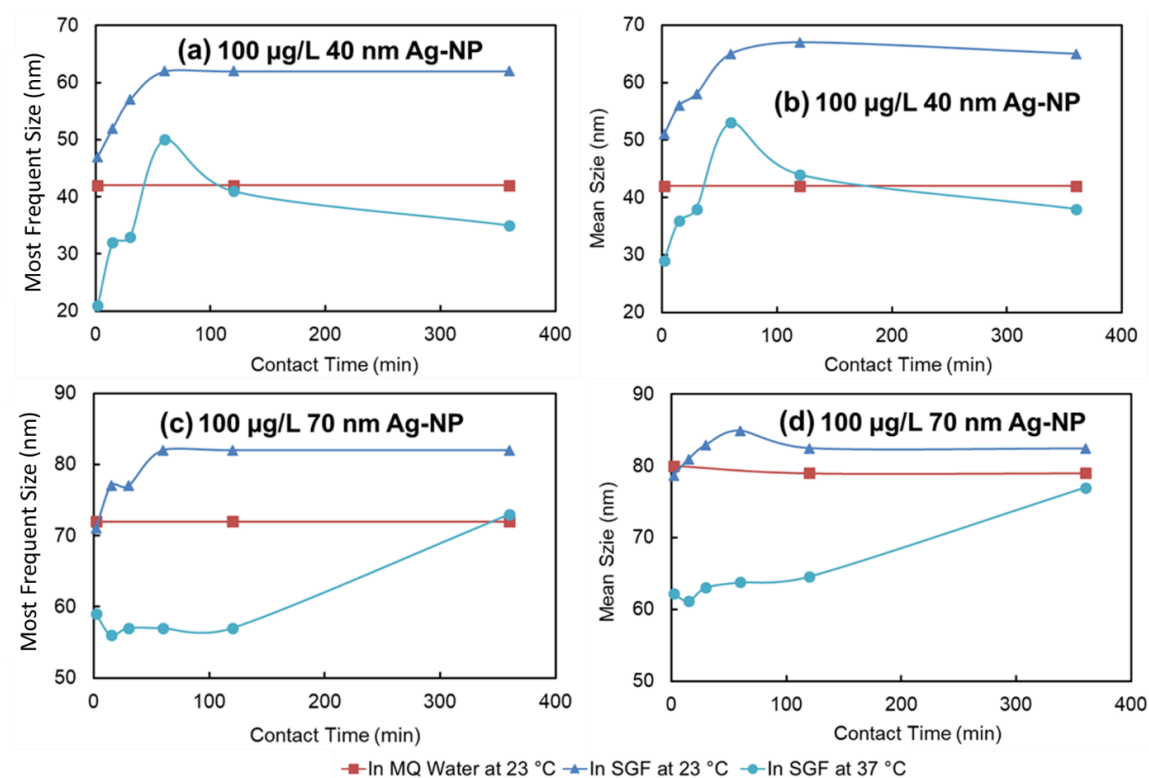
Figure 2. Most frequent size and mean size profiles of 100 µg/L Ag-NPs in MQ water and SGF with time

3.3. FATE OF Au-NPs IN SGF

The fates of 40 and 80 nm AuNPs in SGF with different initial concentrations were studied using SP-ICP-MS. The changes in particle concentrations and the most frequent and mean sizes of Au-NPs are shown in Figures 3 and 4. All suspensions of Au-NPs in MQ water at 23 °C show no change in either particle concentration (Figure 3a) or the size distribution histograms (Figures S5a-c and S6a-c). The same result was observed at 37 °C (data are not shown here). For the 40 nm Au-NPs, the particle concentrations decreased during incubation in SGF at 23 and 37 °C with all concentrations of 1, 10, and 100 µg/L.

Table 3. Dissolved metal ion concentration in MQ water and SGF at different contact times[a]

.nanoparticle species	contact time	dissolved metal ion concentration (µg/L)								
		in MQ Water at 23 °C			in SGF at 23 °C			in SGF at 37 °C		
		1 µg/L[b]	10 µg/L	100 µg/L	1 µg/L	10 µg/L	100 µg/L	1 µg/L	10 µg/L	100 µg/L
40 nm Ag-NP	2 min	<LOD[c]	<LOD	<LOD	0.60	5.77	28.78	0.66	6.14	39.89
	15 min	<LOD	<LOD	<LOD	0.75	8.07	28.96	0.99	8.42	42.76
	30 min	<LOD	<LOD	<LOD	1.00	8.46	29.37	1.02	11.07	45.75
	60 min	<LOD	<LOD	<LOD	0.92	9.77	36.98	1.04	10.61	74.79
	120 min	<LOD	<LOD	<LOD	0.94	10.04	37.81	0.97	11.24	75.96
	360 min	<LOD	<LOD	<LOD	0.99	10.64	54.96	0.94	11.38	78.61
70 nm Ag-NP	2 min	<LOD	<LOD	<LOD	0.45	3.1	19.33	0.51	4.32	25.76
	15 min	<LOD	<LOD	<LOD	0.75	6.47	23.77	0.99	9.95	43.22
	30 min	<LOD	<LOD	<LOD	1.07	8.87	27.64	1.03	10.16	46.40
	60 min	<LOD	<LOD	<LOD	1.11	9.44	29.31	1.11	11.40	46.95
	120 min	<LOD	<LOD	<LOD	1.05	11.18	29.51	1.10	11.16	50.26
	360 min	<LOD	<LOD	<LOD	1.04	11.21	43.93	1.14	11.75	70.54
40 nm Au-NP	2 min	<LOD	<LOD	<LOD	<LOD	<LOD	<LOD	<LOD	<LOD	<LOD
	360 min	<LOD	<LOD	<LOD	<LOD	<LOD	<LOD	<LOD	<LOD	<LOD
80 nm Au-NP	2 min	<LOD	<LOD	<LOD	<LOD	<LOD	<LOD	<LOD	<LOD	<LOD
	360 min	<LOD	<LOD	<LOD	<LOD	<LOD	<LOD	<LOD	<LOD	<LOD
30-50 nm CeO$_2$-NP	2 min	<LOD	<LOD	<LOD	<LOD	<LOD	<LOD	<LOD	<LOD	<LOD
	360 min	<LOD	<LOD	<LOD	<LOD	<LOD	<LOD	<LOD	<LOD	<LOD
<100 nm ZnO-NP	2 min	0.79	7.78	54.00	1.17	9.08	84.21	1.13	11.50	113.64
	120 min	0.88	8.36	80.70	1.15	9.33	97.35	1.07	11.40	103.61
	360 min	1.09	10.64	98.26	1.15	9.53	99.22	1.14	11.67	110.39
80-200 nm ZnO-NP	2 min	0.82	3.71	45.15	1.10	11.03	114.04	NA[d]	NA	NA
	120 min	1.13	5.19	60.85	1.13	11.21	112.27	NA	NA	NA
	360 min	1.18	7.85	73.49	1.09	11.27	115.62	NA	NA	NA

[a]Note: For Au- and CeO$_2$-NPs, all the measured dissolved concentrations at different contact times (2, 15, 30, 60, 120, 360 min) are lower than the detection limits. ZnO-NPs dissolve rapidly in SGF in a couple of minutes. Partial data are presented in the table. [b]Dosing concentration of ENPs into MQ water and SGF. [c]LOD means limit of detection of dissolved ions, which is shown in Table 2. [d]NA means not analyze.

The rate of decrease in the particle concentration was inversely dependent on the initial particle concentration (Figure 3b, c). Parts a and b of Figure 4 show that both the most frequent and mean size of the 40 nm Au-NPs increased more at 100 µg/L than at 10 or 1 µg/L, indicating that the particles tend to aggregate at a higher concentration.

Additionally, the results tested at temperatures of 23 and 37 °C did not affect the fate of 40 nm Au-NPs in SGF at the spiked concentration of 1 µg/L. However, at higher concentrations of 10 and 100 µg/L, increased temperatures enhanced aggregation rates.
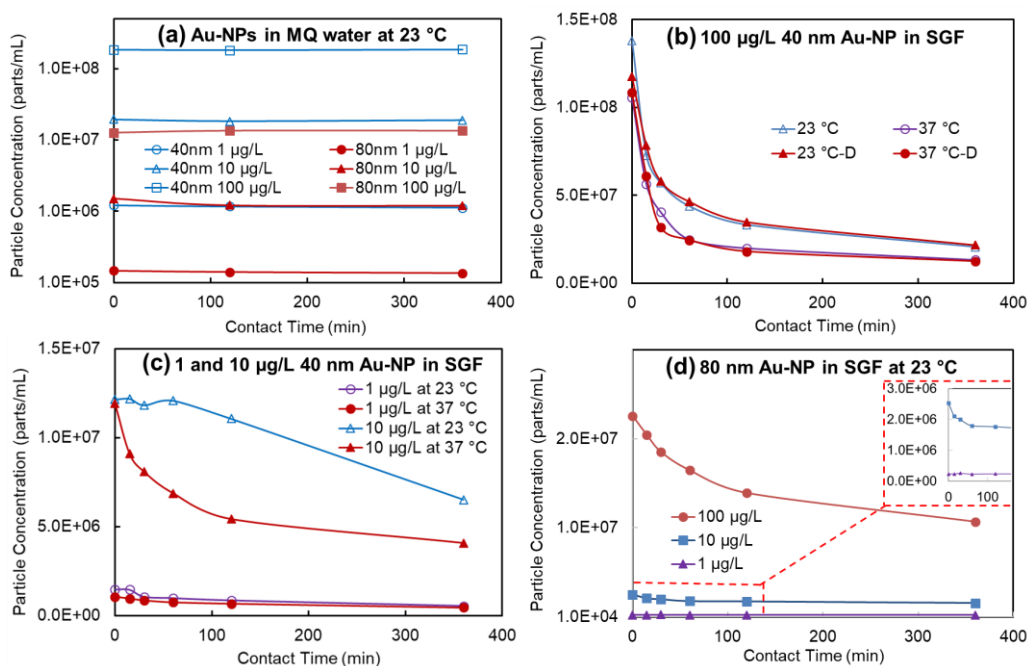
Figure 3. Particle concentration profiles of Au-NPs with time in MQ and SGF at different temperatures. -D means duplicate sample. The samples were diluted appropriately at the time of SP-ICP-MS analysis, and the concentrations were before the dilutions

A similar trend was observed for the 80 nm Au-NPs (Figures 3d and 4c, d). The rate of decrease in the particle concentration was inversely dependent on the initial particle concentration, and aggregation was positively dependent on the initial particle concentration. However, the concentration of the 80 nm Au-NPs decreased at a slower rate, and the most frequent and the mean particle sizes increased at a slower rate than the 40 nm Au-NPs at the same concentration. The size, initial spike concentration, and temperature of the particles play a significant role in the aggregation of Au-NPs in SGF. No dissolved

Au was detected in any suspensions during the experiment, as shown in Table 3, which indicates that no dissolution of Au-NPs occurred in SGF. The Au-NPs size increased while their particle concentration decreased, indicating that the reduced concentration was solely due to the aggregation of Au-NPs in SGF.
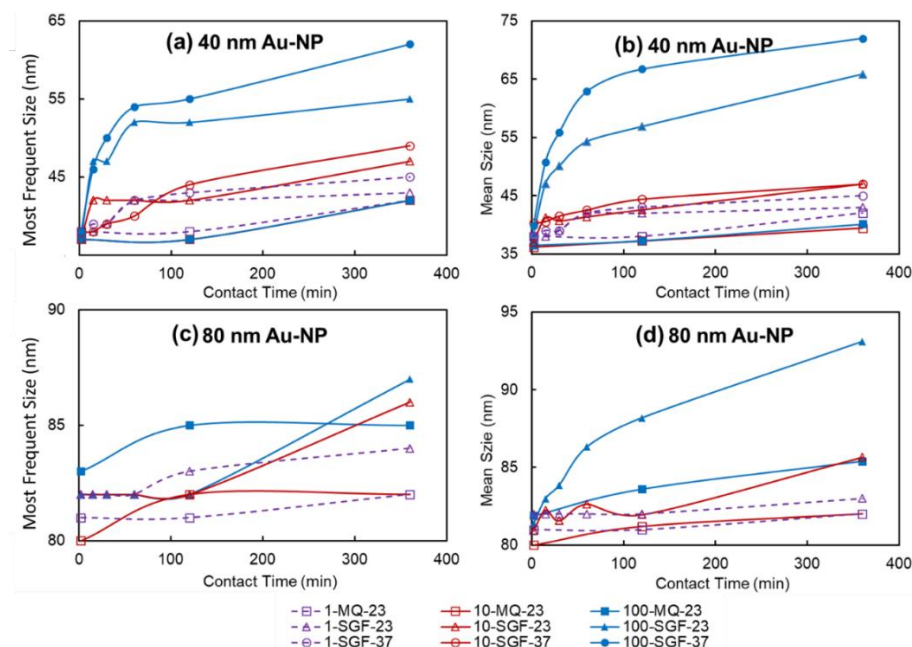
Figure 4. Most frequent size and mean size profiles of Au-NPs in MQ water and SGF with time. (Note: First number in the labels represents Au-NP concentration, second number represents temperature of SGF)

3.4. FATE OF CeO$_2$-NPs IN SGF

The fate of CeO$_2$-NPs in SGF was studied using CeO$_2$-NPs (30-50 nm, a SEM image is shown in Figure S1). These ENPs were spiked into SGF at concentrations of 1, 10, and 100 μg/L CeO$_2$-NPs (calculated Ce element concentration), incubated at 23 or 37 °C for different times, and samples were collected at the set time and analyzed by SP-ICP-MS. In MQ water, the particle concentrations of CeO$_2$-NPs did not change over extended

periods at different concentrations and particle sizes (Figure 5a). When spiked these different concentrations of CeO$_2$-NPs in SGF, the particle concentration profiles versus contact time are shown in Figure 5b-d. The particle concentration decreased only slightly for mass concentrations of 1 and 10 µg/L CeO$_2$-NPs. However, the particle concentration rapidly reduced for the high concentration of 100 µg/L, with a more than 50% decrease in
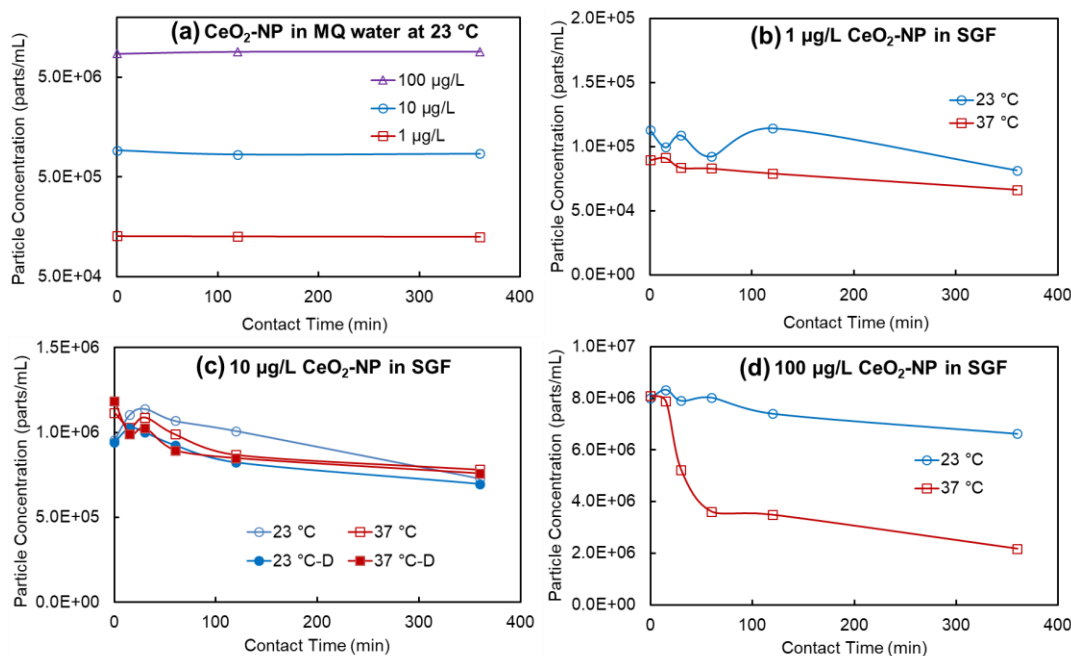
Figure 5. Particle concentration profiles of 30-50 nm CeO$_2$-NPs with time in MQ and SGF at different temperature. -D means duplicate sample. The samples were diluted appropriately at the time of SP-ICP-MS analysis, and the concentrations were before the dilutions

the first 60 min at 37 °C, while there was only a slight decrease at 23 °C. Figure 6 shows the changes in the mean and most frequent particle sizes of CeO$_2$-NPs in MQ water and SGF. The mode and the mean particle sizes did not change significantly at low mass concentrations of 1 and 10 µg/L. But, the mode and the mean particle sizes of CeO2-NPs increased significantly for 100 µg/L at body temperature (37 °C), while remaining stable

at 23 °C (Figure 6). The dissolved Ce concentration was below the detection limit in all suspensions (Table 3). These results concluded that CeO_2- NPs are stable in SGF at low concentrations but aggregate at a high concentration at body temperature. It has been proven that some redox reactive elements, such Fe^{2+} and Mn^{2+}, react with CeO_2-NPs and produce dissolved Ce^{3+} after being absorbed on the surface of CeO_2-NPs.[50, 51] In addition, the redox action of CeO_2-NPs can be more complicated when CeO_2-NPs absorbed the polymers and Fe^{2+}. These reactions have a significant impact on the fate, transport, and toxicity of CeO_2-NPs.[50, 51] Therefore, the biological gastric fluid with unique redox properties,[52] which may affect the fate of CeO_2- NPs, deserves further study. Again, SP-ICP-MS has limited capability to distinguish species of Ce, and ion chromatography in combination with ICP-MS may be applied to the further study fate of CeO_2-NPs, in biological gastric fluid.
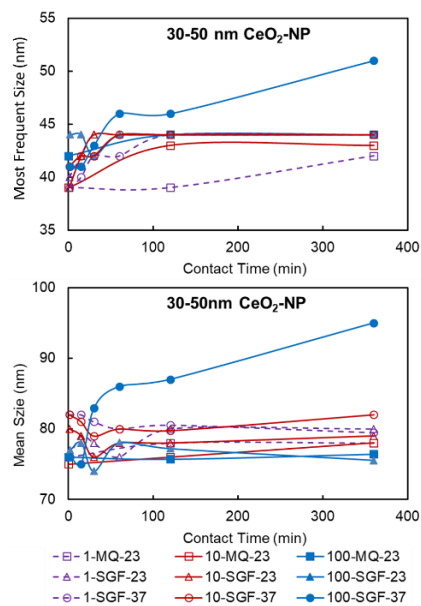
Figure 6. Most frequent size and mean size profiles of 30-50 nm CeO_2-NPs in MQ water and SGF with time (Note: First number in the labels represents CeO_2-NP concentration, the second number represents temperature of SGF.)

3.5. FATE OF ZnO-NPs IN SGF

The fate of ZnO-NPs in SGF was investigated for two different particle size ranges, one with a manufacture specified size less than 100 nm and the other one with a product specified size 80-200 nm. The SEM images of both types of ZnO-NPs show the irregular shape and broad range of particle size distributions (Figure S2). SP-ICP-MS experiments were performed by spiking selected concentrations of 1, 10, and 100 μg/L ZnO-NPs (calculated Zn element concentration) into MQ water and SGF, and then, samples were collected and analyzed at different contact times. The particle concentrations decreased very rapidly with time. Thus, the reliable particle concentration, particle size, and size distribution histogram could not be obtained with this technique due to such rapid dissolution of this ENP. Table 3 shows dissolved Zn concentrations at 2 and 360 min contact times. In MQ water, most of the ZnO-NPs at low concentration dissolved quickly within 2 min contact time and about 50% dissolved at a high concentration of 100 μg/L. Larger sized ZnO-NPs dissolved slower than the smaller sized ones. In SGF, all the ZnO-NPs dissolved quickly and all dissolved within 2 min of contact time (during mixing and SP-ICP-MS analysis). At high concentration (100 μg/L), ZnO-NPs appeared to dissolve faster at body temperature (37 °C) (113.6 μg/L dissolved Zn) than at room temperature (23 °C) (84.21 μg/L). However, these dissolution differences compared with the real concentration (100 μg/L) might not be significant enough to make this conclusion. Other researchers have also reported the complete dissolution of ZnO-NPs in the gastric system or under low pH fluid.[4, 21, 23] Therefore, our experimental results in this study confirmed that ZnO-NPs dissolved very rapidly under gastric pH.

Because biological gastric fluid has more complicated compositions and unique properties, it will be interesting to study real biological gastric systems, such as using an animal study and evaluating the fates of the nanoparticles in the real biological gastric system. However, SP-ICP-MS is a powerful tool for nanoanalysis with advantages of high performance for detecting, characterizing, and quantifying nanoparticles. The limitations of SP-ICP-MS on the exact form of NPs and chemical species determination make it necessary to combine with the other technologies, such as ion chromatography-ICPMS and field flow fractionation-ICP-MS, for a more comprehensive study of a real biological system.

4. CONCLUSIONS

We have developed and validated sensitive and selective SPICP-MS methods capable of analyzing particle concentration, size, size distribution, aggregation, and dissolution for four types of broadly used ENPs. The fates of these ENPs in SGF are investigated systemically with the new methods. The experimental results indicated that particle size, initial concentration, and temperature all played significant roles in the fates of these nanoparticles when exposed to SGF. For Ag-NPs, the alterations of particle concentration, size distribution, and dissolved Ag concentration were affected by the initial concentration, particle size, and temperature. The Ag-NPs, and/or another form of particulate Ag, are still present at up to 6 h of contact time. The original chemical form of the particulate Ag could not be confirmed by the SP-ICP-MS method, and there is a desire to further study by combination with other technology. Au-NPs are stable at low concentrations and progressively aggregated with increasing concentrations. No dissolved

Au ions were found at or the above detection limit, which confirmed that Au-NPs were present in the gastric system as Au-NPs particulates form without dissolution. The CeO$_2$-NPs in SGF is stable at low concentrations and aggregate at high concentrations only at body temperature (37 °C). These particles also do not dissolve in SGF. On the contrary, ZnO-NPs behave differently from the other three types of ENPs in this study. They dissolved very quickly in SGF. Thus, Zn-NPs do not present in particulate form in the gastric system and should not get into other biological fluids and organs after intake through food and drink.

This study adds to the growing knowledge of the fates of ENPs under conditions that simulate the human stomach. The fates of different nanoparticles after exposure to a simulated human digestion system is highly relevant to understanding the impact of ENPs overall as they become more integrated into daily life, potentially resulting in increased exposures. Various factors such as species, size, the concentration of ingested ENPs, and body temperature on the fates of nanoparticles in the human digestion system proved to be varied and complex. This research highlights the need for a better understanding of nanomaterials' properties in the digestive system under other physiologically relevant conditions. This work contributes to an improved understanding of the fates of ENPs in gastric fluid, which gives insights into the gastrointestinal uptake of these ENPs before they enter into the blood circulation and organ systems. It is especially crucial for nanoparticles not completely solubilized in the digestive system's physiological contact time because these ENPs will enter into the other body systems and potentially circulate through the body as particulates. Using this study framework, sequentially studying in other tissues, especially for those ENPs not dissolved in SGF, including Ag-NPs, Au-NPs,

and CeO$_2$-NPs, would be valuable to evaluate the potential risk of ENPs to human health.

ACKNOWLEDGEMENT

REFERENCES

(1)   Laborda, F.; Bolea, E.; Cepria, G.; Gomez, M. T.; Jimenez, M. S.; Perez-Arantegui, J.; Castillo, J. R. Detection, characterization and quantification of inorganic engineered nanomaterials: A review of techniques and methodological approaches for the analysis of complex samples. *Anal Chim Acta*. **2016**, 904, 10-32.

(2)   Dan, Y. B.; Zhang, W. L.; Xue, R. M.; Ma, X. M.; Stephan, C.; Shi, H. L. Characterization of gold nanoparticle uptake by tomato plants using enzymatic extraction followed by single-particle inductively coupled plasma-aass spectrometry analysis. *Environ Sci Technol*. **2015**, 49, 3007-3014.

(3)   Sohal, I. S.; O'Fallon, K. S.; Gaines, P.; Demokritou, P.; Bello, D. Ingested engineered nanomaterials: state of science in nanotoxicity testing and future research needs. *Part Fibre Toxicol*. **2018**, 15:29.

(4)   Sohal, I. S.; Cho, Y. K.; O'Fallon, K. S.; Gaines, P.; Demokritou, P.; Bello, D. Dissolution behavior and biodurability of ingested engineered nanomaterials in the gastrointestinal environment. *Acs Nano*. **2018**, 12, 8115-8128.

(5)   Mei, W.; Wu, Q. Applications of metal nanoparticles in medicine/metal nanoparticles as anticancer agents. *Metal Nanoparticles: Synthesis and Applications in Pharmaceutical Sciences*. Wiley-VCH, New Jersey, **2018**. Chapter 7, pages 169-190.

(6)   Harish, K.; Nagasamy, V.; Himangshu, B.; Anuttam, K. Metallic nanoparticle: a review. *Biomedical Journal of Scientific & Technical Research*. **2018**, 4, 3765-3775.

(7)   Li, C. H.; Shen, C. C.; Cheng, Y. W.; Huang, S. H.; Wu, C. C.; Kao, C. C.; Liao, J. W.; Kang, J. J. Organ biodistribution, clearance, and genotoxicity of orally administered zinc oxide nanoparticles in mice. *Nanotoxicology*. **2012**, 6, 746-756.

(8)   Dufour, E. K.; Kumaravel, T.; Nohynek, G. J.; Kirkland, D.; Toutain, H. Clastogenicity, photo-clastogenicity or pseudo-photo-clastogenicity: Genotoxic effects of zinc oxide in the dark, in pre-irradiated or simultaneously irradiated Chinese hamster ovary cells. *Mutat Res*. **2006**, 607, 215-224.

(9)   Hackenberg, S.; Scherzed, A.; Technau, A.; Kessler, M.; Froelich, K.; Ginzkey, C.; Koehler, C.; Burghartz, M.; Hagen, R.; Kleinsasser, N. Cytotoxic, genotoxic and pro-inflammatory effects of zinc oxide nanoparticles in human nasal mucosa cells in vitro. *Toxicol In Vitro*. **2011**, 25, 657-663.

(10)   Sajid, M.; Ilyas, M.; Basheer, C.; Tariq, M.; Daud, M.; Baig, N.; Shehzad, F. Impact of nanoparticles on human and environment: review of toxicity factors, exposures, control strategies, and future prospects. *Environ Sci Pollut Res Int*. **2015**, 22, 4122-4143.

(11)   Williams, K. M.; Gokulan, K.; Cerniglia, C. E.; Khare, S. Size and dose dependent effects of silver nanoparticle exposure on intestinal permeability in an in vitro model of the human gut epithelium. *J Nanobiotechnology*. **2016**, 14:62. DOI 10.1186/s12951-016-0214-9

(12)   Lichtenstein, D.; Ebmeyer, J.; Knappe, P.; Juling, S.; Bohmert, L.; Selve, S.; Niemann, B.; Braeuning, A.; Thunemann, A. F.; Lampen, A. Impact of food components during in vitro digestion of silver nanoparticles on cellular uptake and cytotoxicity in intestinal cells. *Biol Chem*. **2015**, 396, 1255-1264.

(13)   Smolkova, B.; El Yamani, N.; Collins, A. R.; Gutleb, A. C.; Dusinska, M. Nanoparticles in food. Epigenetic changes induced by nanomaterials and possible impact on health. *Food Chem Toxicol*. **2015**, 77, 64-73.

(14)   Wu, W.; Zhang, R.; McClements, D. J.; Chefetz, B.; Polubesova, T.; Xing, B. Transformation and speciation analysis of silver nanoparticles of dietary supplement in simulated human gastrointestinal tract. *Environ Sci Technol*. **2018**, 52, 8792-8800.

(15)   Liu, Q.; Zhou, Q.; Jiang, G. Nanomaterials for analysis and monitoring of emerging chemical pollutants. Trends in Analytical Chemistry. 2014, 58, 10-22.

(16)   Corma, A.; Atienzar, P.; Garcia, H.; Chane-Ching, J. Y. Hierarchically mesostructured doped CeO2 with potential for solar-cell use. *Nat Mater*. **2004**, 3, 394-397.

(17)   Kosynkin, V.; Arzgatkina, A.; Ivanov, E.; Chtoutsa, M.; Grabko, A.; Kardapolov, A.; Sysina, N. The study of process production of polishing powder based on cerium dioxide. *Journal of Alloys and Compounds*. **2000**, 303, 421-425.

(18)   Mwilu, S. K.; El Badawy, A. M.; Bradham, K.; Nelson, C.; Thomas, D.; Scheckel, K. G.; Tolaymat, T.; Ma, L. Z.; Rogers, K. R. Changes in silver nanoparticles exposed to human synthetic stomach fluid: Effects of particle size and surface chemistry. *Sci Total Environ*. **2013**, 447, 90-98.

(19)   Rogers, K. R.; Bradham, K.; Tolaymat, T.; Thomas, D. Alterations in physical state of silver nanoparticles exposed to synthetic human stomach fluid. *Sci Total Environ*. **2012**, 420, 334-339.

(20)   Walczak, A. P.; Fokkink, R.; Peters, R.; Tromp, P.; Rivera, Z. E. H.; Rietjens, I. M. C. M.; Hendriksen, P. J. M.; Bouwmeester, H. Behaviour of silver nanoparticles and silver ions in an in vitro human gastrointestinal digestion model. *Nanotoxicology*. **2013**, 7, 1198-1210.

(21)   Cho, W. S.; Kang, B.-C.; Lee, J. K.; Jeong, J.; Che, J.-H.; Seok, S. H. Comparative absorption, distribution, and excretion of titanium dioxide and zinc oxide nanoparticles after repeated oral administration. *Part Fibre Toxicol*. **2013**, 10(1):9. https://doi.org/10.1186/1743-8977-10-9

(22)   Böhmert, L.; Girod, M.; Hansen, U.; Maul, R.; Knappe, P.; Niemann, B.; Weidner, S. M.; Thünemann, A. F.; Lampen, A. Analytically monitored digestion of silver nanoparticles and their toxicity on human intestinal cells. *Nanotoxicology*. **2014**, 8, 631-642.

(23)   Gomez-Gomez, B.; Perez-Corona, M. T.; Madrid, Y. Using single-particle ICP-MS for unravelling the effect of type of food on the physicochemical properties and gastrointestinal stability of ZnONPs released from packaging materials. *Anal Chim Acta*. **2020**, 1100, 12-21.

(24)   Kästner, C.; Lichtenstein, D.; Lampen, A.; Thünemann, A. F. Monitoring the fate of small silver nanoparticles during artificial digestion. *Colloids and Surfaces A: Physicochemical and Engineering Aspects*. **2017**, 526, 76-81.

(25)   Laloux, L.; Kastrati, D.; Cambier, S.; Gutleb, A. C.; Schneider, Y. J. The food matrix and the gastrointestinal fluids alter the features of silver nanoparticles. *Small*. **2020**, 1907687.

(26)   Axson, J. L.; Stark, D. I.; Bondy, A. L.; Capracotta, S. S.; Maynard, A. D.; Philbert, M. A.; Bergin, I. L.; Ault, A. P. Rapid kinetics of size and pH-dependent dissolution and aggregation of silver nanoparticles in simulated gastric fluid. *J Phys Chem C Nanomater Interfaces*. **2015**, 119, 20632-20641.

(27)   Telgmann, L.; Nguyen, M. T. K.; Shen, L.; Yargeau, V.; Hintelmann, H.; Metcalfe, C. D. Single particle ICP-MS as a tool for determining the stability of silver nanoparticles in aquatic matrixes under various environmental conditions, including treatment by ozonation. *Anal Bioanal Chem*. **2016**, 408, 5169-5177.

(28)   Laborda, F.; Jiménez-Lamana, J.; Bolea, E.; Castillo, J. R. Critical considerations for the determination of nanoparticle number concentrations, size and number size distributions by single particle ICP-MS. *Journal of Analytical Atomic Spectrometry*. **2013**, 28, 1220-1232.

(29)   Lee, S.; Bi, X. Y.; Reed, R. B.; Ranville, J. F.; Herckes, P.; Westerhoff, P. Nanoparticle size detection limits by single particle ICP-MS for 40 elements. *Environ Sci Technol*. **2014**, 48, 10291-10300.

(30)   Montoro Bustos, A. R.; Purushotham, K. P.; Possolo, A.; Farkas, N.; Vladar, A. E.; Murphy, K. E.; Winchester, M. R. Validation of single particle ICP-MS for routine measurements of nanoparticle size and number size distribution. *Anal Chem*. **2018**, 90, 14376-14386.

(31)   Donovan, A. R.; Adams, C. D.; Ma, Y.; Stephan, C.; Eichholz, T.; Shi, H. Detection of zinc oxide and cerium dioxide nanoparticles during drinking water treatment by rapid single particle ICP-MS methods. *Anal Bioanal Chem*. **2016**, 408, 5137-5145.

(32)   Donovan, A. R.; Adams, C. D.; Ma, Y.; Stephan, C.; Eichholz, T.; Shi, H. Single particle ICP-MS characterization of titanium dioxide, silver, and gold nanoparticles during drinking water treatment. *Chemosphere*. **2016**, 144, 148-153.

(33)   Dan, Y. B.; Ma, X. M.; Zhang, W. L.; Liu, K.; Stephan, C.; Shi, H. L. Single particle ICP-MS method development for the determination of plant uptake and accumulation of CeO2 nanoparticles. *Anal Bioanal Chem*. **2016**, 408, 5157-5167.

(34)   Li, C. C.; Dang, F.; Li, M.; Zhu, M.; Zhong, H.; Hintelmann, H.; Zhou, D. M. Effects of exposure pathways on the accumulation and phytotoxicity of silver nanoparticles in soybean and rice. *Nanotoxicology*. **2017**, 11, 699-709.

(35)   Proulx, K.; Wilkinson, K. J. Separation, detection and characterisation of engineered nanoparticles in natural waters using hydrodynamic chromatography and multi-method detection (light scattering, analytical ultracentrifugation and single particle ICP-MS). *Environmental Chemistry*. **2014**, 11, 392-401.

(36)   Londono, N.; Donovan, A. R.; Shi, H.; Geisler, M.; Liang, Y. Effects of environmentally relevant concentrations of mixtures of TiO2, ZnO and Ag ENPs on a river bacterial community. *Chemosphere*. **2019**, 230, 567-577.

(37)   Londono, N.; Donovan, A. R.; Shi, H.; Geisler, M.; Liang, Y. Impact of TiO2 and ZnO nanoparticles on an aquatic microbial community: effect at environmentally relevant concentrations. *Nanotoxicology*. **2017**, 11, 1140-1156.

(38)   Peters, R. J.; Rivera, Z. H.; van Bemmel, G.; Marvin, H. J.; Weigel, S.; Bouwmeester, H. Development and validation of single particle ICP-MS for sizing and quantitative determination of nano-silver in chicken meat. *Anal Bioanal Chem*. **2014**, 406, 3875-3885.

(39)   Weigel, S.; Peters, R.; Loeschner, K.; Grombe, R.; Linsinger, T. P. J. Results of an interlaboratory method performance study for the size determination and quantification of silver nanoparticles in chicken meat by single-particle inductively coupled plasma mass spectrometry (sp-ICP-MS). *Anal Bioanal Chem*. **2017**, 409, 4839-4348.

(40)   Dan, Y. B.; Shi, H. L.; Stephan, C.; Liang, X. H. Rapid analysis of titanium dioxide nanoparticles in sunscreens using single particle inductively coupled plasma-mass spectrometry. *Microchem J*. **2015**, 122, 119-126.

(41)   Schwertfeger, D. M.; Velicogna, J. R.; Jesmer, A. H.; Saatcioglu, S.; McShane, H.; Scroggins, R. P.; Princz, J. I. Extracting metallic nanoparticles from soils for quantitative analysis: method development using engineered silver nanoparticles and SP-ICP-MS. *Anal Chem*. **2017**, 89, 2505-2513.

(42)   Pace, H. E.; Rogers, N. J.; Jarolimek, C.; Coleman, V. A.; Higgins, C. P.; Ranville, J. F. Determining transport efficiency for the purpose of counting and sizing nanoparticles via single particle inductively coupled plasma mass spectrometry. *Anal Chem*. **2011**, 83, 9361-9369.

(43)   Laborda, F.; Bolea, E.; Jiménez-Lamana, J. Single particle inductively coupled plasma mass spectrometry: a powerful tool for nanoanalysis. *Anal Chem*. **2014**, 86, 2270-2278.

(44)   Liu, H.; Gong, F.; Wei, F.; Wu, H. Artificial simulation of salivary and gastrointestinal digestion, and fermentation by human fecal microbiota, of polysaccharides from Dendrobium aphyllum. *RSC advances*. **2018**, 8, 13954-13963.

(45)   Liu, J.; Murphy, K. E.; Winchester, M. R.; Hackley, V. A. Overcoming challenges in single particle inductively coupled plasma mass spectrometry measurement of silver nanoparticles. *Anal Bioanal Chem*. **2017**, 409, 6027-6039.

(46)   Clark, R. W.; Bonicamp, J. M. The Ksp-solubility conundrum. *Journal of chemical education*. **1998,** *75*, (9), 1182-1185.

(47)   Bekkby, T.; Bjørge, A. Variation in stomach temperature as indicator of meal size in harbour seal. *Phoca vitulina. In*. 1995. ICES.

(48)   Bateman, D. N. Effects of meal temperature and volume on the emptying of liquid from the human stomach. *J Physiol*. **1982**, 331, 461-467.

(49)   Mohan, S.; Princz, J.; Ormeci, B.; DeRosa, M. C. Morphological Transformation of Silver Nanoparticles from Commercial Products: Modeling from Product Incorporation, Weathering through Use Scenarios, and Leaching into Wastewater. *Nanomaterials*. **2019**, 9, 1258-1272.

(50)   Liu, X.; Ray, J. R.; Neil, C. W.; Li, Q.; Jun, Y.-S. Enhanced colloidal stability of CeO_2 nanoparticles by ferrous ions: adsorption, redox reaction, and surface precipitation. *Environ Sci Technol*. **2015**, 49, 5476-5483.

(51)   Ray, J. R.; Wu, X. H.; Neil, C. W.; Jung, H. S.; Li, Z. C.; Jun, Y. S. Redox chemistry of CeO2 nanoparticles in aquatic systems containing Cr(VI)(aq) and Fe2+ ions. *Environ. Sci.: Nano*, **2019**, 6, 2269-2280.

(52)   Gorelik, S.; Kohen, R.; Ligumsky, M.; Kanner, J. Saliva plays a dual role in oxidation process in stomach medium. Arch Biochem Biophys. 2007, 458 (2), 236-243.

SUPPLEMENTARY INFORMATION

SEM Images of NPs

The scanning electron microscopy (SEM) samples were prepared by diluting stock suspensions of nanoparticles to appropriate concentrations in ultra-pure water. Each sample was ultrasonicated for 10 min to reduce aggregation before being transferred onto the SEM state (silica wafer) and the liquid was evaporated over 5 min. After drying, the samples were sputtered with Au/Pd and imaged under vacuum with a S-4700 model field emission scanning electron microscope. The SEM images are presented in Figure S1 and S2.
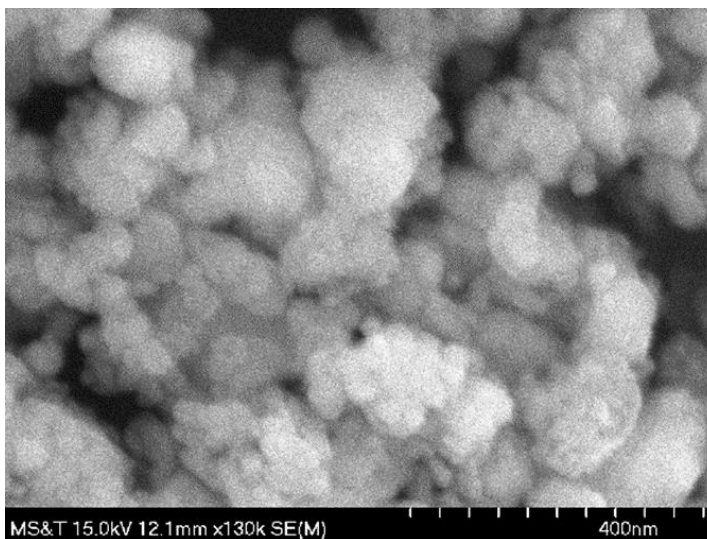
Figure S1. SEM image of CeO_2–NPs with manufacture specified size of 30-50 nm

MS&T 15.0kV 8.1mm x180k SE(M) |—— 200 nm ——|

| mode | HV | curr | WD | det | mag ⊞ | ———— 2 µm ———— |
| SE | 10.00 kV | 0.17 nA | 5.2 mm | TLD | 20 000 x | |
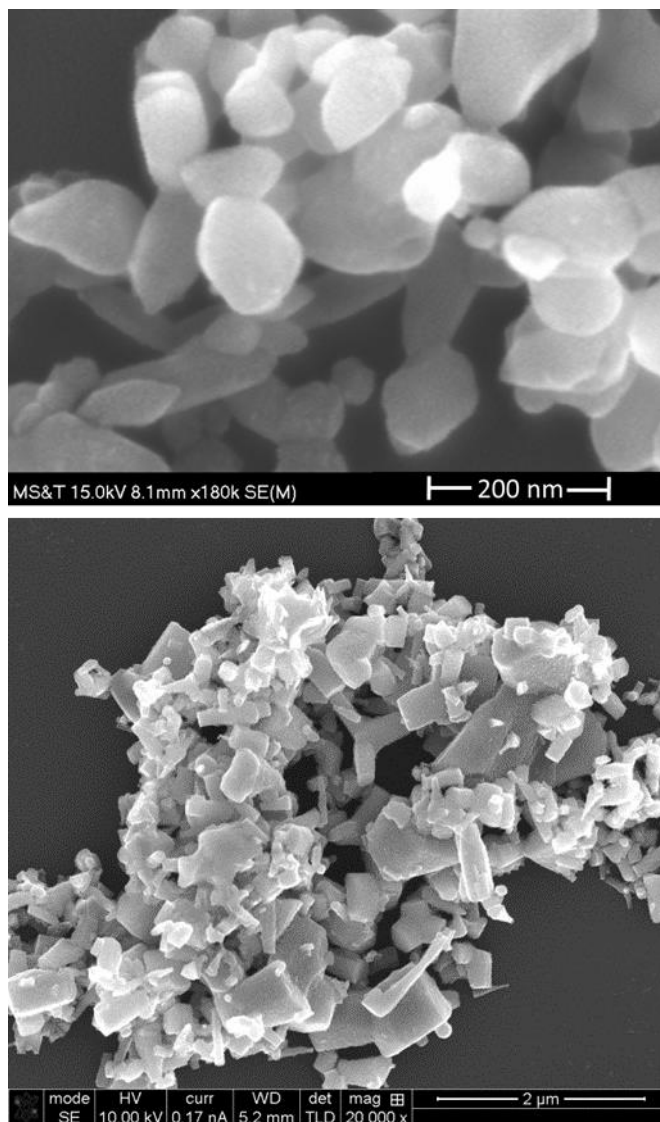
Figure S2. SEM images of ZnO-NPs. Top panel is the SEM image of ZnO-NPs with manufacture specified size of <100 nm and the bottom panel is the SEM image of ZnO-NPs with manufacture specified size of 80-200 nm

Size distribution of NPs
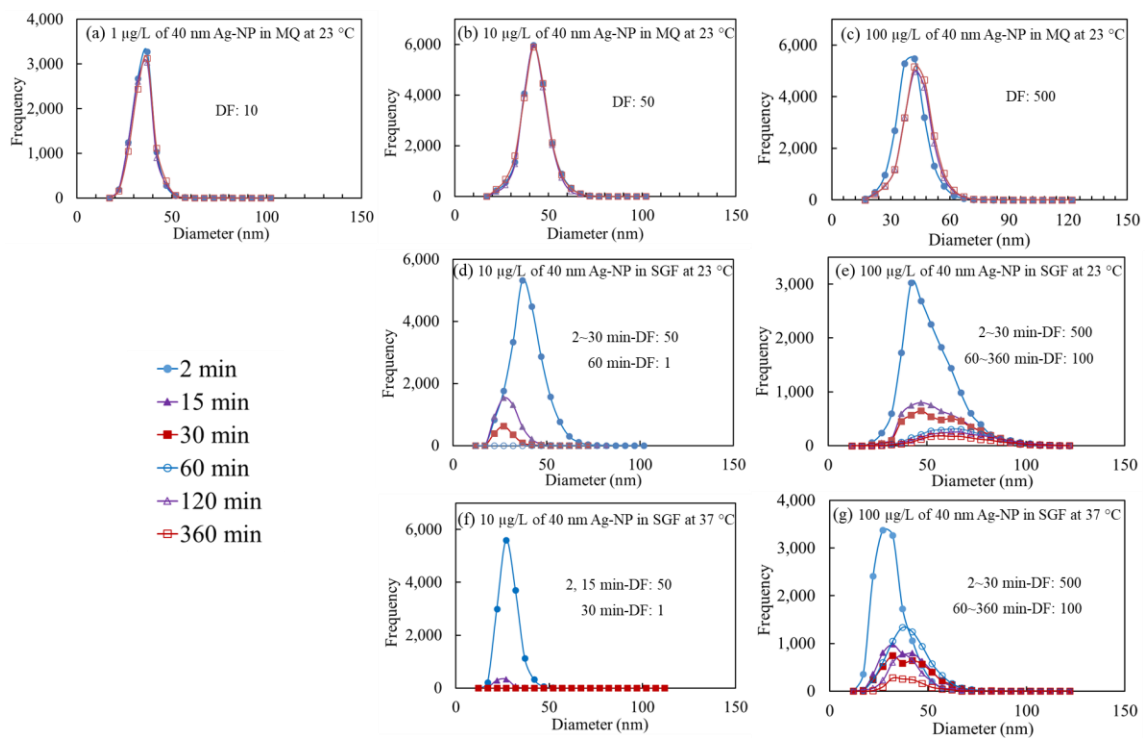
Figure S3. Size distribution histograms of 40 nm Ag-NPs with time in MQ water and SGF. DF means dilution factor
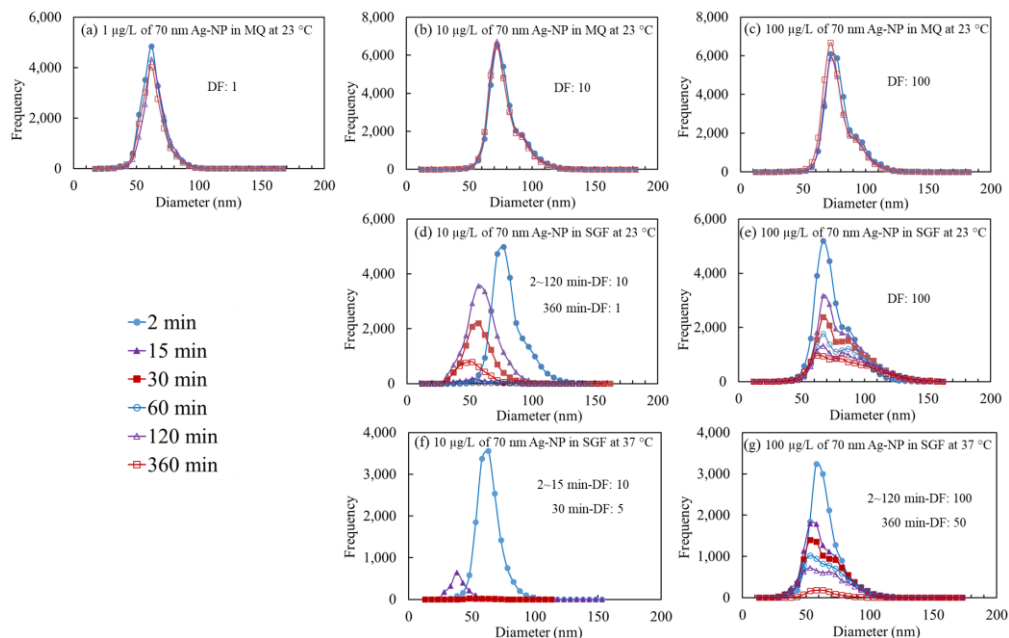
Figure S4. Size distribution histograms of 70 nm Ag-NPs with time in MQ water and SGF. DF means dilution factor
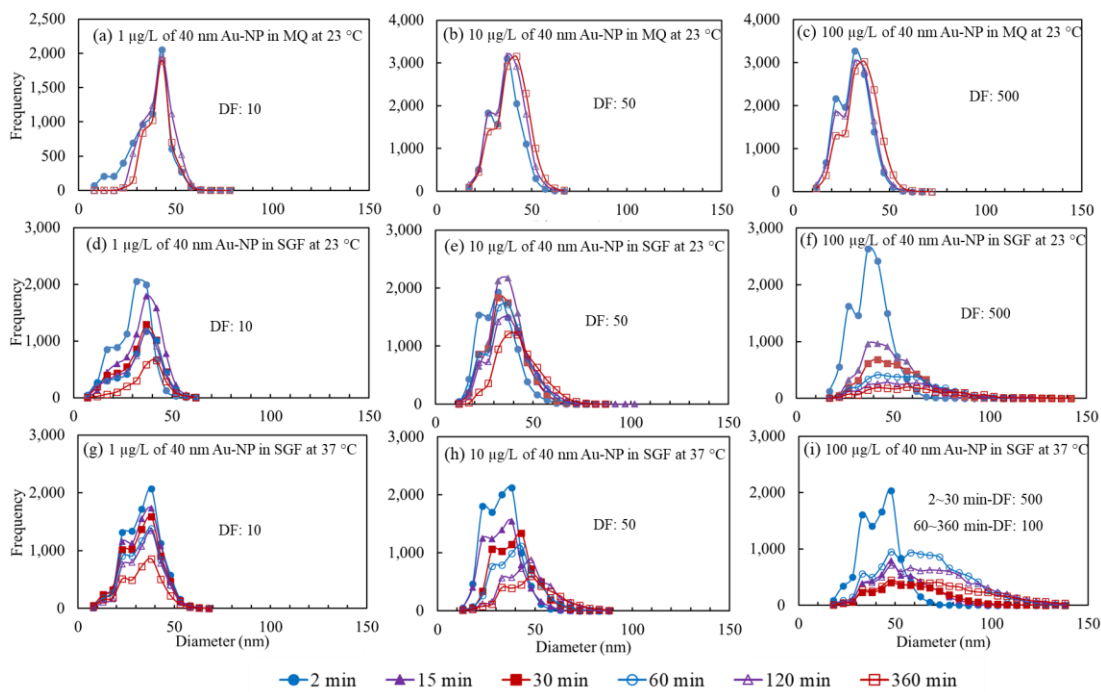
Figure S5. Size distribution histograms of 40 nm Au-NPs with time in MQ water and SGF. DF means dilution factor
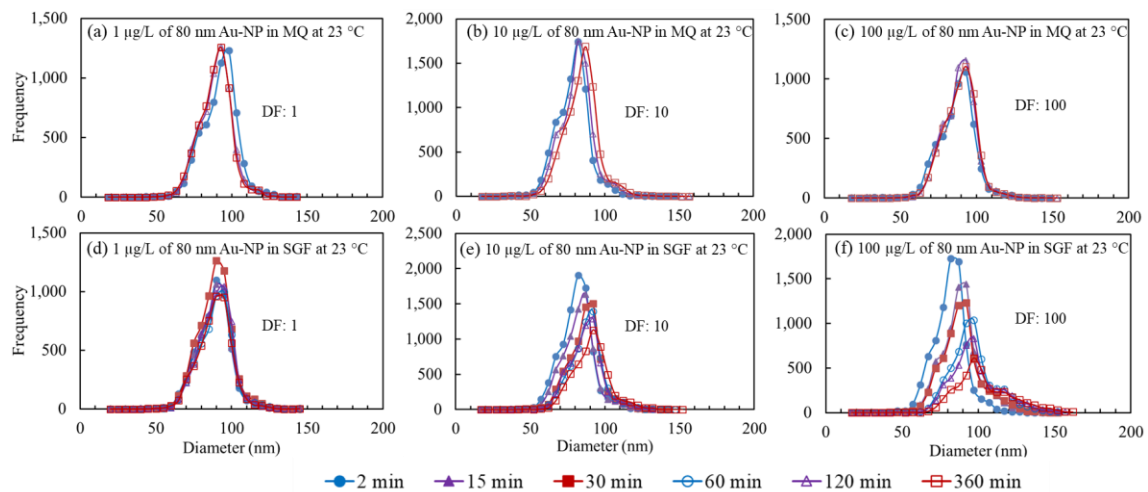
Figure S6. Size distribution histograms of 80 nm Au-NPs with time in MQ water and SGF. DF means dilution factor
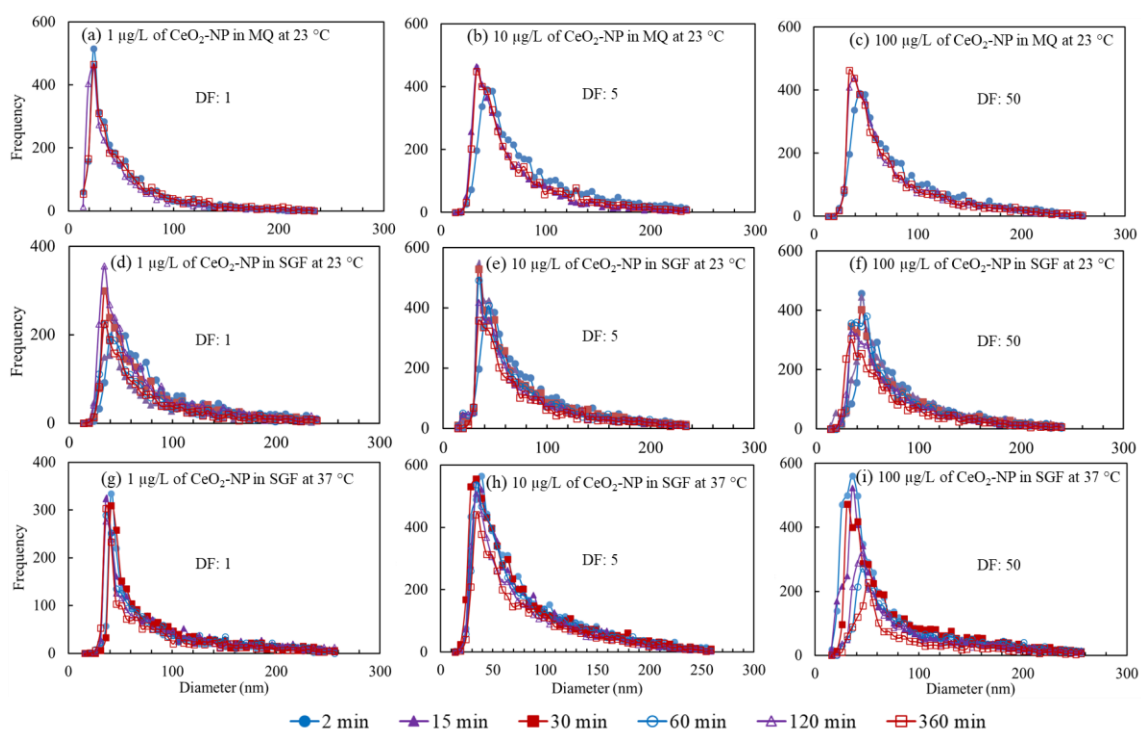
Figure S7. Size distribution histograms of 30-50 nm CeO₂-NPs with time in MQ water and SGF. DF means dilution factor

SECTION

2. CONCLUSIONS

2.1. THE ANALYTICAL METHODS OF EFCs IN PLANT SAP AND TISSUES

This work developed a high throughput freeze-thaw-centrifugal filtration followed by HPLC-MS/MS analysis method to analyze 11 representative EFCs with different properties in three species of crop plant sap. The method can quantify these EFCs in crop plant sap without using complicate multi-step sample extraction and purification procedures. The second method, a rapid, simple, and reliable method based on freeze-thaw equilibration followed by HS-SPME extraction and GC-MS analysis for the determination of volatile EFCs in three representative crop stems was also developed. The method shows good performance for the quantification of volatile EFCs in the plant stems without the need of complicated pretreatment procedure and losses of analytes. These two novel methods provide rapid screening tools to evaluate the brownfields and food crop plant contaminations of EFCs. These methods can also potentially be used as a preliminary screening for degradation of pollutants in plants, an ideal choice for identifying plant metabolites and plant metabolic pathways.

2.2. THE FATES OF ENPs IN SIMULATED GASTRIC FLUID

In this part of the research, we developed sensitive and selective SP-ICP-MS method to analyze nanoparticle concentrations, sizes, size distributions, aggregations, and dissolutions for four types of broadly used ENPs. The fates of these ENPs in SGF and the effects of particle size, initial concentration, and temperature of SGF on the fates of ENPs

in SGF were investigated. This study should help us to understand the fates of ENPs in gastric fluid and to access their potential toxicity and health risks after they enter into the blood circulation and organ systems.

BIBLIOGRAPHY

1. Groom, C. A.; Halasz, A.; Paquet, L.; Morris, N.; Olivier, L.; Dubois, C.; Hawari, J., Accumulation of HMX (octahydro-1,3,5,7-tetranitro-1,3,5,7-tetrazocine) in indigenous and agricultural plants grown in HMX-contaminated anti-tank firing-range soil. Environ Sci Technol 2002, 36, (1), 112-8.

2. Huelster, A.; Mueller, J. F.; Marschner, H., Soil-Plant Transfer of Polychlorinated Dibenzo-p-dioxins and Dibenzofurans to Vegetables of the Cucumber Family (Cucurbitaceae). Environ Sci Technol 1994, 28, (6), 1110-5.

3. Wu, W. Z.; Schramm, K. W.; Xu, Y.; Kettrup, A., Contamination and distribution of polychlorinated dibenzo-p-dioxins and dibenzofurans (PCDD/F) in agriculture fields in Ya-Er Lake area, China. Ecotoxicol Environ Saf 2002, 53, (1), 141-7.

4. Pereira, L. S.; Oweis, T.; Zairi, A., Irrigation management under water scarcity. Agricultural water management 2002, 57, (3), 175-206.

5. Manas, P.; Castro, E.; de Las Heras, J., Irrigation with treated wastewater: effects on soil, lettuce (Lactuca sativa L.) crop and dynamics of microorganisms. J Environ Sci Health A Tox Hazard Subst Environ Eng 2009, 44, (12), 1261-73.

6. Pal, A.; He, Y.; Jekel, M.; Reinhard, M.; Gin, K. Y., Emerging contaminants of public health significance as water quality indicator compounds in the urban water cycle. Environ Int 2014, 71, 46-62.

7. Rochester, J. R., Bisphenol A and human health: a review of the literature. Reprod Toxicol 2013, 42, 132-55.

8. Hussain, G.; Rasul, A.; Anwar, H.; Aziz, N.; Razzaq, A.; Wei, W.; Ali, M.; Li, J.; Li, X., Role of Plant Derived Alkaloids and Their Mechanism in Neurodegenerative Disorders. Int J Biol Sci 2018, 14, (3), 341-357.

9. Niemuth, N. J.; Klaper, R. D., Emerging wastewater contaminant metformin causes intersex and reduced fecundity in fish. Chemosphere 2015, 135, 38-45.

10. Pal, S.; Blais, J. M.; Robidoux, M. A.; Haman, F.; Krummel, E.; Seabert, T. A.; Imbeault, P., The association of type 2 diabetes and insulin resistance/secretion with persistent organic pollutants in two First Nations communities in northern Ontario. Diabetes Metab 2013, 39, (6), 497-504.

11. McKinney, M. A.; De Guise, S.; Martineau, D.; Beland, P.; Lebeuf, M.; Letcher, R. J., Organohalogen contaminants and metabolites in beluga whale (Delphinapterus leucas) liver from two Canadian populations. Environ Toxicol Chem 2006, 25, (5), 1246-57.

12. Richardson, S. D.; Kimura, S. Y., Water Analysis: Emerging Contaminants and Current Issues. Anal Chem 2016, 88, (1), 546-82.

13. EPA, U. S., Technical Fact Sheet –1,4-Dioxane. 2017.

14. EPA, U. S., Technical Fact Sheet –1,2,3-Trichloropropane (TCP). 2017.

15. Wu, C.; Spongberg, A. L.; Witter, J. D.; Sridhar, B. B., Transfer of wastewater associated pharmaceuticals and personal care products to crop plants from biosolids treated soil. Ecotoxicol Environ Saf 2012, 85, 104-9.

16. Holling, C. S.; Bailey, J. L.; Vanden Heuvel, B.; Kinney, C. A., Uptake of human pharmaceuticals and personal care products by cabbage (Brassica campestris) from fortified and biosolids-amended soils. J Environ Monit 2012, 14, (11), 3029-36.

17. Aitchison, E. W.; Kelley, S. L.; Alvarez, P. J.; Schnoor, J. L., Phytoremediation of 1, 4-dioxane by hybrid poplar trees. Water Environment Research 2000, 72, (3), 313-321.

18. De Paoli, M.; Taccheo Barbina, M.; Damiano, V.; Fabbro, D.; Bruno, R., Simplified determination of combined residues of prochloraz and its metabolites in vegetable, fruit and wheat samples by gas chromatography. J Chromatogr A 1997, 765, (1), 127-31.

19. Briggs, G. G.; Bromilow, R. H.; Evans, A. A., Relationships between lipophilicity and root uptake and translocation of non-ionised chemicals by barley. Pesticide science 1982, 13, (5), 495-504.

20. Limmer, M. A.; Burken, J. G., Plant translocation of organic compounds: molecular and physicochemical predictors. Environmental Science & Technology Letters 2014, 1, (2), 156-161.

21. Laborda, F.; Bolea, E.; Cepria, G.; Gomez, M. T.; Jimenez, M. S.; Perez-Arantegui, J.; Castillo, J. R., Detection, characterization and quantification of inorganic engineered nanomaterials: A review of techniques and methodological approaches for the analysis of complex samples. Anal Chim Acta 2016, 904, 10-32.

22. Li, C.-H.; Shen, C.-C.; Cheng, Y.-W.; Huang, S.-H.; Wu, C.-C.; Kao, C.-C.; Liao, J.-W.; Kang, J.-J., Organ biodistribution, clearance, and genotoxicity of orally administered zinc oxide nanoparticles in mice. Nanotoxicology 2012, 6, (7), 746-756.

23. Bonner, J. C., Nanoparticles as a potential cause of pleural and interstitial lung disease. Proceedings of the American Thoracic Society 2010, 7, (2), 138-141.

24. Dufour, E. K.; Kumaravel, T.; Nohynek, G. J.; Kirkland, D.; Toutain, H., Clastogenicity, photo-clastogenicity or pseudo-photo-clastogenicity: Genotoxic effects of zinc oxide in the dark, in pre-irradiated or simultaneously irradiated Chinese hamster ovary cells. Mutation Research/Genetic Toxicology and Environmental Mutagenesis 2006, 607, (2), 215-224.

25. Sharma, V.; Shukla, R. K.; Saxena, N.; Parmar, D.; Das, M.; Dhawan, A., DNA damaging potential of zinc oxide nanoparticles in human epidermal cells. Toxicology letters 2009, 185, (3), 211-218.

26. Petosa, A. R.; Jaisi, D. P.; Quevedo, I. R.; Elimelech, M.; Tufenkji, N., Aggregation and deposition of engineered nanomaterials in aquatic environments: role of physicochemical interactions. Environ Sci Technol 2010, 44, (17), 6532-49.

27. Smolkova, B.; El Yamani, N.; Collins, A. R.; Gutleb, A. C.; Dusinska, M., Nanoparticles in food. Epigenetic changes induced by nanomaterials and possible impact on health. Food Chem Toxicol 2015, 77, 64-73.

28. Emamhadi, M. A.; Sarafraz, M.; Akbari, M.; Thai, V. N.; Fakhri, Y.; Linh, N. T. T.; Mousavi Khaneghah, A., Nanomaterials for food packaging applications: A systematic review. Food Chem Toxicol 2020, 146, 111825.

29. Bumbudsanpharoke, N.; Choi, J.; Ko, S., Applications of Nanomaterials in Food Packaging. J Nanosci Nanotechnol 2015, 15, (9), 6357-72.

30. Guo, H.; Zhang, Z.; Xing, B.; Mukherjee, A.; Musante, C.; White, J. C.; He, L., Analysis of silver nanoparticles in antimicrobial products using surface-enhanced Raman spectroscopy (SERS). Environmental science & technology 2015, 49, (7), 4317-4324.

31. Wang, M.; Gao, B.; Tang, D., Review of key factors controlling engineered nanoparticle transport in porous media. J Hazard Mater 2016, 318, 233-246.

32. Keller, A. A.; McFerran, S.; Lazareva, A.; Suh, S., Global life cycle releases of engineered nanomaterials. Journal of nanoparticle research 2013, 15, (6), 1-17.

33. Zhao, D.; Tang, J.; Ding, X., Analysis of volatile components during potherb mustard (Brassica juncea, Coss.) pickle fermentation using SPME–GC-MS. LWT-Food Science and Technology 2007, 40, (3), 439-447.

34. Yasuhara, A.; Shiraishi, H.; Nishikawa, M.; Yamamoto, T.; Uehiro, T.; Nakasugi, O.; Okumura, T.; Kenmotsu, K.; Fukui, H.; Nagase, M., Determination of organic components in leachates from hazardous waste disposal sites in Japan by gas chromatography–mass spectrometry. Journal of Chromatography A 1997, 774, (1-2), 321-332.

35. Wejnerowska, G.; Gaca, J., Application of headspace solid-phase microextraction for determination of chloro-organic compounds in sewage samples. Toxicology mechanisms and methods 2008, 18, (6), 543-550.

36. Carter, L. J.; Harris, E.; Williams, M.; Ryan, J. J.; Kookana, R. S.; Boxall, A. B., Fate and uptake of pharmaceuticals in soil–plant systems. Journal of agricultural and food chemistry 2014, 62, (4), 816-825.

37. Fu, Q.; Wu, X.; Ye, Q.; Ernst, F.; Gan, J., Biosolids inhibit bioavailability and plant uptake of triclosan and triclocarban. Water Res 2016, 102, 117-124.

38. Navarro, I.; de la Torre, A.; Sanz, P.; Porcel, M. A.; Pro, J.; Carbonell, G.; Martinez, M. L., Uptake of perfluoroalkyl substances and halogenated flame retardants by crop plants grown in biosolids-amended soils. Environ Res 2017, 152, 199-206.

39. Yang, C. Y.; Chang, M. L.; Wu, S. C.; Shih, Y. H., Partition uptake of a brominated diphenyl ether by the edible plant root of white radish (Raphanus sativus L.). Environ Pollut 2017, 223, 178-184.

40. Hechmi, N.; Ben Aissa, N.; Abdenaceur, H.; Jedidi, N., Uptake and Bioaccumulation of Pentachlorophenol by Emergent Wetland Plant Phragmites australis (Common Reed) in Cadmium Co-contaminated Soil. Int J Phytoremediation 2015, 17, (1-6), 109-16.

41. Montemurro, N.; Postigo, C.; Lonigro, A.; Perez, S.; Barcelo, D., Development and validation of an analytical method based on liquid chromatography-tandem mass spectrometry detection for the simultaneous determination of 13 relevant wastewater-derived contaminants in lettuce. Anal Bioanal Chem 2017, 409, (23), 5375-5387.

42. Picó, Y.; Alfarham, A.; Barceló, D., Analysis of emerging contaminants and nanomaterials in plant materials following uptake from soils. TrAC Trends in Analytical Chemistry 2017, 94, 173-189.

43. Dan, Y.; Ma, X.; Zhang, W.; Liu, K.; Stephan, C.; Shi, H., Single particle ICP-MS method development for the determination of plant uptake and accumulation of CeO 2 nanoparticles. Analytical and bioanalytical chemistry 2016, 408, (19), 5157-5167.

44. Dan, Y.; Zhang, W.; Xue, R.; Ma, X.; Stephan, C.; Shi, H., Characterization of gold nanoparticle uptake by tomato plants using enzymatic extraction followed by single-particle inductively coupled plasma–mass spectrometry analysis. Environmental science & technology 2015, 49, (5), 3007-3014.

45. Taylor, A. F.; Rylott, E. L.; Anderson, C. W.; Bruce, N. C., Investigating the toxicity, uptake, nanoparticle formation and genetic response of plants to gold. PLoS One 2014, 9, (4), e93793.

46. Feichtmeier, N. S.; Walther, P.; Leopold, K., Uptake, effects, and regeneration of barley plants exposed to gold nanoparticles. Environmental Science and Pollution Research 2015, 22, (11), 8549-8558.

47. Donovan, A. R.; Adams, C. D.; Ma, Y.; Stephan, C.; Eichholz, T.; Shi, H., Detection of zinc oxide and cerium dioxide nanoparticles during drinking water treatment by rapid single particle ICP-MS methods. Anal Bioanal Chem 2016, 408, (19), 5137-45.

48. Wei, X.; Hu, L.-L.; Chen, M.-L.; Yang, T.; Wang, J.-H., Analysis of the distribution pattern of chromium species in single cells. Analytical chemistry 2016, 88, (24), 12437-12444.

49. Telgmann, L.; Nguyen, M. T. K.; Shen, L.; Yargeau, V.; Hintelmann, H.; Metcalfe, C. D., Single particle ICP-MS as a tool for determining the stability of silver nanoparticles in aquatic matrixes under various environmental conditions, including treatment by ozonation. Analytical and bioanalytical chemistry 2016, 408, (19), 5169-5177.

50. Donovan, A. R.; Adams, C. D.; Ma, Y.; Stephan, C.; Eichholz, T.; Shi, H., Single particle ICP-MS characterization of titanium dioxide, silver, and gold nanoparticles during drinking water treatment. Chemosphere 2016, 144, 148-153.

51. Li, C. C.; Dang, F.; Li, M.; Zhu, M.; Zhong, H.; Hintelmann, H.; Zhou, D. M., Effects of exposure pathways on the accumulation and phytotoxicity of silver nanoparticles in soybean and rice. Nanotoxicology 2017, 11, (5), 699-709.

52. Sohal, I. S.; Cho, Y. K.; O'Fallon, K. S.; Gaines, P.; Demokritou, P.; Bello, D., Dissolution Behavior and Biodurability of Ingested Engineered Nanomaterials in the Gastrointestinal Environment. ACS Nano 2018, 12, (8), 8115-8128.

53. Wu, W.; Zhang, R.; McClements, D. J.; Chefetz, B.; Polubesova, T.; Xing, B., Transformation and Speciation Analysis of Silver Nanoparticles of Dietary Supplement in Simulated Human Gastrointestinal Tract. Environ Sci Technol 2018, 52, (15), 8792-8800.

54. Mwilu, S. K.; El Badawy, A. M.; Bradham, K.; Nelson, C.; Thomas, D.; Scheckel, K. G.; Tolaymat, T.; Ma, L.; Rogers, K. R., Changes in silver nanoparticles exposed to human synthetic stomach fluid: effects of particle size and surface chemistry. Sci Total Environ 2013, 447, 90-8.

55. Cho, W. S.; Kang, B. C.; Lee, J. K.; Jeong, J.; Che, J. H.; Seok, S. H., Comparative absorption, distribution, and excretion of titanium dioxide and zinc oxide nanoparticles after repeated oral administration. Part Fibre Toxicol 2013, 10, 9.

56. Gomez-Gomez, B.; Perez-Corona, M. T.; Madrid, Y., Using single-particle ICP-MS for unravelling the effect of type of food on the physicochemical properties and gastrointestinal stability of ZnONPs released from packaging materials. Analytica chimica acta 2020, 1100, 12-21.

57. Axson, J. L.; Stark, D. I.; Bondy, A. L.; Capracotta, S. S.; Maynard, A. D.; Philbert, M. A.; Bergin, I. L.; Ault, A. P., Rapid Kinetics of Size and pH-Dependent Dissolution and Aggregation of Silver Nanoparticles in Simulated Gastric Fluid. J Phys Chem C Nanomater Interfaces 2015, 119, (35), 20632-20641.

VITA

Xiaolong He was born in Lüliang, Shanxi Province, China. In 2011, he graduated with a Bachelor degree of Environmental Engineering from Yanshan University in Qinhuangdao, China. After he received his BS degree, he started to work in the Yema environment protection company in Shanghai for 4 years. In 2017, he joined in Missouri University of Science and Technology to continue his graduate study in Dr. Honglan Shi's research group. He received his Ph.D. degree in Chemistry in May 2021 from Missouri University of Science and Technology.